Periphery Decorated and Core Initiated Neutral and Polyanionic Borane large molecules: Forthcoming and Promising properties for medicinal applications

Clara Viñas,[a,*] Rosario Núñez,[a] Ines Bennour[a] and Francesc Teixidor[a]

[a] Institut de Ciència de Materials de Barcelona (ICMAB-CSIC). Campus UAB, 08193 Bellaterra, Barcelona, Spain.

Phone: 34 93 5801853

e-mail: clara@icmab.es

Keywords: carboranes, metallacarboranes, boranes, dendrimers, macromolecules, cellular imaging, markers, antimicrobial, fluorescent probes, octasilselquioxanes, photoluminescence.

Abstract

A mini review based on radial growing macromolecules and core initiated Borane periphery decorated with *o*-carboranes and metallacarboranes that has been developed in the authors laboratories is reported. The review is divided into four sections; three of them are related to the design and synthesis of these large boron containing molecules and the fourth deals with the unique properties of anionic metallacarborane molecules that provide a glimpse of their potential for their promising use in medicinal applications. Their unique stability along with their geometrical and electronic properties, as well as the precise steric structure of 1,2-*closo*-$C_2B_{10}H_{12}$ (*o*-carborane) that has the potential for the incorporation of many substituents: at the carbon (C_c), at the boron and at both carbon and boron vertices, suggests this cluster as an innovative building block or platform for novel applications that cannot be achieved with organic hydrocarbon compounds. Poly(aryl-ether) dendrimers grown from fluorescent cores, such as 1,3,5-triarylbenzene or *meso*-porphyrins, have been decorated with boron clusters to attain rich boron containing dendrimers. Octasilsesquioxane cubes have been used as core for its radial growth to get boron rich large molecules. The unique properties of cobaltabisdicarbollide cluster for: i) self-assembly in water to produce monolayer nano-vesicles, ii) crossing lipid bilayer membranes, iii) interacting with membrane cells, iv) facilitating its visualization within cells by Raman and fluorescence techniques and v) their use as molecular platform for "*in vivo*" imaging are discussed in detail.

INDEX:

Introduction

Boron, which is not present on the Earth in its elemental form but only in the form of compounds such as borax, boric acid and borates, is distributed in the nature as in air, in soils and in surface freshwaters. Boron is probably a prebiotic element with special relevance.[1] Despite that high boron concentration in the soils is toxic to plants and some boron derivatives are used as herbicides, though boron is an essential micronutrient for plant's growth as well as for some animals.[2] In humans, boron deficiency apparently affects the function or the composition of skeleton, kidney, and brain.[3] In addition, boron deficiency is associated with the metabolism of several other nutrients including calcium, copper, potassium, magnesium, nitrogen or vitamin D, among others.[4] It is well documented that ancient civilizations (Babylonians, Egyptians, Chinese, Romans as well as Arabians) used boron compounds as drugs. Since the eighteenth century, boric acid (H_3BO_3) has been widely used for topic administration because of its strong reactivity against bacteria and fungi.[5]

Boron is located at the left side of carbon in the Periodic Table. Boron and carbon are the elements that have the property to build molecules of unlimited size by covalent self-bonding; these polyhedral compounds are named boranes.[6] The term electron deficient is usually applied when discussing boron clusters.[7] The bonding in such boron compounds may be adequately described by the use of delocalized three-centre two-electron bonds (3c-2e).[7] Therefore, a line drawn in a structural representation of a molecule indicates an interaction or connectivity, not a bond in the two-centre two-electron (2c-2e) sense. Most of the known polyhedral compounds of this type contain four to twelve atoms but icosahedral cages are the most studied.[8]

The polyhedral *closo* $[B_{12}H_{12}]^{2-}$ borane is a robust icosahedral cage stabilized by three-dimensional delocalization of thirteen bonding electron pairs (Chart 1).[9] This charge-delocalized ion $[B_{12}H_{12}]^{2-}$ may be considered the 3D parent aromatic species[10] that serves borane chemistry as benzene serves organic chemistry.[11] Isoelectronic substitution of one or two B-H vertices in

closo $[B_{12}H_{12}]^{2-}$ by C-H provides the carborane derivatives: *closo* $[1\text{-}CB_{11}H_{12}]^{-}$ and *closo* $C_2B_{10}H_{12}$.[8] The word carborane, a contraction of the IUPAC name, carbaborane, is used for cluster compounds containing carbon and boron atoms. Largely, the twelve-vertex *closo* $C_2B_{10}H_{12}$ icosahedral carboranes have been the most widely studied (Chart 1). The three known isomers, in which the carbon atoms occupy *ortho*- (1,2), *meta*- (1,7), or *para*- (1,12) vertices are white solids that rank among the most stable molecular compounds known (Chart 2). IUPAC approved prefix designations indicate the degree of "closed" and "open" polyhedral character for the carboranes.[12] The term "*closo*" is used for closed polyhedra having triangular faces only and "*nido*" for closed polyhedra in which a boron vertex has been removed from the parent *closo* polyhedron.[12]

The principal feature of boranes and carboranes is a triangular face polyhedral or polyhedral fragment framework of carbon and boron atoms. The boron and carbon atoms are located at the polyhedron vertices. A terminal hydrogen atom is bonded to the cluster vertex via a classical 2c-2e bond. Metallacarboranes, $[M(C_2B_{11}H_{12}]^{-}$, are derivatives of boron hydrides that contain carbon and metal atoms into the fragment. Many metals have been incorporated as cluster vertices.[13] These Boron cluster families (Chart 1) display many particular characteristics that do not find parallel in their organic counterparts. In addition, the shape of the stable icosahedral clusters, $[B_{12}H_{12}]^{2-}$, $[CB_{11}H_{12}]^{-}$, $C_2B_{10}H_{12}$ brings the possibility to build larger high boron containing molecules having the icosahedral boron cluster as the core, allowing for a maximum of twelve primary branches in a unique spatial disposition.

Dendrimers are hyperbranched and mono-dispersed macromolecules that have a perfectly defined, multifunctionalized and reproducible structure.[14] The well-defined size, molecular weight and specific number of end groups of dendrimers can be well controlled thus improving their physical and chemical characteristics compared with classical polymers.[15],[16] The structural diversity and special properties make dendrimers suitable for a wide range of different applications, such as catalysis, magnetic applications, redox, molecular electronics, energy

conversion, sensing, photo-optical materials and nanomedicine, among others.[17],[18],[19] The advantage of introducing changes in their structures (nucleus, branches and terminal groups) allows to modulate their behaviour with the goal focused to designing and synthesizing dendrimers more specific for certain areas, such as carriers for drug delivery.[20],[21],[22]

An efficient Boron Neutron Capture Therapy (BNCT) treatment needs effective boron delivery agents that fulfil the following requirements: 1) an accumulation of approximately 10-30 μg of ^{10}B per gr of tumor cells; 2) a low systemic toxicity; 3) a high tumor-to-healthy tissue and tumor-to-blood boron concentration ratios; 4) an efficient retention of ^{10}B in the tumor during the irradiation; and 5) an easy quantification and monitoring systems of the boron carrier concentration and biodistribution in the patient. Plesek reported that most of the polyhedral boranes are essentially nontoxic due to their inertness to biochemical reactions.[23] Lethal doses 60 (LD_{60}) of $[B_{12}H_{12}]^{2-}$ to rats by oral administration has been estimated as 7g/kg.[24]

Along the years, several research groups have been involved in the development of boron enriched macromolecules, by incorporating boron clusters in the interior or at the periphery of different dendrimeric systems, such as PAMAM, Poly-L-lysine and Pentaerythritol based dendrimers,[25] which possess a great potential as boron carrier for BNCT.[26] In addition to these, other macromolecules as star-shaped molecules having cores made of 1,3,5-triarylbenzene and hexaphenylbenzene decorated with boron clusters,[27] high boron content aliphatic polyester dendrimers,[28] as well as carbosilane dendrimers decorated with *closo*-carboranes and cobaltabisdicarbollide derivatives have also been developed.[29],[30],[31]

Apart from dendrimers-based macromolecules, another type of scaffolds used to functionalize with carborane clusters to obtain high boron content systems are Polyhedral Oligomeric Silsesquioxanes (POSS) $(RSiO_{1.5})_n$ (n = 8) or octasilsesquioxanes. POSS are nanosized building blocks for organic/inorganic hybrid materials of general formulae $[RSiO_{1.5}]_8$ with a 3-D scaffold that are easy to synthesise and exhibit versatile functionality, high robustness and thermal stability.[32] These POSS frameworks can be modified to control the nanostructure

assembly and tailor chemical properties as oxidative stability and catalytic activity, as well as mechanical, electrical, optical or electronic properties.[32d],[33] These exceptional characteristics make silsesquioxane based materials very useful for a wide variety of applications, including emitting layers in OLEDs,[34] thermally and chemically resistant polymers and ceramics,[35] or nanomedicine,[36] among others.

So, focusing on the carborane cluster, their versatile vertices allow the icosahedral cage to act as a scaffold to extend the dendron from the carbon cluster atoms to the periphery or to be modified as a focal point. Yamamoto *et al.* reported on the synthesis of serving as water-solubilizing groups of *o*-carborane cluster derivatives for BNCT. These compounds were synthesized via a palladium-catalysed reaction under essentially neutral conditions (Scheme 1).[37]

The high stability of $[B_{12}H_{12}]^{2-}$ to strong bases, strong acids and oxidizing agents is unique for boron hydride structures. However, most of boron hydride borates react smoothly with certain reagents, particularly electrophilic species, to give stable derivatives in which hydrogen atoms are replaced by the attacking group.[38] The perhydroxylated *closo* $[B_{12}(OH)_{12}]^{2-}$ in which the icosahedral cage is retained was successfully synthesized in Hawthorne's group by treating alkali metal salts of $[B_{12}H_{12}]^{2-}$ with 30% hydrogen peroxide.[11],[39] The hydrogen bonded arrays observed in the new cages point to the potential that *closo* $[B_{12}(OH)_{12}]^{2-}$ has in the development of species as central cores for the divergent growth of dendrimers. The twelve-fold functional icosahedral dodecaborate core is rigid and the directions of the arms within the first generation should be sterically favorable. The total esterification of the *closo* $[B_{12}(OH)_{12}]^{2-}$ with acetic anhydride or benzoyl chloride produced organoderivatized molecules of the icosahedral cluster.[11],[39],]40] The resulting scaffold named homo functional "closomer", in which each vertex is substituted with an organic moiety represent the first example of such structural motif known in chemistry (Scheme 2). Spherical high boron containing closomer synthesis was achieved in 2001 with the synthesis of: i) the dianionic homo functional closomer that contains an

icosahedral $[B_{12}]^{2-}$ cluster as a core and twelve branches ending with neutral *closo* C_2B_{10} units and ii) the synthesis of the fourteen anionic closomer that is formed by the icosahedral $[B_{12}]^{2-}$ cluster core and twelve anionic *nido* $[C_2B_9]^-$ units at the end of the twelve branches.[41] The negative charges impart hydrophilicity to the closomer molecules, which attains solubility in hot water, while maintaining solubility in polar organic solvents. These boron-rich macromolecular anionic nanospheres possess great potential for their use in future as drug delivery platforms for cancer treatment using the BNCT technique. Homo functional closomers serving contrast agent functionalities for diagnostic in high-performance MRI were also developed.[42] Later, a bifunctional closomer probe for fluorine (^{19}F) magnetic resonance and optical bimodal cellular imaging was also reported.[43] Scheme 2 displays the reported icosahedral $[B_{12}]^{2-}$ homo functional "closomers".

Boron neutron capture therapy (BNCT) is a promising binary therapy for the treatment of cancer, because malignant cells can be selectively targeted and destroyed in the presence of healthy normal cells.[44],[45] Along decades, many carriers have been designed as boron delivery vehicles, including porphyrins, amino acids, peptides, nucleosides and liposomes.[44],[46],[47],[48] Moreover, improved BNCT agents with higher tumor selectivity for being accumulated in tumor cells, such as glioblastoma multiform, neck and head cancers and melanomas have been reported.[49] Despite the number of boron drug delivery agents developed, delivery of adequate amounts of B to tissues, which would enhance the effectiveness of the treatment is still a challenge. To achieve the required amount of boron concentration dendrimers-based drug delivery agents are found to be superior in terms of accumulation and retention in the tumour tissues. Furthermore, tagging imaging contrast agents such as fluorescent dyes, optical or magnetic nanoparticles (Fe_2O_3), radioisotopes to the boron delivery agents will generate theranostic nanohybrids, that allows a better visualization of the drugs *in vitro* and *in vivo*.

The most studied metallacarborane is cobaltabisdicarbollide $[3,3'\text{-}Co(1,2\text{-}C_2B_9H_{11})_2]^-$ that was synthesized in 1965.[50] This anion has a great chemical stability, high molecular volume, low

nucleophilic character and low charge density because the negative charge is distributed between 45 atoms.[51] The derivative chemistry of the cobaltabisdicarbollide remains very much unexplored.[52] The fundamental reason is the lack of a comprehensive synthetic strategy leading to these derivatives. As for the *closo* $C_2B_{10}H_{12}$ carborane compounds, substitutions may occur on $[3,3'\text{-}Co(1,2\text{-}C_2B_9H_{11})_2]^-$ either on carbon or on boron. With few exceptions,[53] substitutions on carbon have been achieved only at an early stage of the synthetic process, i.e. on the starting *o*-carborane,[54] but not by direct reaction at the $[3,3'\text{-}Co(1,2\text{-}C_2B_9H_{11})_2]^-$ cage.

In this review, we report on the results from our laboratories based on the radial growing of different cores to obtain periphery borane decorated macromolecules, which achieve high boron content. Icosahedral c*loso o*-carborane cluster, organic centers (aryl-ether dendrons, 1,3,5-triarylbenzene and *meso*-porphyrins) and purely inorganic octasilsesquioxane cubes are the different cores that have been functionalized with several branches ending with neutral or anionic boron clusters to achieve high boron containing macromolecules. The unique properties of the small cobaltabisdicarbollide molecule of self-assembly to form monolayer nano-vesicles that cross lipid bilayer membranes facilitating its cells' uptake and posterior visualization within the cells by Raman Spectroscopy are discussed in detail. Furthermore, the more recent advances on the biological assessment of some cobaltabisdicarbollide derivatives, such as their antimicrobial activity, cells' cytotoxicity, accumulation and visualization in living cells by fluorescence, as well as *in vivo* imaging by Positron Emission Tomography combined with X-ray Computed Tomography (PET-CT) have being included.

Results and Discussion

1. Neutral 1,2-*closo*-$C_2B_{10}H_{12}$ Carborane as Core for Radial Growing to Achieve High Boron Containing Macromolecules.

The unique stability and geometrical properties, as well as the precise steric structure of *closo* isomers $C_2B_{10}H_{12}$, suggest that these species are potential building blocks or platforms for novel applications that cannot be achieved with organic hydrocarbon compounds. Each one of the three isomeric *closo* $C_2B_{10}H_{12}$ carboranes has the potential for the incorporation of many substituents: at the carbon (C_c) and boron vertices (Chart 3).[55],[38b] These species have two moderately acidic C_c-H vertices that are deprotonated with strong bases and subsequently can be functionalized using electrophilic reagents. The chemistry of boron-substituted carboranes is less developed than that of the carbon-substituted analogues because of the higher difficulty to introduce functional groups at the boron atoms of the carborane cage. The 10 B-H vertices present in each of the icosahedral carborane isomers have electrophilic substitution chemistry in many ways reminiscent of arenes. Thus, most reactions that occur at the boron vertices do not affect the carbon vertices, and *vice-versa*. Previous calculated charges[56] on 1,2-*closo*-$C_2B_{10}H_{12}$ show that B(8,9,10,12), *i.e*. the boron atoms located farthest from the cluster carbon atoms, are the boron atoms richest in electron density, whilst boron atoms B(3,6), which are closest to the cluster carbons are the poorer. B(3,6) are the most positive vertices (0.204 e), followed by B(4,5,7,11) (0.024 e), and finally B(8,9,11,12) (in the range -0.146 / -0.168 e) so, each vertex can selectively achieve a different reactivity according to its different electron density.[57] The rigid three-dimensional icosahedra hold substituents in well-defined spatial relationships and most transformations maintain the integrity of the underlying geometry.

o-Carborane, 1,2-*closo*-$C_2B_{10}H_{12}$, has been adapted to perform as a core of globular macromolecules, dendrons or dendrimers by substitution only at the C_c-H, only at the B-H or at both vertices C_c-H and B-H (Charter 3).

1.1.- Neutral 1,2-*closo*-$C_2B_{10}H_{12}$ Carborane as Core through substitution at the carbon vertices.

The *o*-carborane cluster provides a unique platform for the construction of molecules with a variable degree of branches and a wide range of derivatization. The large number of cluster vertices offers a unique core for the construction of highly branched macromolecules with full control over the substitution' position (Chart 3), which may convert the cluster molecules as multifunctional molecules. How? By the capacity to functionalize the different vertices with branches terminated with distinct functionalities (fluorescent dyes, radiopharmaceuticals, MRI, contrast agents, …) to provide multi-modal treatments, e.g. diagnostic and therapy in addition to drug delivery nanocarriers.[5a]

Small carbosilane dendrons in which a *closo* carborane is located at the focal point have been prepared by a sequence of steps involving hydrosilylation and reduction reactions.[58] For this purpose, compounds **1**-**5** were used as scaffolds for peripheral functionalization with styrene, chlorovinylstyrene, or suitable carboranes, while keeping the $C_{cluster}$-Si (C_c-Si) bond to produce compounds **6**-**8** (Scheme 3). Besides, the reaction involving nucleophilic attack by fluoride or other nucleophiles, and the subsequent cleavage of C_c-Si bonds, is a well-documented process in carboranylsilane chemistry.[59] Thus, the possibility to use carboranes as a platform for dendron functionalization and cluster elimination by nucleophilic cleavage of the C_c-Si bond offers a new strategy to introduce other functions. The modification of the carborane by reduction with Mg/$BrCH_2CH_2Br$ was also achieved.[58] The possibility of the cluster modification by reducing agents, while keeping the C_c-Si bonds, represents another alternative to prepare new carboranylsilane dendrons.

In addition, following our studies on cobaltabisdicarbollides' direct substitution[60]to produce novel high boron content polyanionic species with enhanced water solubility, we explored the possibility of using lithiated boron clusters as nucleophiles to produce a new family of high boron content polyanionic large molecules.[60],[61],[62] The zwitterionic compound [3,3'-Co(8-$(CH_2CH_2O)_2$-1,2-$C_2B_9H_{10}$)(1',2'-$C_2B_9H_{11}$)] has been shown to be susceptible to nucleophilic

attack on the positively charged oxygen atom, e.g. by pyrrolyl,[63] imide, cyanide or amines,[64] phenolate, dialkyl or diarylphosphite,[65] N-alkylcarbamoyldiphenylphosphine oxides,[66] alkoxides[67],[68] and nucleosides[69] yielding in one anionic species formed by the opening of the dioxane ring.[61]

Trying to synthesize high boron content polyanionic multicluster macromolecules, we studied the nucleophilic behavior of the mono- and di-lithiated salts of 1,2-*closo*-$C_2B_{10}H_{12}$, 1,7-*closo*-$C_2B_{10}H_{12}$ and 1,12-*closo*-$C_2B_{10}H_{12}$ isomers toward [3,3'-Co(8-$(CH_2CH_2O)_2$-1,2-$C_2B_9H_{10}$)(1',2'-$C_2B_9H_{11}$)].[70] It was concluded that mono- and di-litiated salts of 1,2-*closo*-, 1,7-*closo*- and 1,12-*closo*-$C_2B_{10}H_{12}$ isomers act as nucleophiles (Scheme 4) in the ring opening reaction of [3,3'-Co(8-$(CH_2CH_2O)_2$-1,2-$C_2B_9H_{10}$)(1',2'-$C_2B_9H_{11}$)] leading to: i) the monoanionic type species [1-X-2-R-1,2-*closo*-$C_2B_{10}H_{10}]^-$, (R= H, (**9**); CH_3, (**10**); C_6H_5; (**11**)); [1-X-1,7-*closo*-$C_2B_{10}H_{11}]^-$ (**12**) and [1-X-12-*closo*-$C_2B_{10}H_{11}]^-$ (**13**) and ii) the dianionic compounds [1,2-X_2-1,2-*closo*-$C_2B_{10}H_{10}]^{2-}$ (**14**), [1,7-X_2-1,7-*closo*-$C_2B_{10}H_{10}]^{2-}$ (**15**) and [1,12-X_2-1,12-$C_2B_{10}H_{10}]^{2-}$ (**16**), (where X= [3,3'-Co(8-$(CH_2CH_2O)_2$-1,2-$C_2B_9H_{10}$)(1',2'-$C_2B_9H_{11}$)]$^-$). These two sets of compounds contain both structural motifs, cobaltabisdicarbollide and *closo*-carborane within the same molecule.[61]

Even though the *closo* carborane clusters are structures showing high stability with respect to strong acids, they react with Lewis bases yielding more opened structures, known as *nido*, by a partial deboronation process that implies the loss of a B-H cluster's vertex. Several nucleophiles such as alkoxides,[71] amines,[72] fluorides,[73] phosphanes[74] have been used in the deboronation reaction. The nucleophilic attack takes place at one of the boron atoms directly bonded to both carbon atoms, the B(3) or its equivalent B(6), since they both present electronic deficiency. Scheme 5 shows that regioselective removal of one B-H vertex from 1,2-*closo*-$C_2B_{10}H_{12}$ cluster of the double cluster monoanion of type [1-X-2-R-1,2-*closo*-$C_2B_{10}H_{10}]^-$ species (where X= [3,3'-Co(8-$(CH_2CH_2O)_2$-1,2-$C_2B_9H_{10}$)(1',2'-$C_2B_9H_{11}$)]$^-$ and R= H, (**17**); CH_3 (**18**), C_6H_5, (**19**)) takes place by heating with ethanolic KOH to give a series of dianions [7-X-8-R-7,8-*nido*-$C_2B_9H_{10}]^{2-}$. As anticipated, the same degradation procedure applied to the dianionic triple-cluster compound

[1,2-X_2-1,2-*closo*-$C_2B_{10}H_{10}]^{2-}$ gave rise to the trianionic species [7,8-X_2-7,8-*nido*-$C_2B_9H_{10}]^{3-}$ (**20**), substituted at both carbon atoms of the eleven-vertex dicarborane cluster. The fact that these high boron content large molecules are polyanionic, makes them more soluble in water, and increases their potential for biological uses. The presence of *closo* or *nido* carborane subclusters permits a ready modification of these molecules by attaching variable substituents onto the carbon and boron vertices. This may add new properties to the boron clusters and, in fact, give rise to new species that can be used potentially in medicine as good candidates to improve the BNCT techniques' efficiency.[61]

1.2.- Neutral 1,2-*closo*-$C_2B_{10}H_{12}$ Carborane as Core through substitution at the boron vertices.

Keeping in mind the afore mentioned properties of carborane to be functionalized at the boron vertices, two families of *o*-carborane derivatives with precisely defined patterns of substitution have been built starting with the diiodinated (9,12-I_2-1,2-*closo*-$C_2B_{10}H_{10}$), (**21**), and tetra iodinated (8,9,10,12-I_4-1,2-*closo*-$C_2B_{10}H_8$), (**22**), *o*-carboranes (Chart 3b and Scheme 6). The cross coupling reaction with allylmagnesium chloride in the presence of [$PdCl_2(PPh_3)_2$] as catalyst and CuI as cocatalyst proceeded to completion after a few hours, yielding the di or tetra substituted derivatives (**23** and **24**, respectively) (Scheme 6).[75] The terminal olefinic groups are free to be further reacted. As an example for the development of these dendrimers, a hydroboration/oxidation reaction was carried out to transform the terminal double bonds to terminal hydroxyl groups giving compounds **25** and **26**. BH_3·THF was used as the hydroborating agent, resulting in a specific anti-Markovnikov process (Schemes 6). Later, the hydroxyl terminated arms, in a specific compact area of the cluster characterized by adjacent boron vertices, were coupled leading to a di and quadruped shaped structure, which might serve as a versatile dendritic, dendron or globular precursor macromolecules (Chart 3) containing multiple carborane or metallacarborane clusters at their periphery (Schemes 7 and 8).[75] The resulting arborol structures, comprising the pendant arms that end with reactive

organic groups, and residing at reactive vertices located on opposite sides of a central *o*-carborane core, can be envisaged as versatile precursors for dendritic growth.

Schemes 7 and 8 show that the esterification reaction of the di and tetra alcohols (compounds **25** and **26**,respectively) by organic acids or the click reaction on the di and tetra azides obtained from the tetra chloride derivative are possible. Further, the synthesis of the polyanionic dendron like molecules (**27** and **35**) containing metallabisdicarbollide at the periphery and carborane as a core in the molecule, was achieved.[75] Moreover, these borane cage subunits can be further modified by attaching different and varied substituents either on the cage carbon or boron vertices, which makes these structurally flexible compounds potential candidates for BNCT of cancer cells and HIV-PR inhibition.[76]

In addition, the presence of the two C_c-H on these Boron substituted *o*-carborane cluster allows their derivatization through coordination elements S or P providing the type of molecules shown in Figure 1 that can be fixed in surfaces such as gold nanoparticles (NPs), Magnetic nanoparticles (MNPs), Quantum Dots (QDs) or silica,… among others as reported by the parent *o*-mercaptocarborane 1-SH-1,2-*closo*-$C_2B_{10}H_{11}$ and *m*-carboranylphosphinate 1-OPH(OH)-1,7-*closo*-$C_2B_{10}H_{11}$ synthons (Figure 1).[77] An example of the C cluster derivatization of the 9,12-$(HOCH_2CH_2CH_2)_2$-1,2-*closo*-1,2-$C_2B_{10}H_{10}$ (**25**) compound was to employ the boron cluster for the modification of the physicochemical and biological properties of nucleic acids; this was made possible by designing conjugates of DNA oligonucleotides and oligofunctionalized boron clusters as building blocks for the construction of 2D and 3D nanoframeworks.[78] To reach this goal, two reactions were conducted. The first one was the protection of hydroxyl functions of dialcohol with acid labile trityl group (compound **25**) and then the functionalization of C_c-H vertices using the ring opening reaction method of lithiated carborane with ethylene oxide (Scheme 9)[79] obtaining 1-$HOCH_2CH_2CH_2$-9,12-$(TrOCH_2CH_2CH_2)_2$-1,2-*closo*-$C_2B_{10}H_9$ compound (**31**). To anchor this compound through the Carbon cluster on Controlled Porous Glass (borosilicate) and run Automated DNA synthesis, the terminal alcohol group was transformed to succinate (**43**) and

then into the *p*-nitrophenyl ester (**44**) as shown in Scheme 9. Subsequent condensation of the active ester with the primary amino groups of the long chain alkylamino-controled porous glass (LCA-CPG) provided the required modified solid support (Scheme 10a). The oligonucleotide synthesis on the modified LCA-CPG support was achieved by using standard phosphoramidite chemistry (Scheme 10b).[80] At the end of the automated DNA synthesis, the cleavage of the support and the phosphate deprotection of the oligonucleotide (**45**) was performed in 25% aqueous solution.

Another example is the substitution of the two C_c cluster vertices of di and tetra branched *o*-carborane to obtain the globular tetra branched and hexa branched *o*-carborane derivative as it will be described in the next section.

1.3.- Neutral 1,2-*closo*-$C_2B_{10}H_{12}$ Carborane as Core through substitution at both carbon and boron vertices.

The substitution of the two C_c cluster vertices of the terminal diallyl (**23**) and tetra allyl (**24**) branched *o*-carboranes by two allyl groups was achieved by the reaction of the corresponding dilitiated compounds with two equivalents of allylbromide. The globular tetra branched and hexaallyl branched *o*-carborane derivatives (**46** and **47**) were obtained as shown in Schemes 11 and 12.[81] The posterior hydroboration/oxidation reaction of the allyl groups provide the tetra 9,12-$(HOCH_2CH_2CH_2)_2$-1,2-$(HOCH_2CH_2CH_2)_2$-1,2-*closo*-1,2-$C_2B_{10}H_8$, (**48**) and hexa-alcohol 8,9,10,11-$(HOCH_2CH_2CH_2)_4$-1,2-$(HOCH_2CH_2CH_2)_2$-1,2-*closo*-1,2-$C_2B_{10}H_6$, (**49**), which react with four or six molecules of the zwitterionic compound [3,3'-Co(8-$(CH_2CH_2O)_2$-1,2-$C_2B_9H_{10}$)(1',2'-$C_2B_9H_{11}$)] by the well-known cycle opening reaction producing a new class of globular polybranched macromolecules that contain multiple anionic metallacarborane clusters at the *o*-carborane cluster periphery (compounds **50** and **51**, respectively).[81] These polyanionic globular high boron rich containing molecules, which are water soluble, were isolated as

tetramethylammonium salt. The reinforced electrostatic noncovalent interactions between anionic PEG-COSAN branches and the ammonium cation have been proved by ESI-MS.[81]

These new class of water soluble high boron rich containing globular polybranched macromolecules that contain multiple anionic metallacarborane clusters at the *o*-carborane periphery could be of interest for BNCT as well as for drug delivery.[81]

2.- Organic Cores to Obtain High Boron Content Decorated Dendrimers.

2.1.- Aryl-ether dendrons and 1,3,5-triarylbenzene as fluorescent cores.

The first set of *closo* and *nido* carborane containing "Fréchet type" dendrons were reported by our group in 2007,[82] followed by a second set published in 2011.[83] The neutral carboranyl-functionalized aryl-ether derivatives **52-55** were synthesized by the reaction of α,α'-bis(3,5-bis(bromomethyl)phenoxy-*p*-xylene or α,α'-bis(3,5-bis(bromomethyl)phenoxy-*m*-xylene with 4 equivalents of the monolithium salt of 1-R-1,2-*closo*-$C_2B_{10}H_{12}$ (R = CH_3, C_6H_5) (Scheme 13). Subsequently, *closo* clusters partial degradation was successfully achieved using an excess of KOH in ethanol at reflux for 20 h to achieve the respective *nido* carboranes, that were easily isolated as K^+ salts or precipitated by adding $[Me_4N]Cl$ to get the tetramethylammonium salts (**56-63** in Scheme 13).[61] Salts were soluble in polar solvents, such as EtOH, DMSO and acetone, but the potassium salts were also soluble in water. All compounds were characterized by IR, ^1H, ^{11}B and ^{13}C NMR, and UV-Vis spectroscopies, as well as elemental analyses to confirm the tetra substitution of the starting molecules.

Another set of boron rich dendrimers decorated with four and eight cobaltabisdicarbollide units (**64-67**) were obtained in moderate yields (41-62%) by the ring opening reaction of cyclic oxonium [3,3'-Co(8-$(CH_2CH_2O)_2$-1,2-$C_2B_9H_{10}$)(1',2'-$C_2B_9H_{11}$)] with the corresponding alkoxides, obtained from the deprotonation of terminal alcohols of different generations of poly(alkyl aryl-ether) dendrimers, such as α,α'-bis[3,5-bis(hydroxymehyl)phenoxy]-*p*-xylene, α,α'-bis[3,5-bis(hydroxymehyl)phenoxy]-*m*-xylene, α,α'-bis[3,5-bis-[3,5-

bis(hydroxymethyl)phenoxy]methylen]phenoxy]-*p*-xylene and α,α,'-bis[3,5-bis-[3,5-bis(hydroxymethyl)phenoxy]methylen]phenoxy]-*m*-xylene dendrimers.[84] Scheme 14 shows the synthesis of dendrimer **67** as one example. The best way to know if the reaction had been completed, is monitoring the $^{11}B\{^{1}H\}$ NMR spectra, since compound[3,3'-Co(8-$(CH_2CH_2O)_2$-1,2-$C_2B_9H_{10}$)(1',2'-$C_2B_9H_{11}$)] shows different ^{11}B resonances before and after the dioxane ring opening.

Another family of high boron content macromolecules are the carboranyl-terminal Fréchet-type poly(aryl-ether) dendrimers that contain 1,3,5-triphenylbenzene moiety as core, along with 9 substituted 1,2-*closo*-$C_2B_{10}H_{10}$ moieties at the periphery (Scheme 15).[85] For this purpose, two different sets of carboranyl-containing hydrosilylating agents were used to perform the functionalization of the starting dendrimers that incorporate nine allyl ether groups (Scheme 15). Regiospecific hydrosilylation reactions on the terminal allyl ether functions with both hydrosilylation agents, using a 9:1 ratio in the presence of Karstedt catalyst,[86] following with further purification by TLC, led to the corresponding Féchet-type dendrimers **69-72** (Scheme 15). One of the requirements to use compounds for biomedical applications is their biocompatibility and water solubility. With this purpose, polyanionic dendrimers **73** and **74** (Scheme 16) were prepared following the partial degradation method through nucleophilic attack on *closo* carboranes of the neutral dendrimers **71** and **72**, (Scheme 16). The corresponding polyanionic macromolecules functionalized with *nido* carboranes were isolated as Na^+ salts, which are soluble in water. These polyanionic dendrimers are "a priori" good candidates for exploring applications in boron delivery platforms.

Using also Fréchet-type poly(aryl-ether) cores, polyanionic dendrimers peripherally functionalized with three, six, or twelve terminal cobaltabisdicarbollide units were prepared in good yields.[61] Hydrosilylation reaction of the terminal allyl ether groups of the dendrimers with the Cs[1,1'-μ-$Si(CH_3)$H-3,3'-Co(1,2-$C_2B_9H_{10})_2$] derivative using 3:1, 6:1 and 12:1 ratios, in the presence of Karstedt catalyst, led to the formation of dendrimers **75**, **76** and **77**, respectively

(Scheme 17).[87] When we attempted to perform the hydrosilylation of dendrimer **68** in order to get the analogue to dendrimers **73** and **74**, but decorated with cobaltabisdicarbollide units, the complete functionalization was impossible to achieve. A Monte Carlo simulation confirmed the difficulty to functionalize this dendrimer due to steric hindrance caused by the bulky metallacarborane.[87]

2.2.- *meso*-Porphyrins as fluorescent cores.

More recently we have reported the synthesis of a set of boron enriched dendrimers, in which the *meso*-porphyrin is the core of the dendrimer whereas the branches are constructed by aryl-ether chains ending with eight, sixteen or thirty-two Me-*o*-carboranyl clusters (**78-84**) (Figure 2).[88] To obtain the desired β-(E) isomers, different generations of porphyrin-cored dendrimers bearing terminal allyl groups were functionalized with the corresponding carboranylsilane by hydrosilylation reactions using Karstedt's catalyst (see Scheme 18, as an example of synthesis of **83**). In all cases, binding of the carboranylsilane to the vinyl-and allyl- terminated dendrimers was monitored by ^{1}H NMR spectroscopy, tracing the vanishing of the alkene protons, as well as the new appearing resonances corresponding to -$SiCH_3$ and -CH_2- for the final dendrimers.

2.3. Photophysical properties of dendrimers

Closo Compounds **52-55** exhibited similar UV-Vis spectra with absorption maxima in the region 309–320 nm in THF, and 329–332 nm in acetone, whereas a red-shift of 10-20 nm for their respective *nido* species **56-63** was observed. Compounds **52-63** exhibited fluorescence emission under UV irradiation, with maxima λ_{em} in the range of 373–381 nm for Ph-*o*-carboranyl, and 363–370 nm for Me-*o*-carboranyl derivatives (Table 1).[82,83] Noticeably, the absorption and emission properties depend on the substituent (Ph or Me) linked to the adjacent C_c, the electronic nature of the cluster (*closo* or *nido*) and the solvent polarity. In general, for all species in any solvent, a red-shift of the emission was observed when the substituent is an electron-

acceptor phenyl group, whereas the emission for those compounds containing an electron-donating methyl group was exhibited at lower wavelengths. Then, the fluorescence emission could be modulated by introducing -Ph or -Me groups as substituents at the C_c of the carborane cluster.

Compounds **69-74** exhibited absorption maxima in the region of 266-269 nm (Table 2); these absorption wavelengths were insignificantly altered when changing the C_c substituents or the electronic nature of the cluster (*closo* and *nido*). These dendrimers showed fluorescence emission maxima at around 366 nm in THF solutions (Table 2), and no influence on the emission wavelengths was observed with the different electron-acceptor (Ph) or electron-donor (Me) substutituents at the adjacent C_c. In general, those dendrimers containing *closo* Me-*o*-carboranyl moieties displayed higher ϕ_F than those bearing Ph-*o*-carborane clusters, which is attributed to a partial charge transfer process from the donor group to the *closo* phenyl-carborane that acts as acceptor.[61],[89] The increase of the dendrimer size and the number of terminal carboranyl moieties imply a loss of fluorescence quantum efficiency (see Table 2). Polyanionic dendrimers exhibited lower $\phi_{F,}$ between 0.09 and 0.22, compared to the neutral ones.

Cobaltabisdicarbollide-containing dendrimers **75-77** show absorption bands in the range of 307-310 nm in acetonitrile, but contrary to the above carboranyl-containing poly(aryl-ether) dendrimers **69-74**, they did not show fluorescence, as a quenching of the fluorescence takes place after functionalization with the metallacarborane derivatives.

All the porphyrin-cored dendrimers **78-84** showed similar absorption and emission properties, which suggested that neither the increase of the dendrimer generation nor the number of peripheral Me-*o*-carboranyl units affect significantly their photophysical properties (Table 2). These dendrimers showed typical Soret bands in the range of 422-424 nm, Q_1-bands at 514-550 nm and Q_2 bands at 550-556 nm, in some cases blue-shifted 1-6 nm, in $CHCl_3$ solutions. The molar extinction coefficients (ε) are in the range of 2.40×10^5 and 4.30×10^5 $M^{-1}cm^{-1}$. The emission maxima for non-metallated dendrimers appeared between 649 and 657 nm, whereas two

emission bands are observed for zinc porphyrin-cored dendrimers, with maxima in the range of 596 and 604 nm (see Table 2).

All these neutral and anionic carboranyl functionalized poly(aryl-ether) dendrimers represent a family of fluorescent macromolecule with high boron content, making them good candidates as boron delivery agents for potential applications in BNCT.

3.- Octasilsesquioxane Cube as Core for Radial Growing to get Boron Rich Macromolecules.

Carboranyl-containing cage-like octasilsesquioxane (POSS) structures (**85** and **86**) were prepared in high yields following two different routes:[90] i) the hydrolytic process based on hydrolysis and condensation of the corresponding carboranylalkylethoxysilane precursors and the nonhydrolytic route based on the specific reactivity of carboranylalkylchorosilane toward DMSO as oxygen source (Scheme 19).[91] Partial degradation of the *closo* carborane clusters in compounds **85** and **86** with KOH/EtOH lead to the respective octaanionic derivatives that were isolated as tetramethylammonium salts (**87** and **88**).[90]

Another set of carboranyl-containing octasilsesquioxanes (**89-91**) were synthesized in high yields via olefin cross-metathesis reaction,[92] between the octavinylsilsesquioxane (OVS) and several carboranyl-styrene derivatives, using the Grubbs' catalyst (1st generation) (Scheme 20a).[93]

Carboranyl-containing octasilsesquioxane hybrids **92-94** were prepared in moderate yield, by Heck coupling reaction of octa(*p*-bromostyrenyl)silsesquioxane (*p*-BrStyrenylOS)[92b] with carboranyl-styrene derivatives,[93] using N,N-dicyclohexylmethylamine (NCy_2Me) as base and [$Pd(^tBu_3P)_2$] and [$Pd_2(dba)_3$] as co-catalysts (Scheme 20b). The same reaction was carried out to synthesize compound **95** that ends with eight Ph-*m*-carboranyl units.[94]

Furthermore, two octasilsesquioxane-based hybrids decorated with metallacarborane derivatives (**96-97**) were synthesized via cross-metathesis reaction (Scheme 21).[95] Following the afore mentioned oxonium ring opening reaction, compounds [3,3'-Co(8-$(CH_2CH_2O)_2$-1,2-

$C_2B_9H_{10}$)(1',2'-$C_2B_9H_{11}$)] and [3,3'-Fe(8-(CH_2CH_2O)$_2$-1,2-$C_2B_9H_{10}$)(1',2'-$C_2B_9H_{11}$)] bearing a terminal styrene group were synthesized by using the deprotonated 4-vinylphenol as the nucleophile. Cross-metathesis reactions of these two compounds with OVS were performed in the presence of the first generation of Grubbs's catalyst to give E-isomers of hybrids **96** and **97** in 83 % and 45 % yield, respectively (Scheme 21). The reactions were monitored by ^{1}H NMR upon the total disappearance of the vinyl proton resonances from the Si-CH=CH_2.

Compounds **89-91** showed maxima absorption values at around 262 nm and emission maxima in the region between 340 and 480 nm in CH_2Cl_2, with very large Stoke's shifts of 14010-11140 cm^{-1} (152-110 nm). POSS compound **89** exhibited the highest fluorescence quantum yield of 44%, in comparison with their counterparts **90** having 9% and **91** having 2%. This was attributed to the effect of the POSS cage, which acts as an organizing scaffold, causing restriction of the intramolecular movement of the arms and avoiding additional interactions between them. These results were corroborated by TD-DFT calculations, which supported the fact that no quenching of the fluorescence had occurred due to an intramolecular electron transfer process. Hybrids **92-94** showed vibronically structured UV-Vis absorption and emission spectra in CH_2Cl_2, with maxima absorption and emission of around 338 nm and 391 nm, respectively. All the compounds showed high molar absorption coefficients ($29.2x10^4$ - $58.1x10^4$ $M^{-1}cm^{-1}$) and fluorescent quantum yields in solution (24% – 59%); the highest value was the one that corresponds to hybrid **92**, which contains *o*-carborane units without substituents at the adjacent C_c atom. On the other hand, a noticeable quenching of the fluorescence was observed in solid state attributed to intermolecular interactions, where absolute Φ_F values of 4-7 % were obtained.

Compound **96** showed the redox potential, near -1.74 V *vs* Fc ($Co^{3+/2+}$ in cobaltabisdicarbollide); whereas for compound **97** the pair appeared around -0.74 V ($Fe^{3+/2+}$ from ferrabisdicarbollide).[95] Despite **96** and **97** containing eight metallacarboranes each, they exhibited only one redox process in the CV, which indicated that all units undergo the redox

process simultaneously while acting independently, so that there is no electronic communication between the electro-active parts.

4.- Biomedical studies of cobaltabisdicarbollide.

Boron, the fifth element in the periodic table has been found to be an essential element for animals and humans, and possesses a broad spectrum of biological activities. In the last few years, there is an increasing interest in possible medicinal application of boron and boron compounds in the chemotherapy for some forms of cancer cells with high malignancy and of inoperable cancer cells.[96] Commercial boron-based drugs are still rare. Bortezomib (anti-cancer drug for multiple myeloma and mantle cell lymphoma and the first therapeutic proteasome inhibitor to be used in humans), tavaborole (AN2690) (to treat fungal or yeast infections of the toenails), crisaborole (AN2728) (to relieve redness, itching, swelling caused by mild to moderate eczema), epetraborole (AN3365) (used in clinical trials studying the treatment of bacterial (intestinal, urinary tract or community-acquired) infections) and SCYX-7158 (AN5568) (an antiprotozoal drug nowadays under clinical assays of sleeping sickness), 4-(dihydroxyboryl)phenylalanine (BPA) and sodium mercapto-undecahydro-*closo*-dodecaborate (BSH) are used as drugs; the last two compounds are used in boron neutron capture therapy (BNCT). All of these boron-containing drugs are derivatives of boronic acids except BSH, that has an anionic boron cluster.

In 2005, the first studies of the anionic [3,3'-Co(1,2-$C_2B_9H_{11})_2]^-$ metallacarborane and some PEG derivatives as specific and potent inhibitors of HIV protease[97] were reported. Later, it was proven that these metallacarborane compounds were potential drugs to overcome antiviral resistance.[98]

4.1.- Self-assembling of H[3,3'-Co(1,2-$C_2B_9H_{11})_2$] and H[8,8'-I_2-3,3'-Co(1,2-$C_2B_9H_{10})_2$] in aqueous solution.

Our group reported in 2011 the unique property of the protonated salt of the cobaltabisdicarbollide, H[3,3'-Co(1,2-$C_2B_9H_{11}$)$_2$], to produce monolayer nano-vesicles of about 20 nm radius in diluted water solutions (concentration range 1-13 mM).[99] When increasing the concentration, nano-vesicles and micelles coexist. The radius of the nano-vesicles increases to 80-890 nm when adding the saline solution. It is very important to emphasize that these nano-vesicles are monolayer in contrast to liposomes and natural membranes that are bilayer. Later, the unique property of the protonated salt of the diiodo-cobaltabisdicarbollide, H[8,8'-I_2-3,3'-Co(1,2-$C_2B_9H_{10}$)$_2$], to produce planar monolayer lamellar membranes with water layers between at a concentration in water above 130 mM at ambient temperature was reported.[100] It was suggested that dihydrogen B-H ··· H-C_c bonds have a major role in the formation of self-assemblies. Recently, we have reported that $^{11}B\{^1H\}$-NMR spectroscopy is an excellent probe to visualize the phase transition between nano-vesicles/monomer and micelles/monomer and that $^1H\{^{11}B\}$-NMR spectra provides complementary information in the dihydrogen B-H ··· H-C_c bonds formation.[101] Additionally, to enlighten on the interactions between adjacent metallabisdicarbollide clusters, DFT and QTAIM computational analysis that proved the intramolecular interactions were run on [3,3'-Co(1,2-$C_2B_9H_{11}$)$_2$]$^-$ and [8,8'-I_2-3,3'-Co(1,2-$C_2B_9H_{10}$)$_2$]$^-$.[101]

4.2.- Purely inorganic monolayer nano-vesicles, H[3,3'-Co(1,2-$C_2B_9H_{11}$)$_2$] and H[8,8'-I_2-3,3'-Co(1,2-$C_2B_9H_{10}$)$_2$], crossing lipid bilayer membranes.

With the former knowledge, we wanted to know if these unique [3,3'-Co(1,2-$C_2B_9H_{11}$)$_2$]$^-$ monolayer membranes interact with natural membranes.[102] First, we studied the transport of metallabisdicarbollides (H[3,3'-Co(1,2-$C_2B_9H_{11}$)$_2$], Na[3,3'-Co(1,2-$C_2B_9H_{11}$)$_2$] and Na[8,8'-I_2-3,3'-Co(1,2-$C_2B_9H_{10}$)$_2$]) amphiphilic anions within planar phospholipidic bilayer membranes, that were prepared by using the Montal Mueller technique, and were analyzed using planar lipid bilayer electrophysiology.[103] The experimental protocol of this study is as follows: Once the

planar lipid bilayer was formed, the metallabisdicarbollide compound was added to the feeding side of the chamber. A current, which was measured by means of Vclamp technique, due to the transport of the anions was recorded for several minutes or hours. At the end of the experiment, the metallabisdicarbollide anion at the stripping solution that has crossed the bilayer membrane was analyzed. The concentration of metallabisdicarbollide was determined from the concentration of boron by inductively coupled plasma mass spectrometry (ICP-MS) measurements. Performing these experiments at different initial concentrations and experimental times, the metallabisdicarbollide transport through synthetic lipid membranes was confirmed and the kinetics of the process studied.[102] Lipid composition does not influence $[3,3'\text{-}Co(1,2\text{-}C_2B_9H_{11})_2]^-$ transport rate, as no significant permeation differences were seen for model membranes of neutral lipid composition that mimic either prokaryotic (DPhPC: 1,2-diphytanoyl-sn-glycero-3-phosphocholine,) or eukaryotic (1,2-dioleoyl-sn-glycero-3-phosphocholine, DOPC) cell membranes. But, a slight reduction of the metallabisdicarbollide anion transport rate was observed when the negatively charged membranes DOPC/DOPS (4:1) were used; DOPS is the anionic dioleoylphosphatidylserine lipid that mimics the surface charge density of a typical plasma membrane. These results revealed unexpected properties at the interface of biological and synthetic membranes.[102]

To directly visualize the transferring behavior of the monolayer nano-vesicles of $[3,3'\text{-}Co(1,2\text{-}C_2B_9H_{11})_2]^-$ through artificial bilayer membranes, mixtures of $[3,3'\text{-}Co(1,2\text{-}C_2B_9H_{11})_2]^-$ nano-vesicles and liposomes' solutions, were examined using cryo-TEM.[102] Figure 3 displays the interaction between $[3,3'\text{-}Co(1,2\text{-}C_2B_9H_{11})_2]^-$ vesicles and liposomes.

4.3.- Interaction of purely inorganic monolayer nano-vesicles, $H[3,3'\text{-}Co(1,2\text{-}C_2B_9H_{11})_2]$ and $H[8,8'\text{-}I_2\text{-}3,3'\text{-}Co(1,2\text{-}C_2B_9H_{10})_2]$, with membrane cells.

Then, we studied the interaction of the purely inorganic membranes, $[3,3'\text{-}Co(1,2\text{-}C_2B_9H_{11})_2]^-$, $[3,3'\text{-}Fe(1,2\text{-}C_2B_9H_{11})_2]^-$ and $[8,8'\text{-}I_2\text{-}3,3'\text{-}Co(1,2\text{-}C_2B_9H_{10})_2]^-$, with living cells. To achieve it,

biological *"in vitro"* studies with different types of cells: Amoeba cells, Mammalian healthy and cancerous cells and bacteria were undertaken.[104] It was observed that for each concentration examined, metallabisdicarbollide compounds had no immediate effect on cell viability, with cells showing no signs of membrane disruption. However, after more than 5 hours blocked cell proliferation with ED_{50} values between 99-157 µM depending on the cells did occur (Table 3); the cells fully recovered in hours to days when metallabisdicarbollide is removed.

Dictyostelium amoeba cells, which are eukaryotic cell evolutionarily close to animal cells but lacking caspase-mediated apoptosis,[105] were chosen to carry on the studies to prove the effect of $[3,3'\text{-}Co(1,2\text{-}C_2B_9H_{11})_2]^-$ and $[8,8'\text{-}I_2\text{-}3,3'\text{-}Co(1,2\text{-}C_2B_9H_{10})_2]^-$ on cell growth. The same number of cells were incubated in three different media: One in the absence of boron metallabisdicarbollide compounds, the second one containing 500 µM of $[3,3'\text{-}Co(1,2\text{-}C_2B_9H_{11})_2]^-$ and the third one containing the same concentration of $[8,8'\text{-}I_2\text{-}3,3'\text{-}Co(1,2\text{-}C_2B_9H_{10})_2]^-$.[104]

As shown in Figure 4, cells grew only in the absence of Boron compounds. After six days, the cells from the three experiments were isolated, washed and re-incubated within a media in the absence of Boron compounds; it can be seen that cells that had been previously in the media containing $[3,3'\text{-}Co(1,2\text{-}C_2B_9H_{11})_2]^-$ start proliferation on the 9th day. On 11th and 17th days, cells were once again isolated, washed and re-incubated within a media in absence of Boron compounds and it was observed that the cells that had been in contact with $[8,8'\text{-}I_2\text{-}3,3'\text{-}Co(1,2\text{-}C_2B_9H_{10})_2]^-$ start growing on the 16th day. Remarkably, metallabisdicarbollide compounds display cytostatic effect that is reversed after removal of the drug from the culture medium and cells resume their growth and proliferation. The $[3,3'\text{-}Co(1,2\text{-}C_2B_9H_{11})_2]^-$ modification by bonding two iodo atoms increases cellular potency (Figure 4 and Table 3). *Dictyostelium* cell recovery after $[8,8'\text{-}I_2\text{-}3,3'\text{-}Co(1,2\text{-}C_2B_9H_{10})_2]^-$ treatment takes longer than $[3,3'\text{-}Co(1,2\text{-}C_2B_9H_{11})_2]^-$ and is dose-dependent, suggesting a stronger interaction with its cellular targets. In addition, the monoanionic and dianionic metallacarboranes displayed in Figure 5 were tested on the more sensitive *Dictyostelium* cells. Substitution of cobalt for iron as the central metal, [3,3'-Fe(1,2-

$C_2B_9H_{11})_2]^-$, made no major difference to compound potency. However, methylation of [3,3'-Co(1,2-$C_2B_9H_{11})_2]^-$, or linking two [3,3'-Co(1,2-$C_2B_9H_{11})_2]^-$ clusters via a PEG chain decreased potency on the cells.

When tested on mammalian cell cultures, again [8,8'-I_2-3,3'-Co(1,2-$C_2B_9H_{10})_2]^-$ was more potent than [3,3'-Co(1,2-$C_2B_9H_{11})_2]^-$.[104] In addition, the influence of different biocompatible cations: Li^+ and Na^+ salts of [3,3'-Co(1,2-$C_2B_9H_{11})_2]^-$, (ED_{50} values were 2.5 and 2.6 μM, respectively); Li^+ and Na^+ salts of [3,3'-Fe(1,2-$C_2B_9H_{11})_2]^-$, (ED_{50} values were 3.2 and 3.1 μM, respectively); H^+ and Na^+ salts of [8,8'-I_2-3,3'-Co(1,2-$C_2B_9H_{10})_2]^-$, (ED_{50} values of both salts was 1.8 μM) were tested, but no significant differences in the effects on cells were found. Consequently, from here on, all biological tests were carried out with Na^+ as the cation of the anionic purely inorganic boron based [3,3'-Co(1,2-$C_2B_9H_{11})_2]^-$ and its derivatives.[104]

4.4.- Visualization of anionic boranes by Raman Spectroscopy and fluorescence.

The presence of the metallacarboranes inside/outside the *Dictyostelium* cells and their drug quantification was visualized by Raman Spectroscopy monitoring the frequency about 2550 cm^{-1} that corresponds to the B-H stretching.[106] The ν(B-H) bonds appear in the range 2500-2600 cm^{-1}; in this very specific region at the Raman and Infrared spectroscopies no other characteristic frequencies of organic compounds resonate. The Raman Microscopy images (Figure 6) clearly showed the presence of the [3,3'-Co(1,2-$C_2B_9H_{11})_2]^-$ within the cytoplasm and to a lesser extent in the nucleus.[104],[106]

The chemical stability of metallabisdicarbollides, [3,3'-Co(1,2-$C_2B_9H_{11})_2]^-$ and [8,8'-I_2-3,3'-Co(1,2-$C_2B_9H_{10})_2]^-$, after being removed from *Dictyostelium* cells was proven by comparison of the MALDI-TOF-MS spectrum of the culture media with the pure metallabisdicarbollide.[104] Although boron clusters share many properties with organic drugs, they are inorganic and therefore not metabolized by cellular enzymes. This makes them attractive candidates for medicinal applications.

Our interest in the development of new boron delivery systems to be used for biological applications, led us to prepare a family of fluorescent organotin compounds that could be good candidates as nucleoli and cytoplasmatic markers *in vitro*.[107] These organotin compounds are based on 4-hydroxy-N'-((2-hydroxynaphthalen-1-yl)methylene)benzohydrazidato that was derivatized to contain $[B_{12}H_{12}]^{2-}$ (**98, 99**) and [3,3'-Co(1,2-$C_2B_9H_{11})_2]^-$ (**100, 101**) following the afored mentioned oxonium ring opening reaction (Scheme 22). These compounds showed photoluminescence properties in solution with quantum yields in the range 24% - 49%, being lower for cobaltabisdicarbollide derivatives. Remarkably, the linking of boron clusters to the tin complexes made them more soluble in the culture media and more readily available for cellular uptake, being internalized by the cells, as they do not aggregate either on the cells surface nor in the extracellular media. Mouse melanoma B16F10 cells were incubated at 10 μg/mL of the different compounds for 2 h and then analysed by confocal laser microscopy. Noticeable different staining effect was observed depending on the type of boron cluster attached to the organotin complexes; compounds bearing the cobaltabisdicarbollide anion showed an important fluorescence in the cytoplasm, whereas those bearing $[B_{12}H_{12}]^{2-}$ produced extraordinary nucleoli and cytoplasmic staining (Figure 7a). The remarkable fluorescence staining properties of these organotin compounds in B16F10 cells make them excellent candidates for fluorescent bioimaging *in vitro*.

Another set of compounds designed as fluorescent dyes for cells are the BODIPY-anionic boron cluster conjugates bearing $[B_{12}H_{12}]^{2-}$ (**102**, **103**), [3,3'-Co(1,2-$C_2B_9H_{11})_2]^-$ (**104**, **105**), and [3,3'-Fe(1,2-$C_2B_9H_{11})_2]^-$ (**106**) anions. These conjugates were readily synthesized from the *meso*-(4-hydroxyphenyl)-4,4-difluoro-4-bora-3a,4a-diaza-*s*-indacene (BODIPY) by ring opening reaction (Scheme 23).[108] The luminescent properties of the BODIPY were not significantly altered by the linking of the anionic boron clusters, showing emission fluorescent quantum yields in the range of 3-6 %. Moreover, the cytotoxicity and cellular uptake of compounds **102-106** were analyzed *in vitro* at different concentrations of B (5, 50 and 100 μg B/ml) using HeLa cells. None of the

compounds showed cytotoxicity at the lowest concentration (5 µg B/ml); compound **103** bearing $[B_{12}H_{12}]^{2-}$ and Na^+ as cation was non cytotoxic at any concentration, while the other compounds showed toxicity at the highest concentrations. The percentage of living cells incubated with compound **102** decreased with the concentration, being 60% and 35% of cell viability at 50 and 100 µg B/ml, respectively. On the contrary, the percentage of viability was lower than 17% and 5% for cells incubated with 50 and 100 µg B/ml of compounds **104-106**, respectively. In general, compounds **102-106** are better internalized by cells than the starting nonfunctionalized BODIPY. The internalization efficiency for all the compounds was assessed at the lowest concentration (5 µg B/ml), in which they are not cytotoxic; remarkably compounds **104-106** were successfully internalized by cells, exhibiting a strong cytoplasmic stain (Figure 7b). The exceptional cellular uptake and intracellular boron release, together with the fluorescent and biocompatibility properties make compounds **104** and **105** good candidates for *in vitro* cell tracking.

4.5.- $[3,3'\text{-}Co(1,2\text{-}C_2B_9H_{11})_2]^-$ as a molecular platform for "*in vivo*" imaging.

In the previous section, we have demonstrated that the *in vitro* cell culture studies indicate that $[3,3'\text{-}Co(1,2\text{-}C_2B_9H_{11})_2]^-$ and its derivatives accumulate within cells. This raises the question of whether $[3,3'\text{-}Co(1,2\text{-}C_2B_9H_{11})_2]^-$ based molecules can distribute and accumulate in organs and tissues, which is particularly important for use in BNCT. The large number of cluster vertices in $[3,3'\text{-}Co(1,2\text{-}C_2B_9H_{11})_2]^-$ offers a unique core for the construction of poly branched macromolecules that might convert the cluster in multifunctional molecules. In addition, the stability of the 3D rigid scaffold might be amalgamated with the capacity to functionalize the different vertices with different functional terminations (fluorescent dyes, radiopharmaceuticals, Magnetic Resonance Imaging (MRI) contrast agents, drugs, targeting ligands, etc.) to provide multi-modal treatments, i.e. diagnosis + therapy (chemo + radio + BNCT + photodynamic) in addition to performing as drug delivery nanocarriers. It can be foreseen that the treatment would speed up while diminishing secondary effects.

With the aim to generate mixed-doubly functionalized [3,3'-Co(1,2-$C_2B_9H_{11}$)$_2$]$^-$ derivatives in mind, we designed the synthesis of new bi-functional (iodine and polyethylene glycol, PEG) [3,3'-Co(8-I-1,2-$C_2B_9H_{10}$)(8'-PEG-1',2'-$C_2B_9H_{10}$)]$^-$ derivative and its unprecedented radiolabelling with either ^{125}I (gamma emitter) or ^{124}I (positron emitter) *via* palladium catalyzed isotopic exchange reaction (Scheme 24).[109] Incorporation of ^{125}I and ^{124}I enabled the determination of the biodistribution pattern of the radiolabeled cobaltabisdicarbollide species by using dissection/gamma counting and real-time, "*in vivo"* and noninvasive imaging (PET-CT), respectively. Comparison with its parent [3,3'-Co(8-I-1,2-$C_2B_9H_{10}$)(1',2'-$C_2B_9H_{11}$)]$^-$, was also carried out.

The labelled [3,3'-Co(8-$^{124/125}$I-1,2-$C_2B_9H_{10}$)(1',2'-$C_2B_9H_{11}$)]$^-$ derivatives were intravenously administered to mice and their bio distribution was investigated. There was a rapid accumulation of [3,3'-Co(8-^{125}I-1,2-$C_2B_9H_{10}$)(1',2'-$C_2B_9H_{11}$)]$^-$ in lungs and liver over 2 hours, matched by a decrease in blood content over the same time period. There was a lower accumulation in heart, kidneys, spleen and stomach over the same time period. Independently, [3,3'-Co(8-^{124}I-1,2-$C_2B_9H_{10}$)(1',2'-$C_2B_9H_{11}$)]$^-$ was administered to mice and then followed using Positron Emission Tomography (PET). Again accumulation was observed in lung, heart, kidneys, liver and stomach. Furthermore, synthesis of a new bi-functional (iodine and PEG) [3,3'-Co(8-$^{124/125}$I-1,2-$C_2B_9H_{10}$)(8'-PEG-1',2'-$C_2B_9H_{10}$)]$^-$ derivative (Scheme 24), which would allow further functional derivatization, was tested and found to have the same distribution as [3,3'-Co(8-^{124}I-1,2-$C_2B_9H_{10}$)(1',2'-$C_2B_9H_{11}$)]$^-$.[109]

These results demonstrate that, as suggested from *in vitro* experiments, [3,3'-Co(1,2-$C_2B_9H_{11}$)$_2$]$^-$ and its derivatives can accumulate in tissues within the body, offering a means to both deliver and track compounds for BNCT. Interestingly, the *in vivo* studies did not show accumulation of radioactivity in the thyroid gland, suggesting the stability of both [3,3'-Co(8-^{124}I-1,2-$C_2B_9H_{10}$)(1',2'-$C_2B_9H_{11}$)]$^-$and [3,3'-Co(8-^{124}I-1,2-$C_2B_9H_{10}$)(8'-PEG-1',2'-$C_2B_9H_{10}$)]$^-$ derivatives.

Due to the non-invasive nature of PET imaging, this unprecedented radiolabelling of [Co(8-I-$C_2B_9H_{10}$)($C_2B_9H_{11}$)]$^-$ with ^{124}I and ^{125}I should be suitable for the radiolabelling of specifically targeted [3,3'-Co(1,2-$C_2B_9H_{11}$)$_2$]$^-$ derivatives, enabling their evaluation *in vivo* and facilitating translation into the clinical setting shortening the time from bench to bed for boron carrier drugs.

4.6.- Antimicrobial activity of [3,3'-Co(1,2-$C_2B_9H_{11}$)$_2$]$^-$ derivatives.

Boron compounds (boronic acids, boron heterocycles, etc.) are reported to be promising antibacterials and antifungal agents.[5] Medical treatment for some microbial illnesses is complicated nowadays by the appearance of new multiresistant strains, and therefore, a new class of highly selective antimicrobial boron containing compounds could be necessary.[110]

Towards this aim, a series of [3,3'-Co(1,2-$C_2B_9H_{11}$)$_2$]$^-$ derivatives (Figure 8) were screened to evaluate their putative antimicrobial properties *in vitro* for their minimum inhibitory concentration (MIC) against Gram-positive and -negative bacteria.[111] Pure cultures of 16 pathogenic bacterial strains (isolated from animals and humans as well as control strains) and 3 strains of Candida *spp* were applied in antimicrobial studies that were performed by the agar-diffusion method of Bauer-Kirby and the method of minimum inhibitory concentrations. The obtained results revealed that among the compounds examined Na[3,3'-Co(8-RO(CH_2CH_2O)$_2$-1,2-$C_2B_9H_{10}$)(1',2'-$C_2B_9H_{11}$)] R= CH_3CH_2- and -CO-(2-OH-C_6H_4) exhibited the highest antimicrobial activity that was equal or even higher than those of the commercially available broad-spectrum antibiotic, thiamphenicol. The cobaltabisdicarbollide H[3,3'-Co(1,2-$C_2B_9H_{11}$)$_2$] was shown to express comparatively lower antibacterial and antifungal properties as compared to its derivatives. From a practical point of view it is important to emphasize that the Methicillin-resistant strain of *Staphylococcus aureus* (TSA MRSA), the poly resistant strains of *Pseudomona aeruginosa*, as well as of *Candida spp*., are sensitive to the compounds Na[3,3'-Co(8-RO(CH_2CH_2O)$_2$-1,2-$C_2B_9H_{10}$)(1',2'-$C_2B_9H_{11}$)] R= CH_3CH_2- and -CO-(2-OH-C_6H_4). Tables 4 and 5

shown the minimum inhibitory concentration (MIC_{50}) and (MIC_{50}), respectively, of some cobaltabisdicarbollide complexes on pathogenic microorganisms (Gram-positive and Gram-negative pathogenic bacterial strains and on Candida *spp*.) versus wide-spectrum antibiotic thiamphenicol (used as positive control).[111]

The effect of cobaltabisdicarbollide complexes displayed in Figure 8 on the viability and proliferation of cultured Madin-Darby bovine kidney cells (MDBK) were studied and their results shown in Table 6. Cytotoxicity concentration (CC_{50}) for each compound was determined by thiazolyl blue tetrazolium bromide test (MTT) and neutral red uptake cytotoxicity assay (NR) after 72 h of treatment. All data points represent an average of three independent assays.[111] Recently, it has been reported that $[3,3'\text{-}Co(8\text{-}CH_3CH_2O)_2\text{-}1,2\text{-}C_2B_9H_{10})(1',2'\text{-}C_2B_9H_{11})]^-$ has a high bacteria-killing efficiency observed with eradication of all TSA MRSA cells within 30 min.[112] More importantly, unlike the vancomycin antibiotic, a repeated treatment with $[3,3'\text{-}Co(8\text{-}CH_3CH_2O)_2\text{-}1,2\text{-}C_2B_9H_{10})(1',2'\text{-}C_2B_9H_{11})]^-$ would not induce drug resistance even after 20 passages of TSA MRSA. The mechanistic study showed that $[3,3'\text{-}Co(8\text{-}CH_3CH_2O)_2\text{-}1,2\text{-}C_2B_9H_{10})(1',2'\text{-}C_2B_9H_{11})]^-$ kills TSA MRSA by inducing an increase in the reactive oxygen species (ROS) production and consequentially inducing irreversible damage to the cell wall/membrane, which ultimately leads to the death of TSA MRSA. These results suggested that $[3,3'\text{-}Co(8\text{-}CH_3CH_2O)_2\text{-}1,2\text{-}C_2B_9H_{10})(1',2'\text{-}C_2B_9H_{11})]^-$ may be used as a promising antimicrobial therapeutic agent against TSA MRSA infections in future clinical practices.

Conclusions

In this review, we report on the results from our laboratories based on the radial growing of different cores to obtain borane decorated macromolecules at the periphery, which achieve high boron content. The families of compounds described in section 1 are based on the unique geometry and precise steric structure of the 1,2-*closo*-$C_2B_{10}H_{12}$ cluster that has the potential for the incorporation of many radial substituents at the carbon, at the boron and both at the carbon

and boron vertices. This cluster is an innovative building block or platform for the design of novel globular large molecules that cannot be achieved with organic hydrocarbon compounds. Section 2 covers a compilation of different type of poly(aryl-ether) dendrimers grown from various cores, such as Fréchet-type dendrons, 1,3,5-triarylbenzene or *meso*-porphyrins, which have been decorated with boranes to attain rich boron-content macromolecules. In Section 3, octasilsesquioxane cubes (POSS) have been used as core for its radial growth to get boron rich large molecules. The most relevant photophysical and electrochemical properties of these borane containing dendrimers and POSS hybrids have also been reviewed. The unique properties of cobaltabisdicarbollide cluster such as: i) self-assembly in water to produce monolayer nano-vesicles, ii) crossing lipid bilayer membranes, iii) interacting with membrane cells, iv) facilitating its visualization within cells by Raman and fluorescence techniques and v) their use as molecular platform for "*in vivo*" imaging are discussed in detail in section 4.

Based on the biological properties of the small anionic cobaltabisdicarbollide molecules reported here, it can be foreseen that the periphery decorated highly boron rich polyanionic borane macromolecules may have a promising future in medicinal applications such as BNCT agents or as drug delivery systems. Research in this direction is undergoing in our laboratories.

Conflict of Interest

The authors have no relevant affiliations or financial involvement with any organization or entity with a financial interest in or financial conflict with the subject matter or materials discussed in the manuscript apart from those disclosed. This includes employment, consultancies, honoraria, stock ownership or options, expert testimony, grants or patents received or pending, or royalties. No writing assistance was utilized in the production of this manuscript.

Acknowledgements

This work has been supported by the Spanish Ministerio de Economía y Competitividad (MINECO, project CTQ2016-75150-R) and Generalitat de Catalunya (2017 SGR 1720).

Chart 1. Icosahedral borane and heteroboranes with their vertex numbering: dianionic *closo* $[B_{12}H_{12}]^{2-}$ borane, neutral *closo* *o*-$C_2B_{10}H_{12}$ carborane and metallacarboranes [3,3'-M(1,2-$C_2B_9H_{11})_2]^-$, M= Co(III); Fe(III).

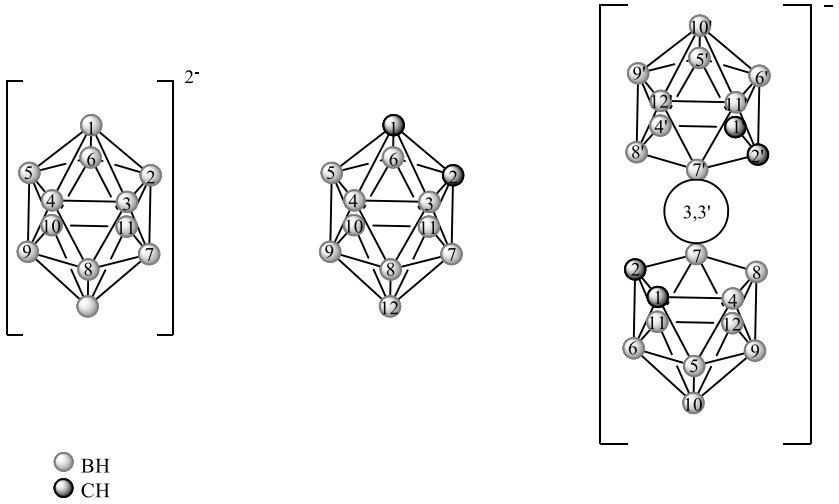

Chart 2. The isomers of the *closo*-$C_2B_{10}H_{12}$: *ortho*- (1,2), *meta*- (1,7), or *para*- (1,12); as well as *nido*-$[C_2B_9H_{12}]^-$ isomers: *ortho*- (7,8) and *meta*- (7,9).

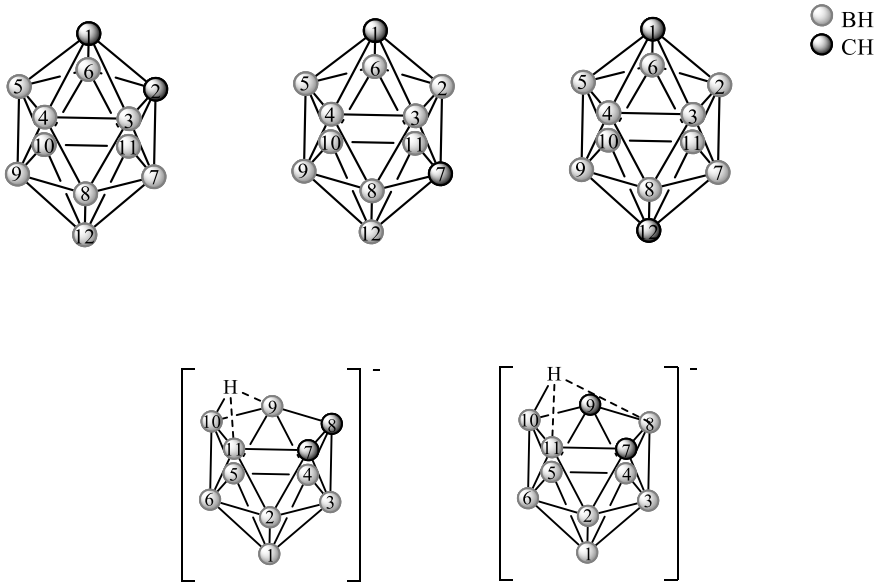

Chart 3.- Schematic representation of the different *o*-carborane branched families: (a) two branches at the C_c vertices (e.g. compounds **9**-**20**); (b) two and four branches at the highly compact B vertices (e.g. compounds **23**, **25**, **27**-**34** and compounds **24**, **26**, **36**-**42**, respectively); (c) multibranched at both C_c and B vertices (e.g. compounds **31**, **43**-**51**).

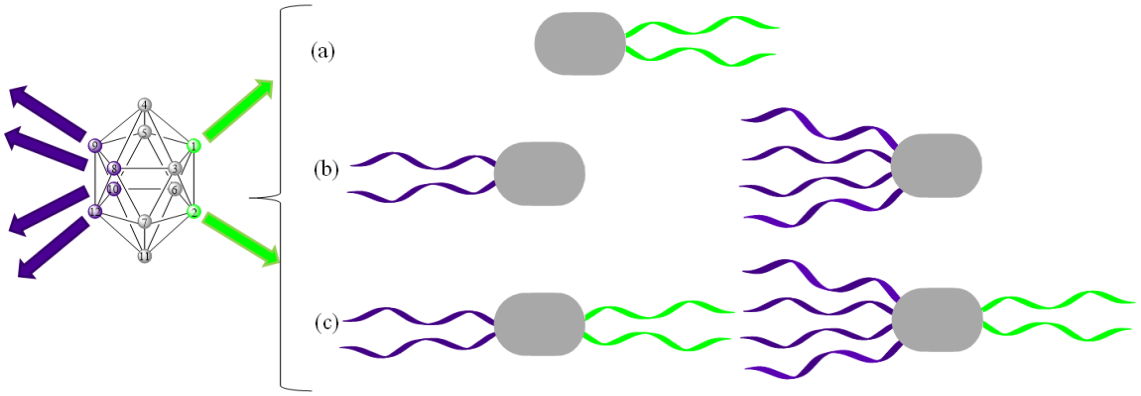

Figure 1.- Compact packing of 3D icosahedral carborane molecules stabilizing gold NPs, MNPs and QDs.

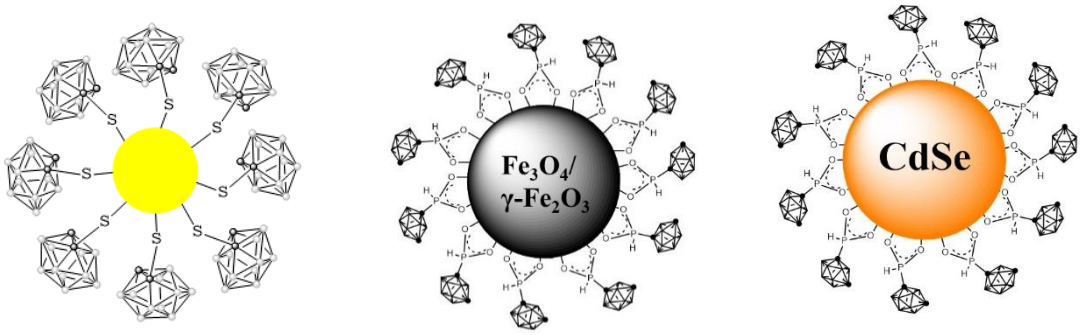

Figure 2. Different generations of high boron rich porphyrin-cored aryl-ether dendrimers.

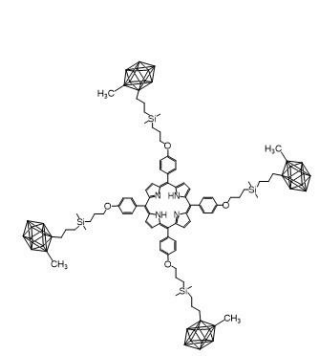

78

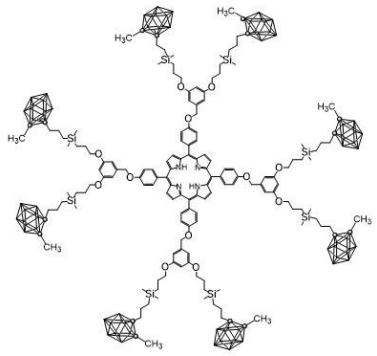

79

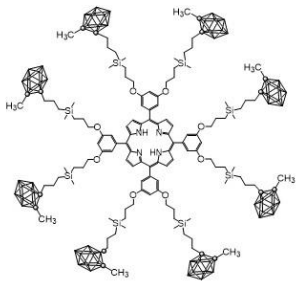

80

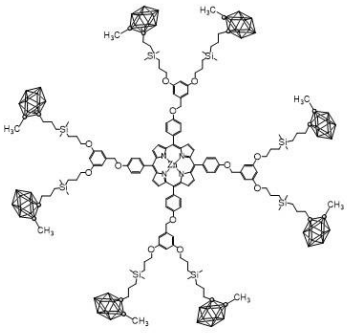

81

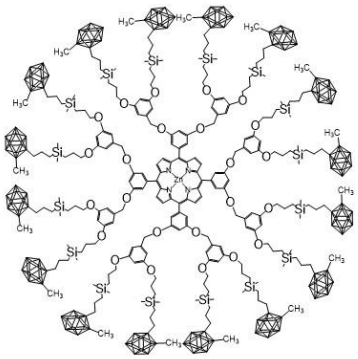

82

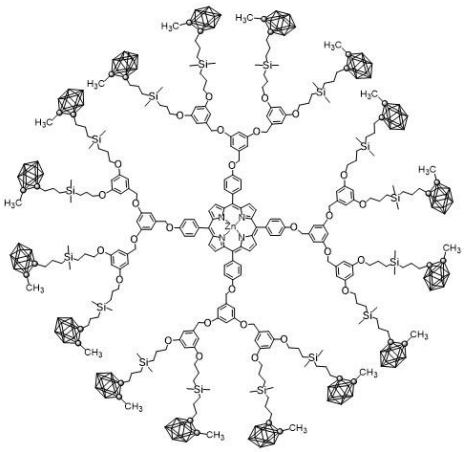

83

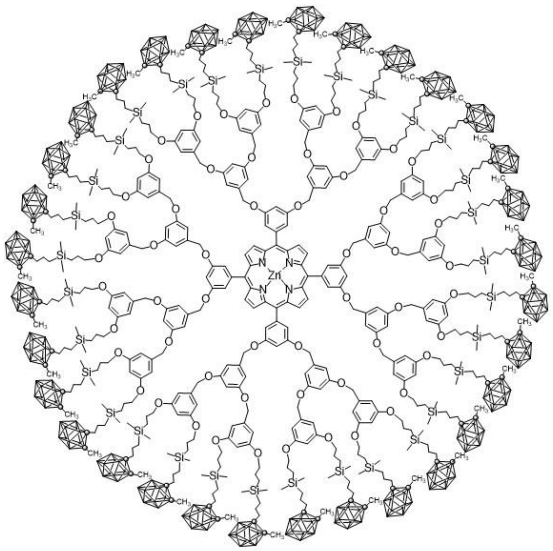

84

Figure 3. CryoTEM image of the interaction between [3,3'-Co(1,2-$C_2B_9H_{11}$)$_2$]$^-$ nano-vesicles and liposomes at the ratio (3:1) suspended in vitreous ice.

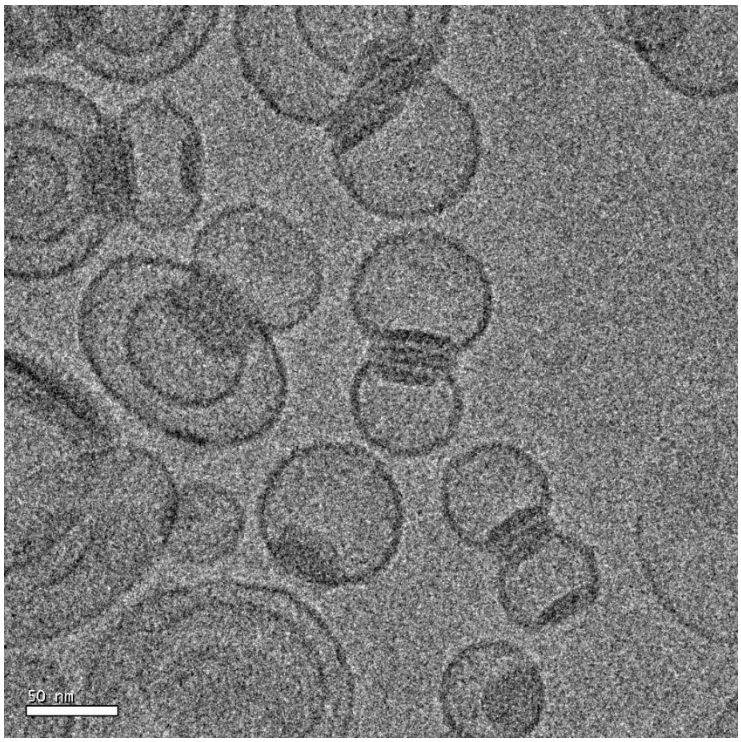

Figure 4. Growth arrest on Amoeba Cells was reversed at 500 µM by Na[3,3'-Co(1,2-$C_2B_9H_{11})_2$] and Na[3,3'-Co(8,8'-I_2-1,2-$C_2B_9H_{10})_2$] after removal the Boron compound of the culture media.

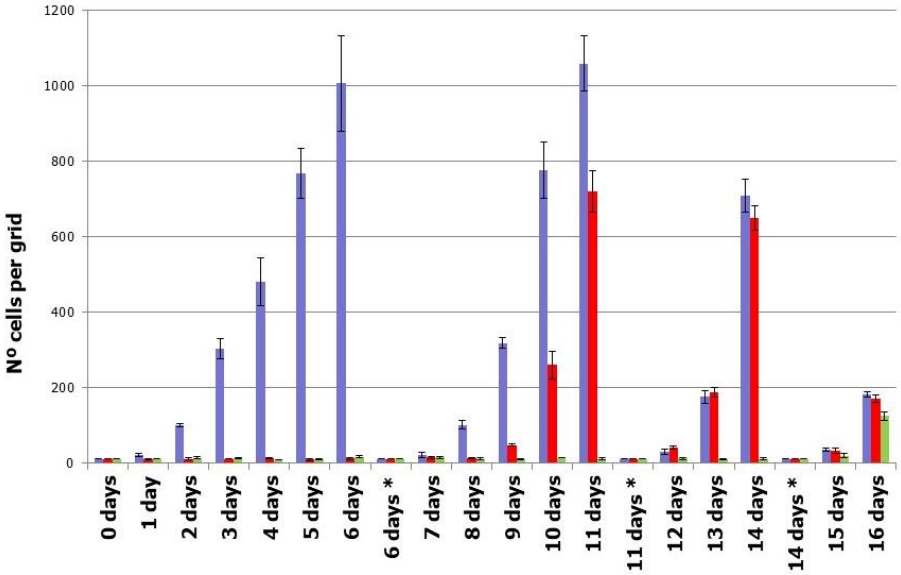

Figure 5. Schematic view of the monoanionic and dianionic metallabisdicarbollide compounds, which ED_{50} was investigated with *Dictyostelium* cells.

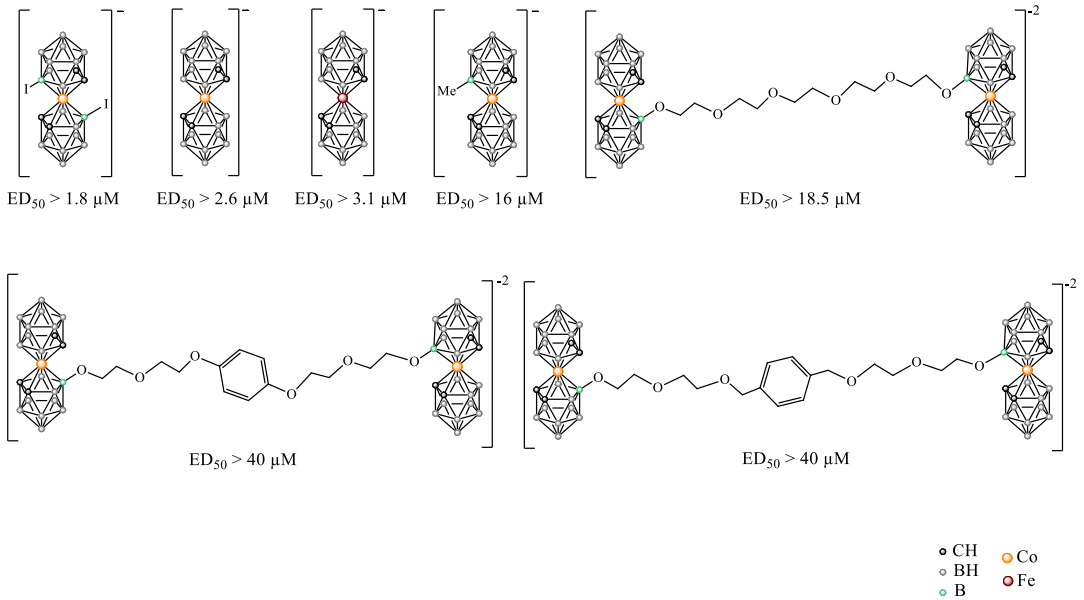

Figure 6. Chemical imaging of HEK293 cell treated with 25mM of Na[3,3'-Co(1,2-$C_2B_9H_{11})_2$] for 1 hour. Image shows phase contrast image and five Raman spectra (Spectra 1-5) show the spectral fingerprint of the cell at 2570 cm^{-1} (B-H peak) at different positions across the cell.

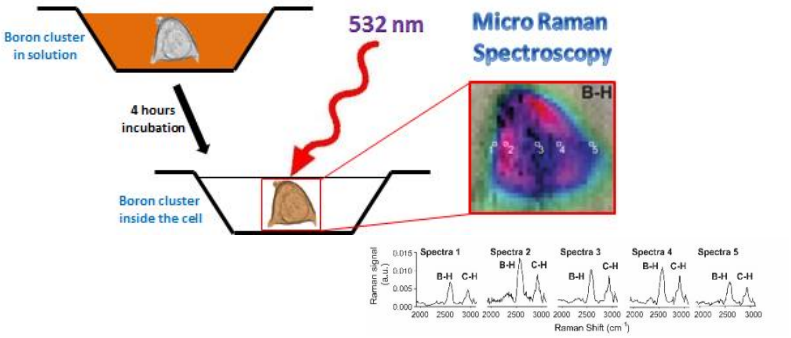

Figure 7. a) Confocal bioimages of B16H10 cells incubated with 10 µg/mL of tin complexes bearing $[B_{12}H_{12}]^{2-}$ (left) and $[3,3'\text{-}Co(1,2\text{-}C_2B_{10}H_{11})]^-$ clusters (right) for 2 hours. b) Confocal bioimages of HeLa cells incubated with BODIPY-cobaltabisdicarbollide conjugates at 5 µg B/ml concentration for 2 hours.

a)

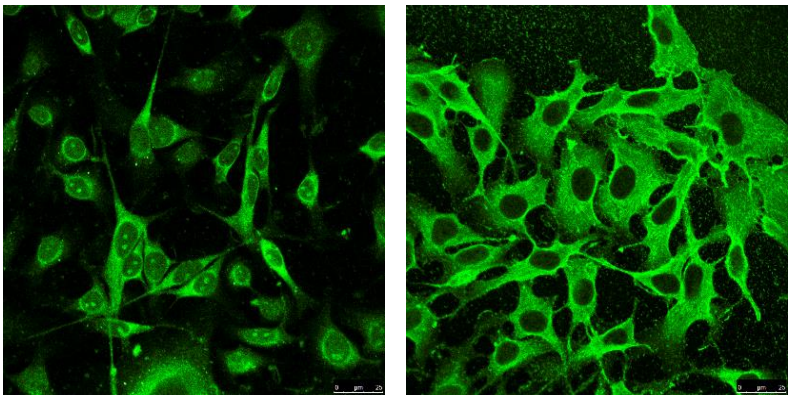

b)

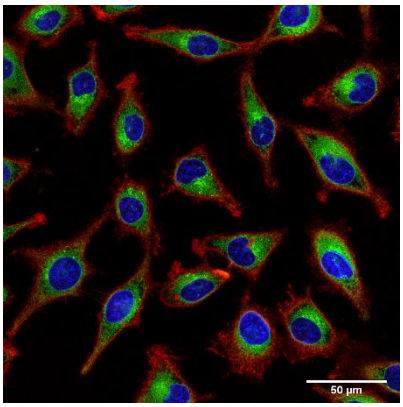

Figure 8. Schematic view of the anionic cobaltabisdicarbollide compounds investigated with cultured Madin-Darby bovine kidney cells (MDBK).

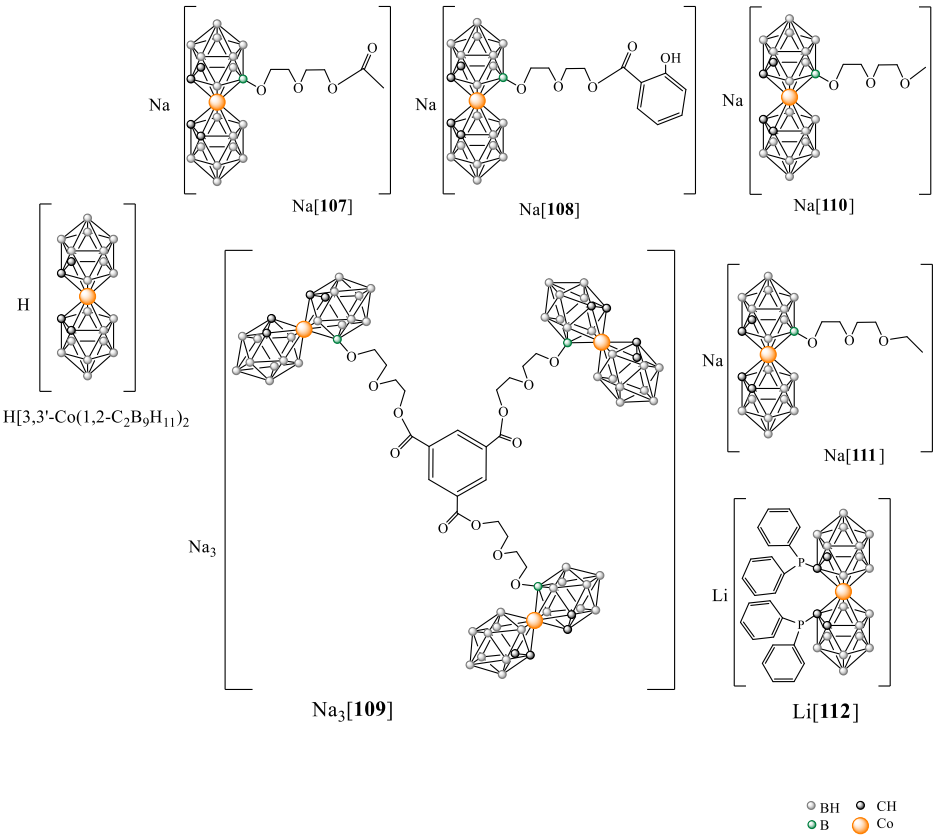

Scheme 1. Synthesis of peripheral carboranyl-functionalized dendrons of polyols cascade type. (a) Epichlorohydrin, $[NBu_4]I$, KOH, H_2O. (b) Propargyl bromide, NaH, DMF. (c) $B_{10}H_{14}$, CH_3CN, toluene.

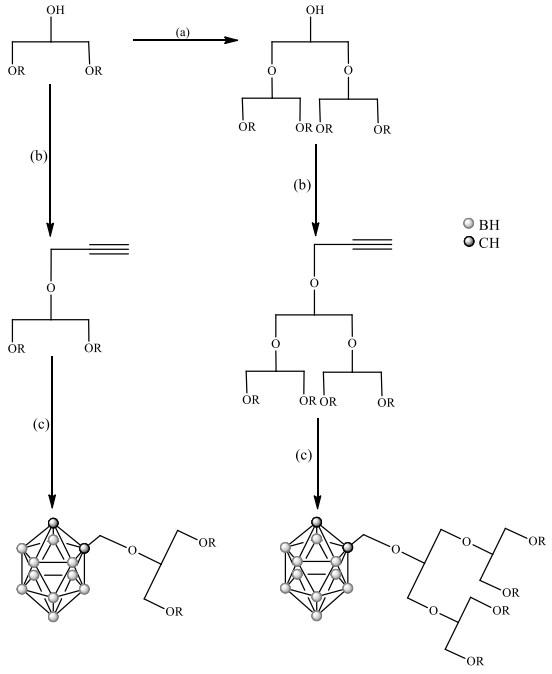

Scheme 2.- The reported icosahedral $[B_{12}]^{2-}$ homo functional “closomers”.

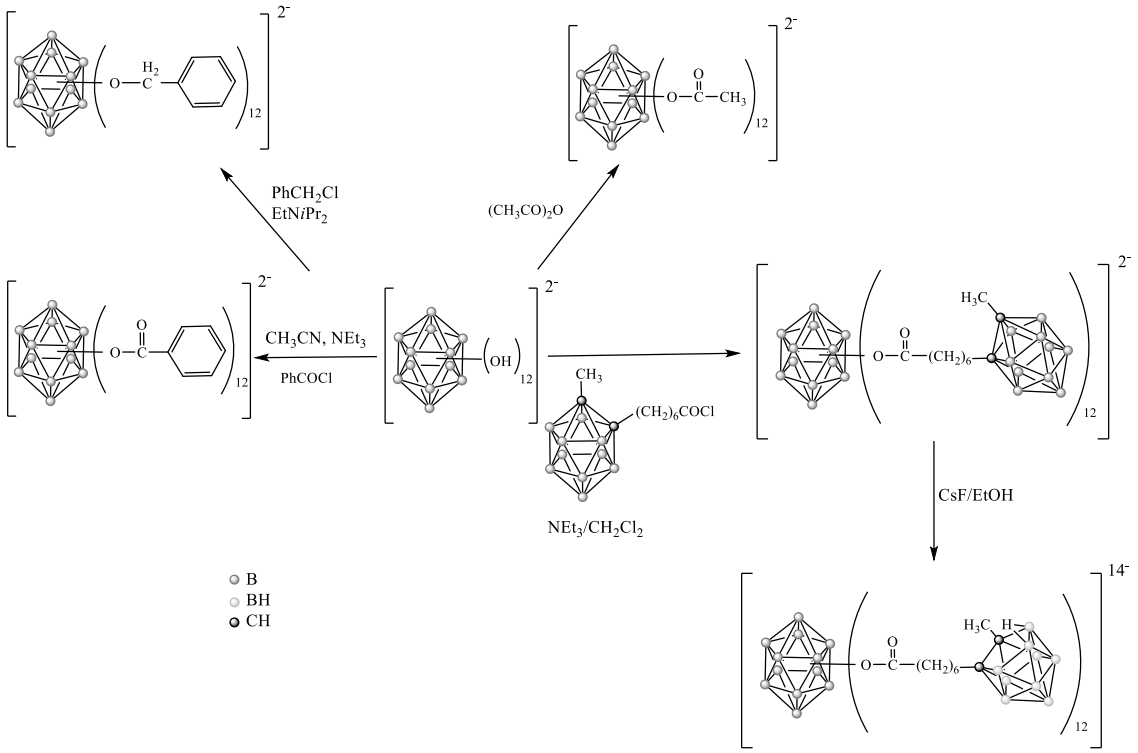

Scheme 3. Preparation of peripheral carboranyl-functionalized dendrons.

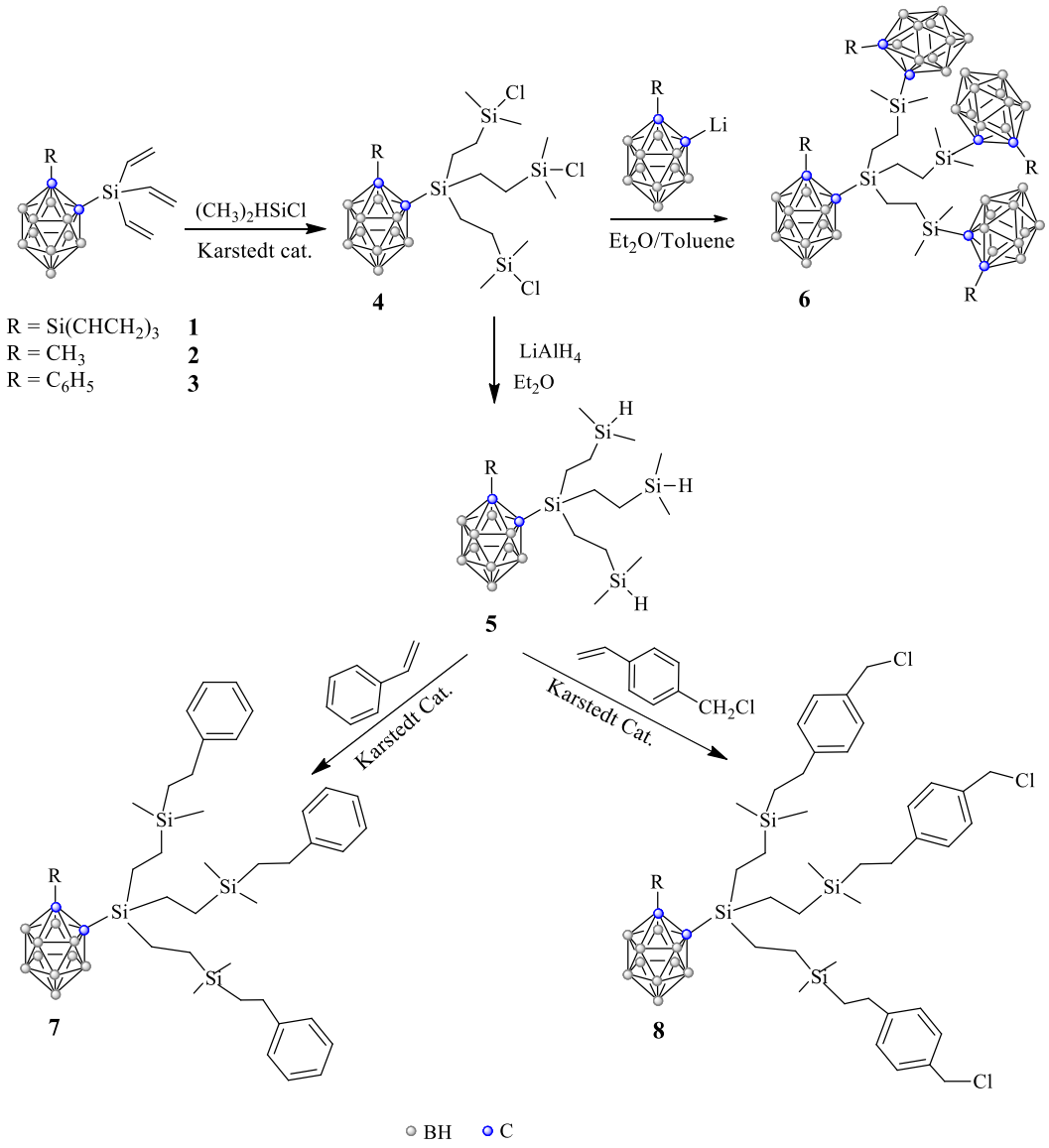

Scheme 4. Formation of the monoanionic and dianionic twelve-vertex dicarboranes modified by the 8-substituted [3,3'-Co(1,2-$C_2B_9H_{11}$)$_2$]$^-$ function via a 1,4-dioxahexane interconnection chain.

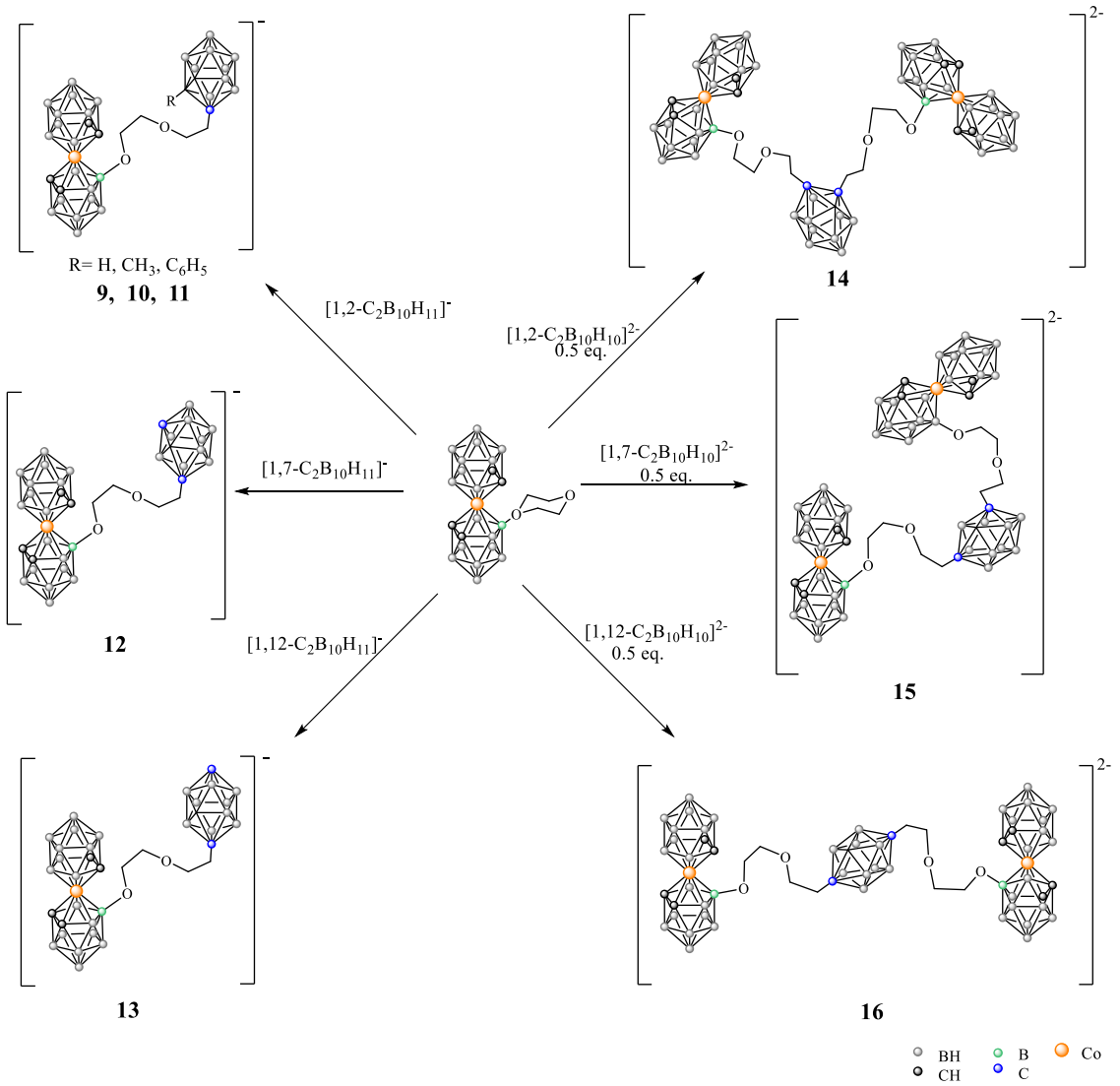

Scheme 5. Partial deboronation reaction of *closo* compounds yielding the corresponding di and trianionic species.

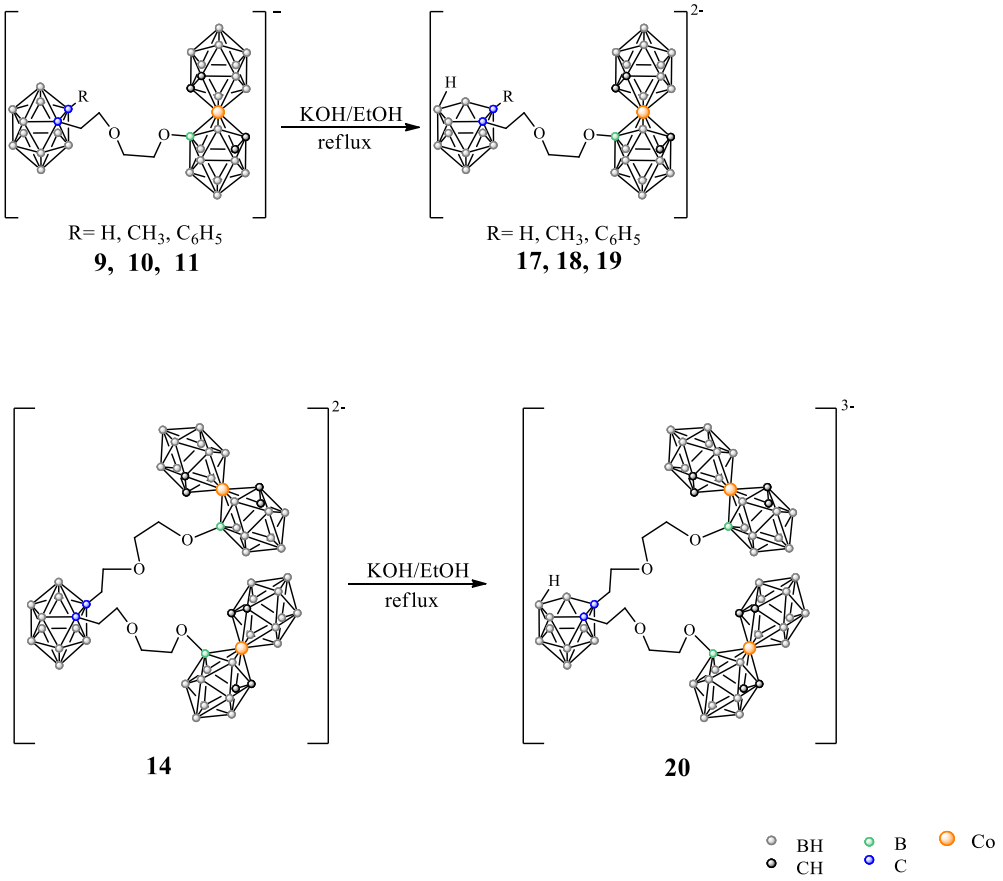

Scheme 6. Derivatization reactions on (a) 9,12-I_2-*closo*-1,2-$C_2B_{10}H_{10}$ and (b) 8,9,10,12-I_4-*closo*-1,2-$C_2B_{10}H_8$.

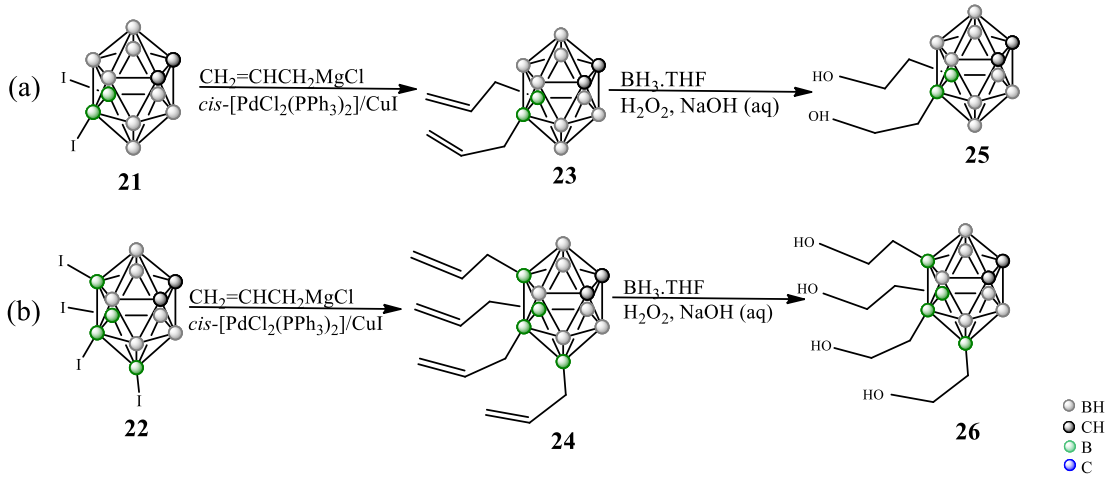

Scheme 7. Derivatization reactions on 9,12-($HOCH_2CH_2CH_2)_2$-*closo*-1,2-$C_2B_{10}H_{10}$.

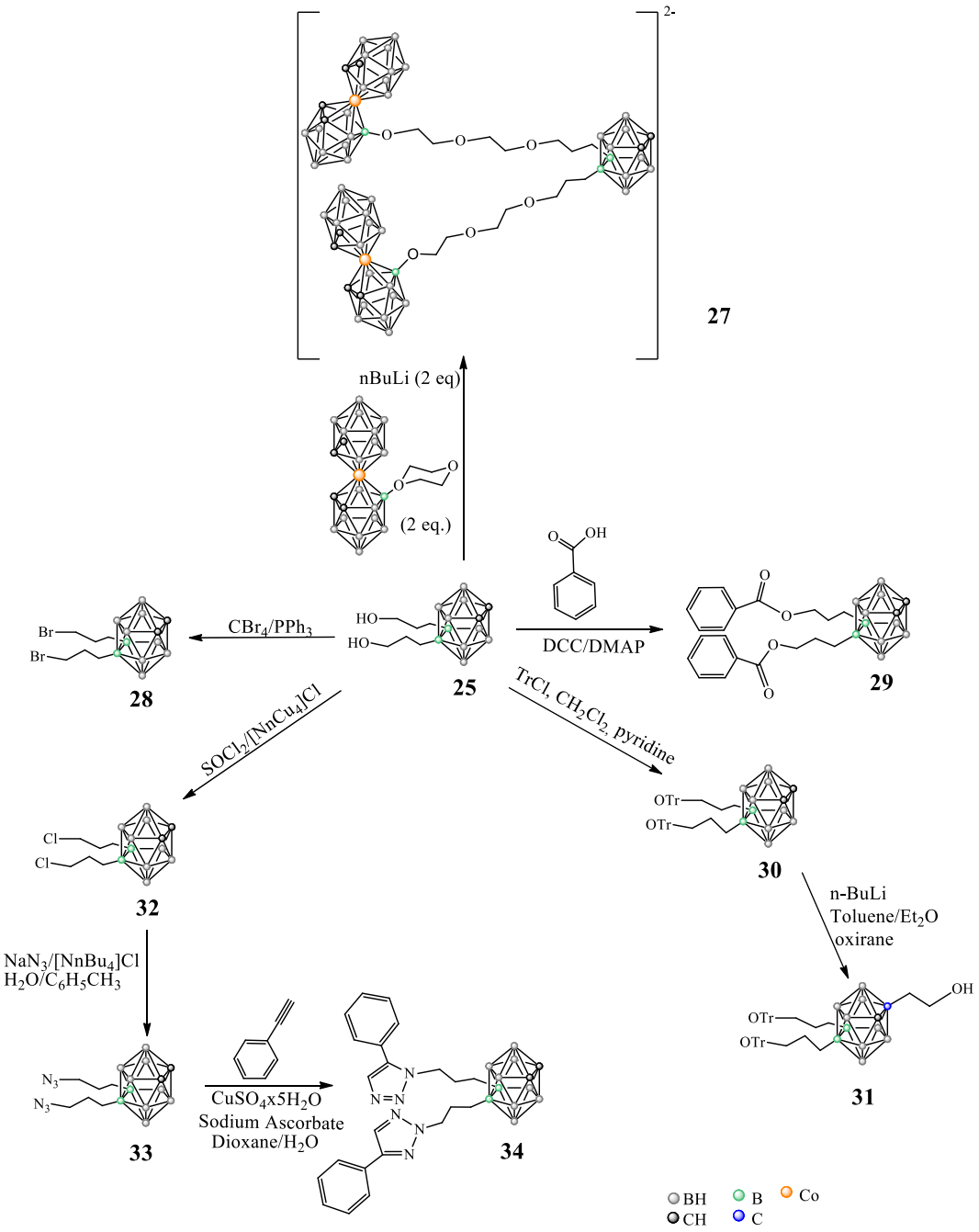

Scheme 8.- Derivatization reactions on 8,9,10,12-(HOCH$_2$CH$_2$CH$_2$)$_4$-*closo*-1,2-C$_2$B$_{10}$H$_8$.

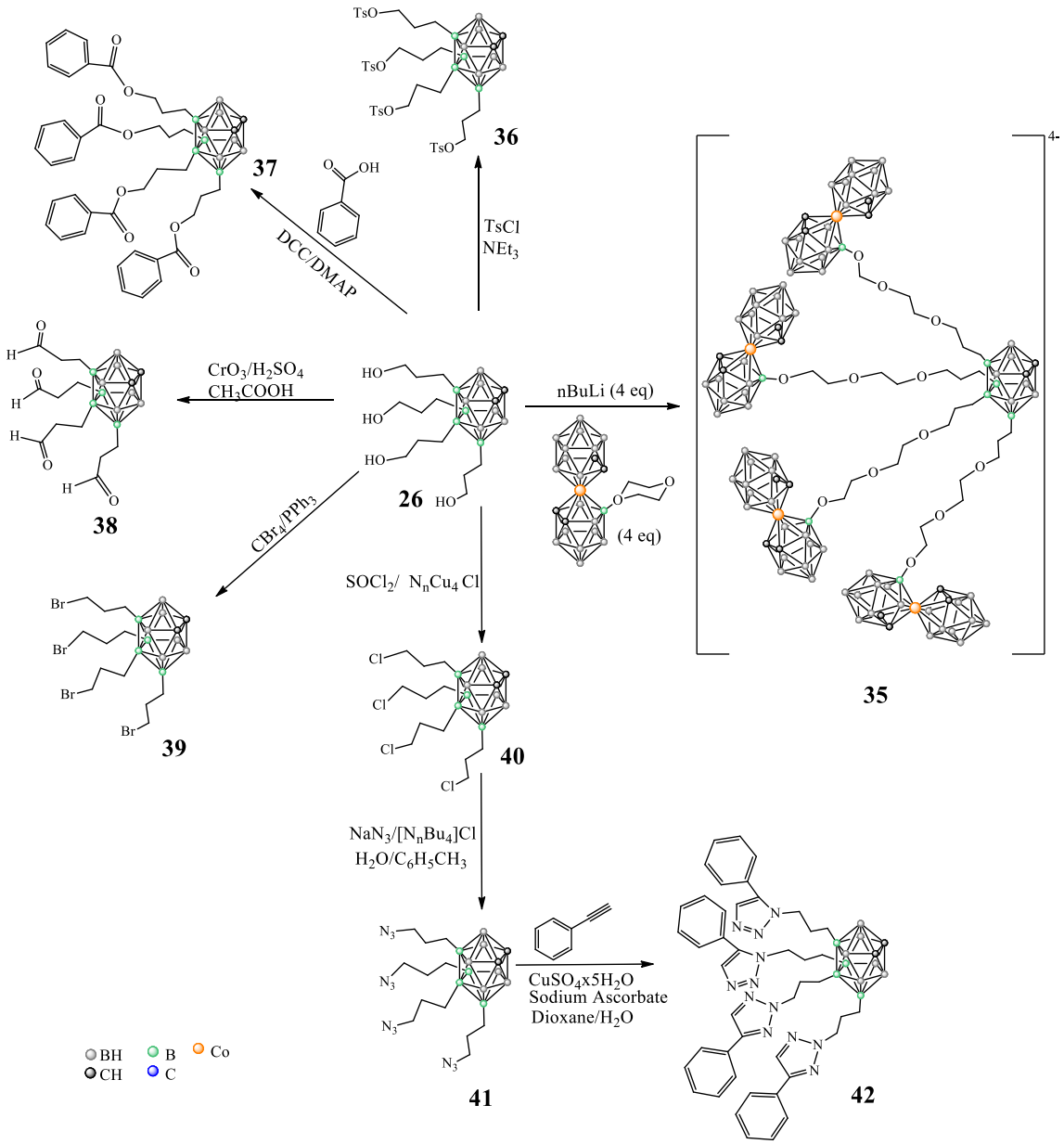

Scheme 9. Derivatization of the tribranched 1-$HOCH_2CH_2$-9,12-$(TrOCH_2CH_2CH_2)_2$-*closo*-1,2-$C_2B_{10}H_9$.

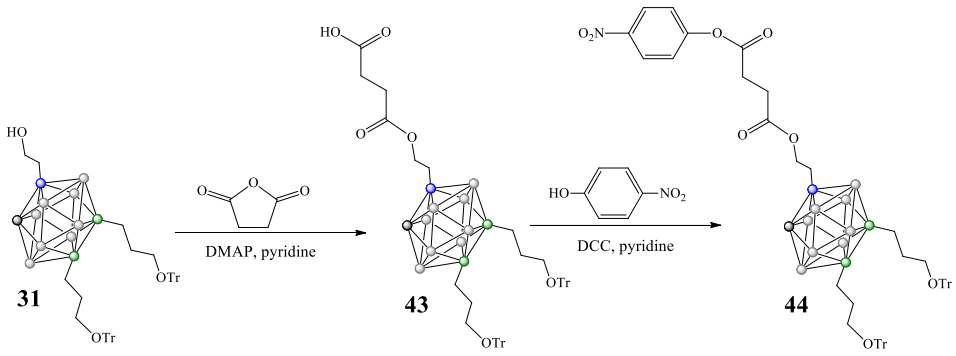

Scheme 10. a) Preparation of the solid (LCA-CPG) with the tribranched 1-$HOCH_2CH_2$-9,12-$(TrOCH_2CH_2CH_2)_2$-*closo*-1,2-$C_2B_{10}H_9$. b) Solid-support synthesis of triplet-shaped 1-$HOCH_2CH_2$-9,12-$(HOTTTTOCH_2CH_2CH_2)_2$-*closo*-1,2-$C_2B_{10}H_9$. T= Thymidine phosphonic. i) detritylation: 3 % DCA in CH_2Cl_2; ii) coupling: 7, 5-ethylothio-1-H-tetrazole in CH_3CN; iii) oxidation: I_2 in THF/2,6-lutidine/H_2O; iv) capping: 1 M acetic anhydride in tetrahydrofuran/pyridine (1:8 v/v); v) cleavage from the support and phosphate deprotection: 25% NH_3 aq.

a)

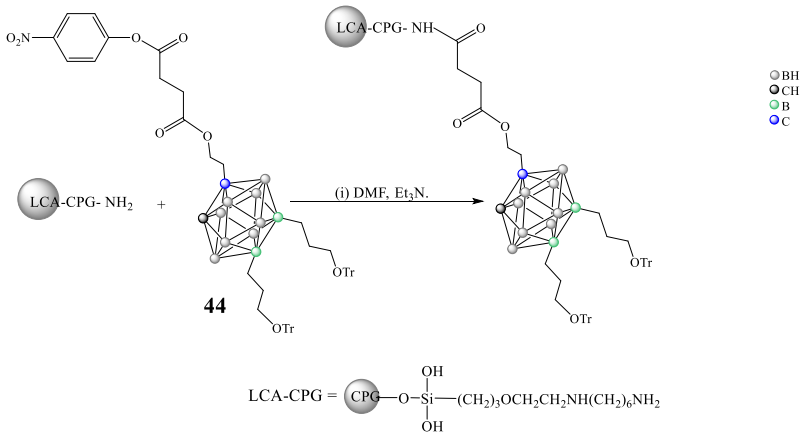

b)

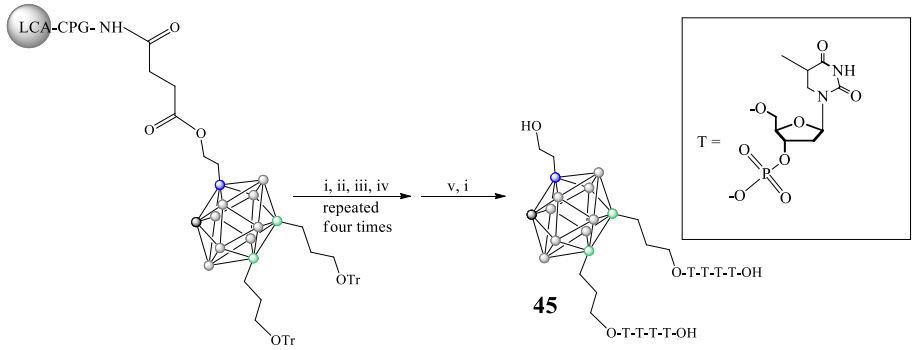

Scheme 11. Deprotonation reaction on C_c-H of the di and tetra *B*-substituted *o*-carborane derivative with *n*-butillitium and nucleophilic substitution with allyl bromide to produce tetra branched compound. Hydroboration/oxidation reaction on the olefinic terminal groups to achieve the corresponding polyalcohols. Nucleophilic oxonium ring opening reaction on zwiterionic compound [3,3'-Co(8-$(C_4H_8O)_2$-1,2-$C_2B_9H_{10}$)(1',2'-$C_2B_9H_{11}$)] by deprotonated hydroxyl compound to obtain the tetra anion [1,2,9,12{3,3'-Co-{8-$(C_4H_8O_2$-1,2-$C_2B_9H_{10}$-1',2'-$C_2B_9H_{11}$}-$O(CH_2)_3$}$_4$-1,2-*closo*-$C_2B_{10}H_8$]$^{4-}$.

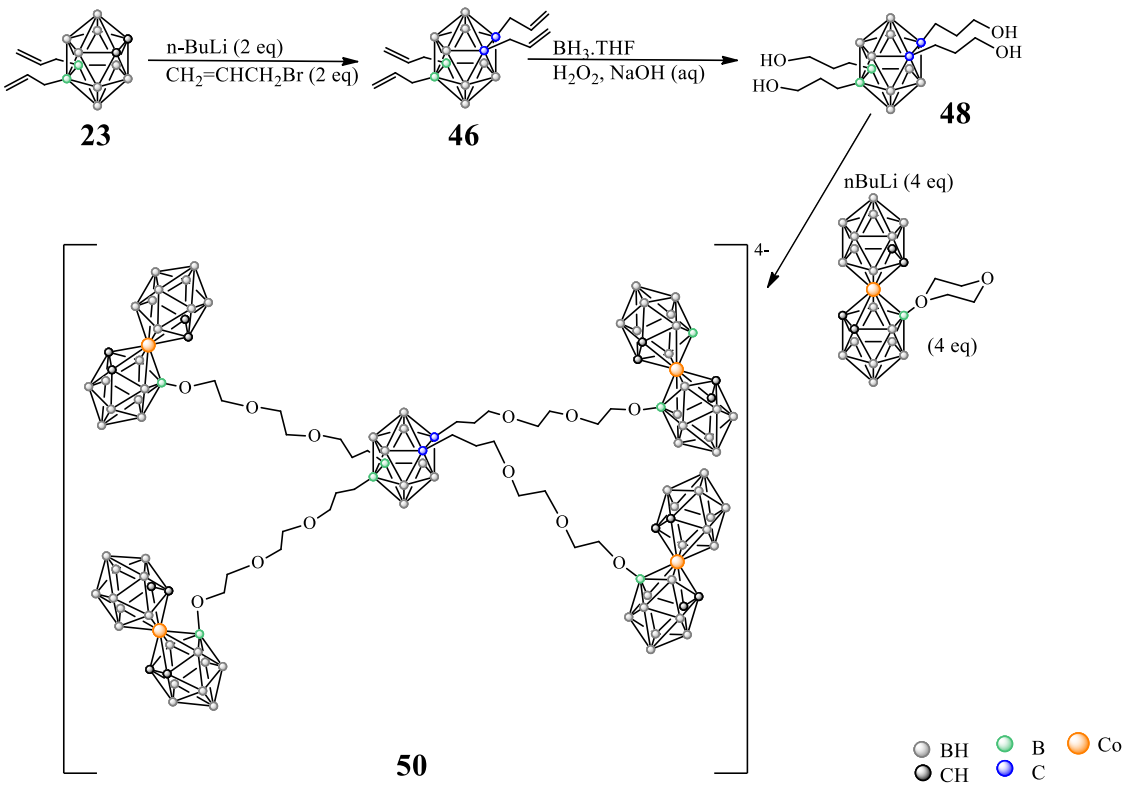

Scheme 12. Deprotonation reaction on C_c-H of the tetra *B*-substituted *o*-carborane derivative with *n*-butillitium and nucleophilic substitution with allyl bromide to produce hexabranched compound. Hydroboration/oxidation reaction on the olefinic terminal groups to achieve the corresponding hexaalcohols. Nucleophilic oxonium ring opening reaction on zwiterionic compound [3,3'-Co(8-$(C_4H_8O)_2$-1,2-$C_2B_9H_{10}$)(1',2'-$C_2B_9H_{11}$)] by deprotonated hydroxyl compound to obtain the hexaanion [1,2,8,9,10,12{3,3'-Co-{8-$(C_4H_8O_2$-1,2-$C_2B_9H_{10}$-1',2'-$C_2B_9H_{11}$}-$O(CH_2)_3$}$_6$-1,2-*closo*-$C_2B_{10}H_6$]$^{6-}$.

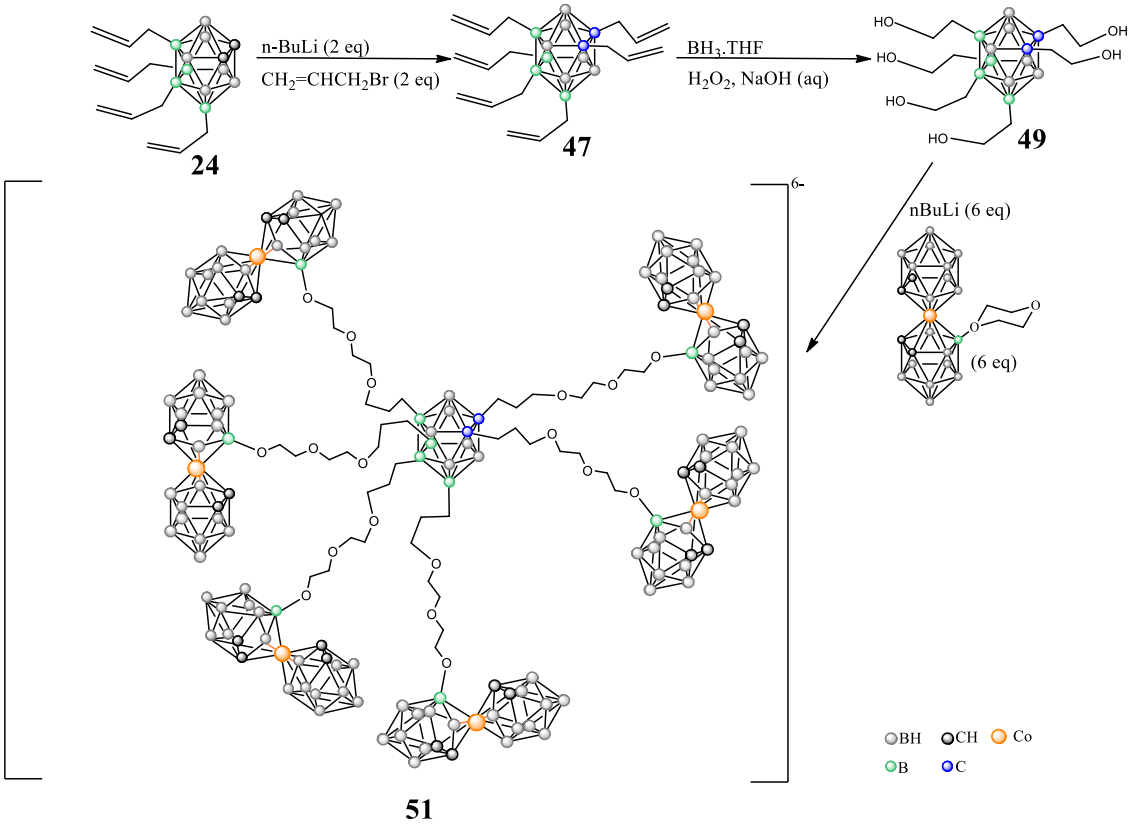

Scheme 13. Frèchet-type aryl-ether derivatives bearing *closo* and *nido*-*o*-carborane clusters.

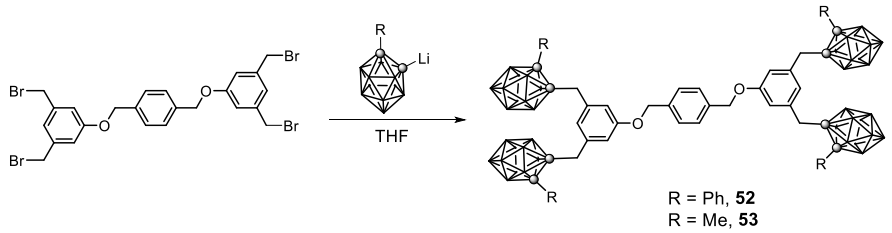

R = Ph, **52**
R = Me, **53**

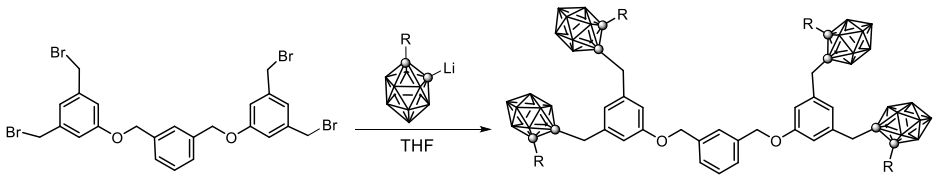

R = Ph, **54**
R = Me, **55**

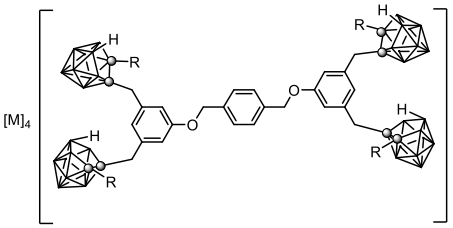

R = Ph, M = K, **56**
R = Ph, M = [NMe_4], **57**
R = Me, M = K, **58**
R = Me, M = [NMe_4], **59**

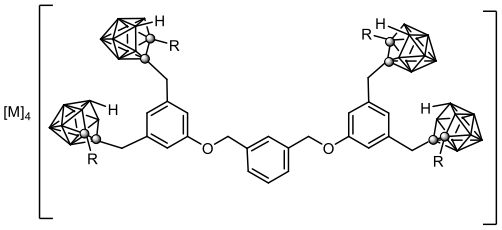

R = Ph, M = K, **60**
R = Ph, M = [NMe_4], **61**
R = Me, M = K, **62**
R = Me, M = [NMe_4], **63**

Scheme 14. Synthesis of a poly(aryl-ether) dendrimer peripherally functionalized with eigth cobaltabisdicarbollide moieties.

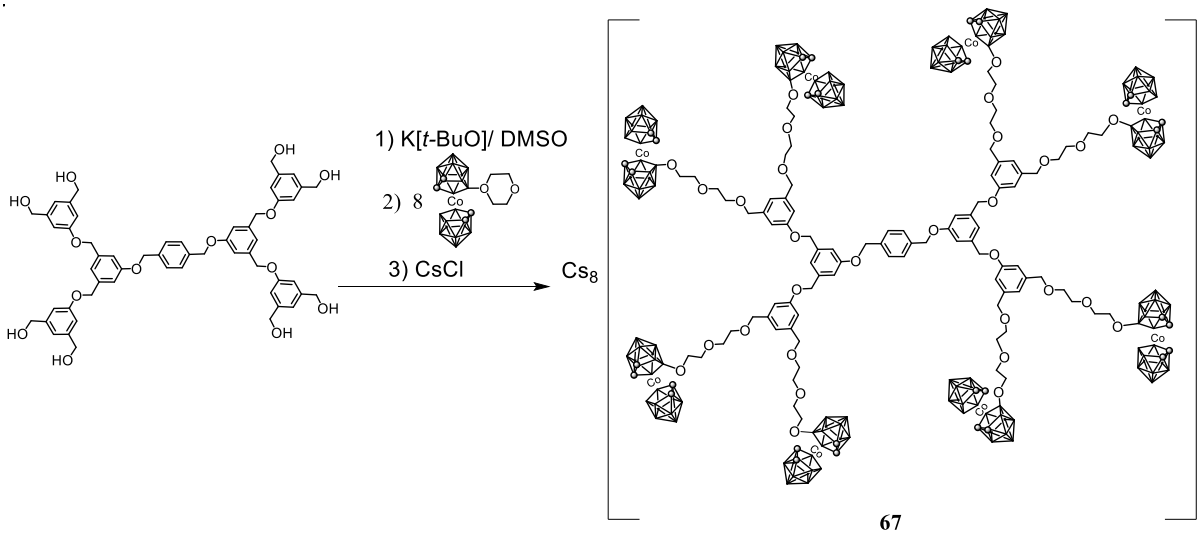

Scheme 15. Synthesis of carboranyl-terminated poly(aryl-ether) dendrimers via hydrosilylation.

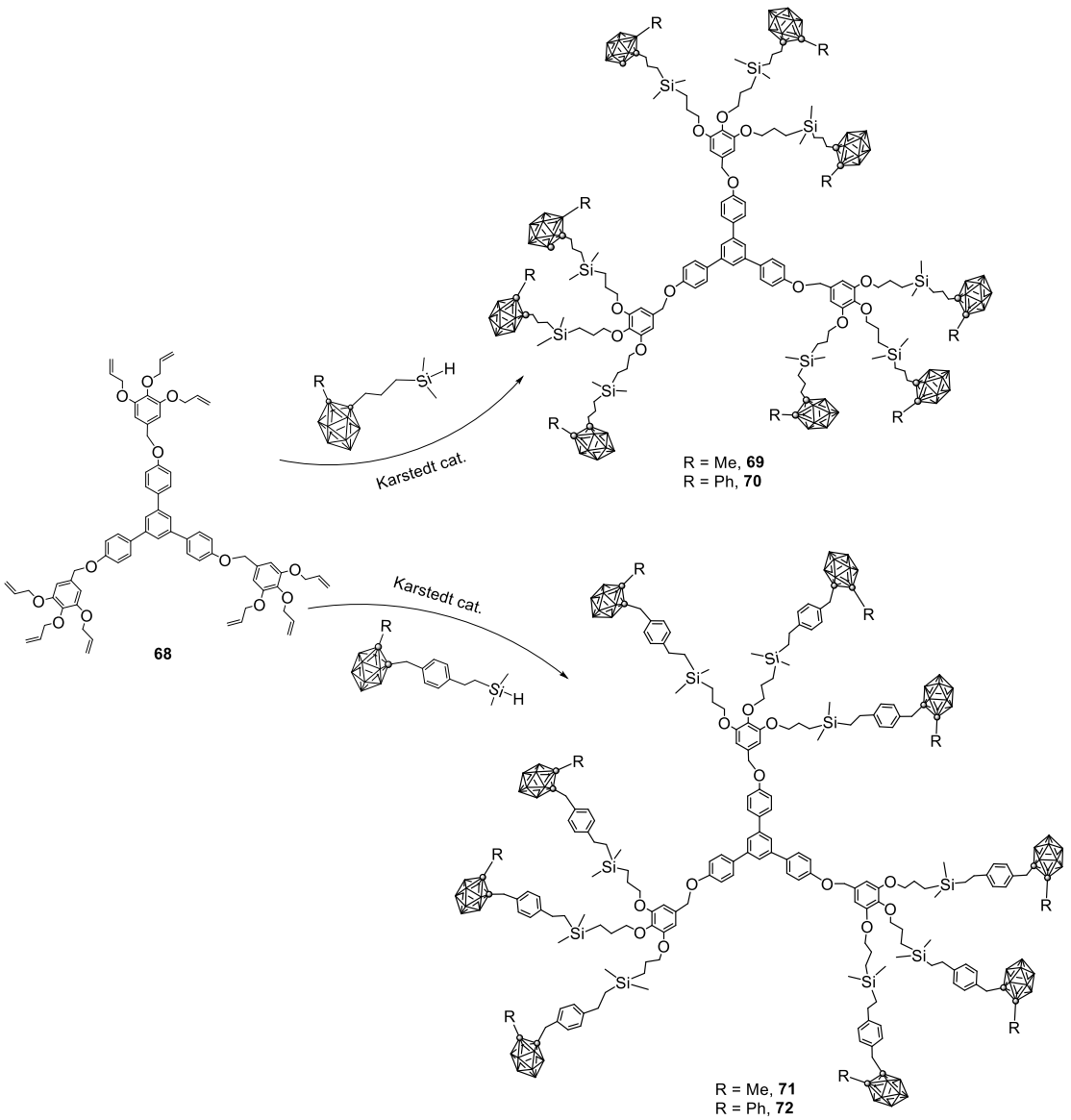

Scheme 16. Partial deboronation of *closo*-carboranes to get polyanionic fluorescent dendrimers.

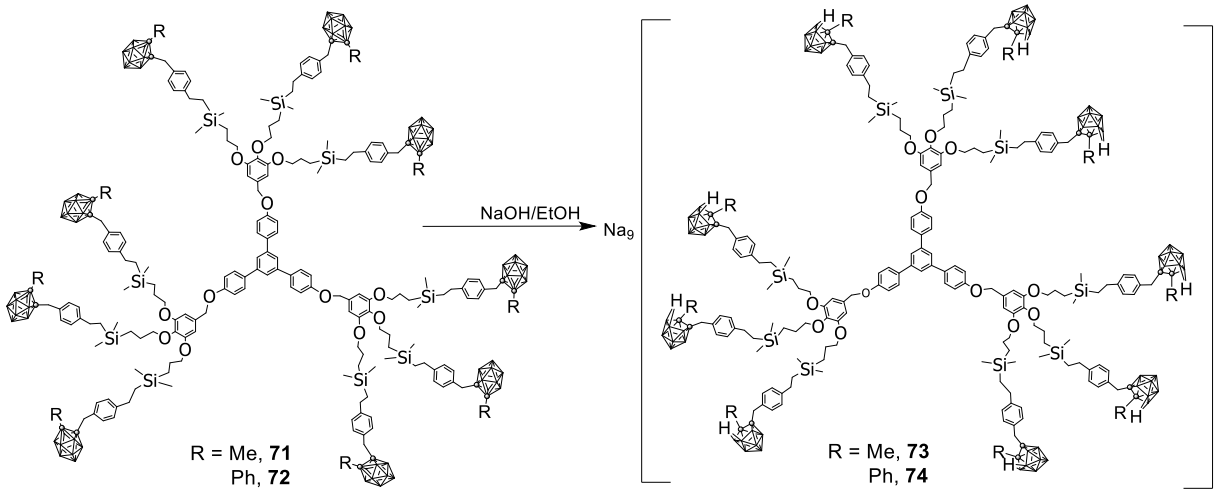

Scheme 17. Cesium salts of polyanionic dendrimers with peripheral cobaltabisdicarbollides.

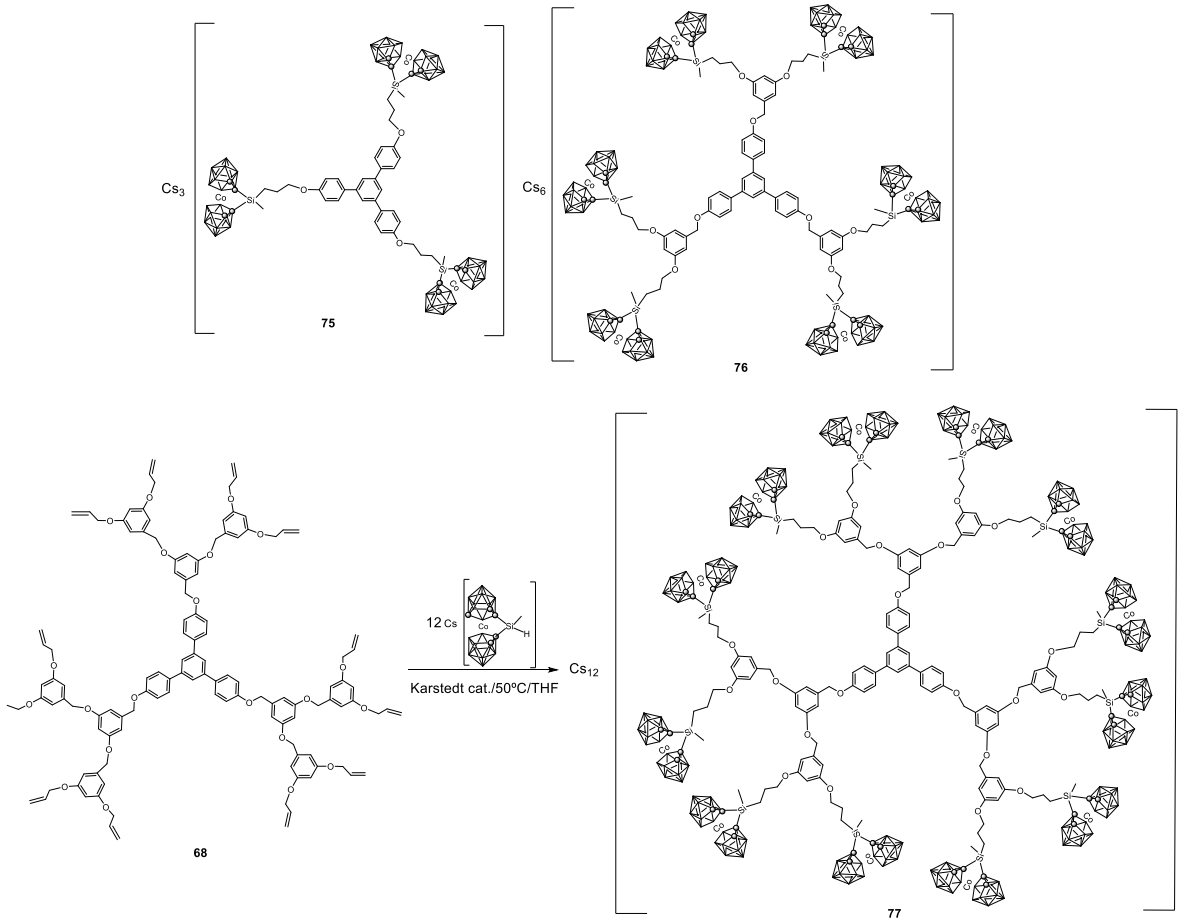

Scheme 18. Synthesis of porphyrin-cored dendrimers decorated with sixteen Me-o-carboranyl units.

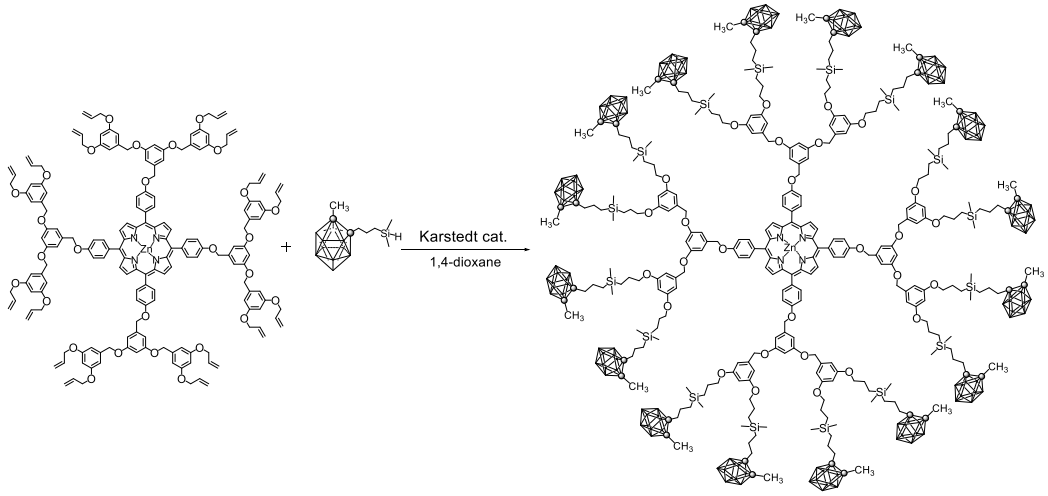

83

Scheme 19. Preparation of neutral and anionic octasilsesquioxane hybrids decorated with *o*-carboranyl units via hydrolytic and nonhydrolytic processes and partial deboronation.

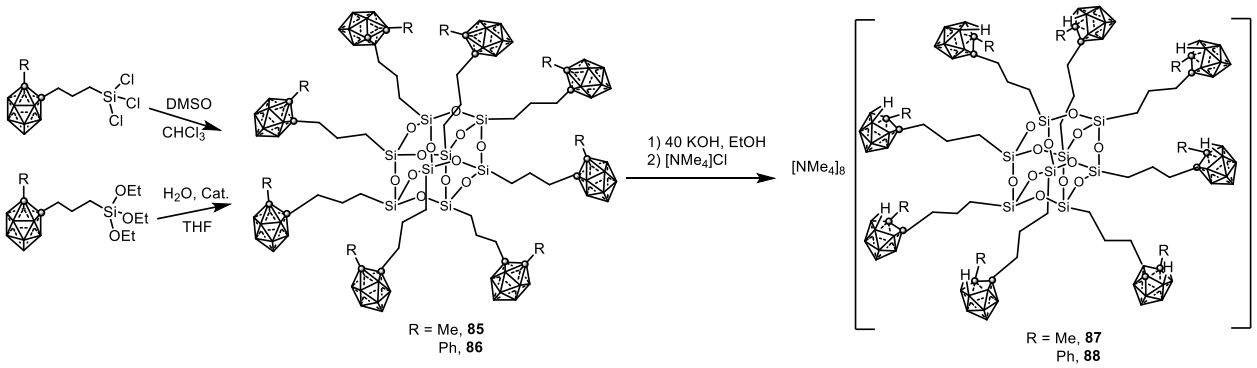

Scheme 20. Synthesis of luminescent POSS hybrids: a) by cross-metathesis reaction of octavinylsilane with styrenyl-carborane derivatives; b) by Heck reaction between the octa(*p*-bromostyrenyl)silsesquioxane and the styrenyl-carborane derivatives.

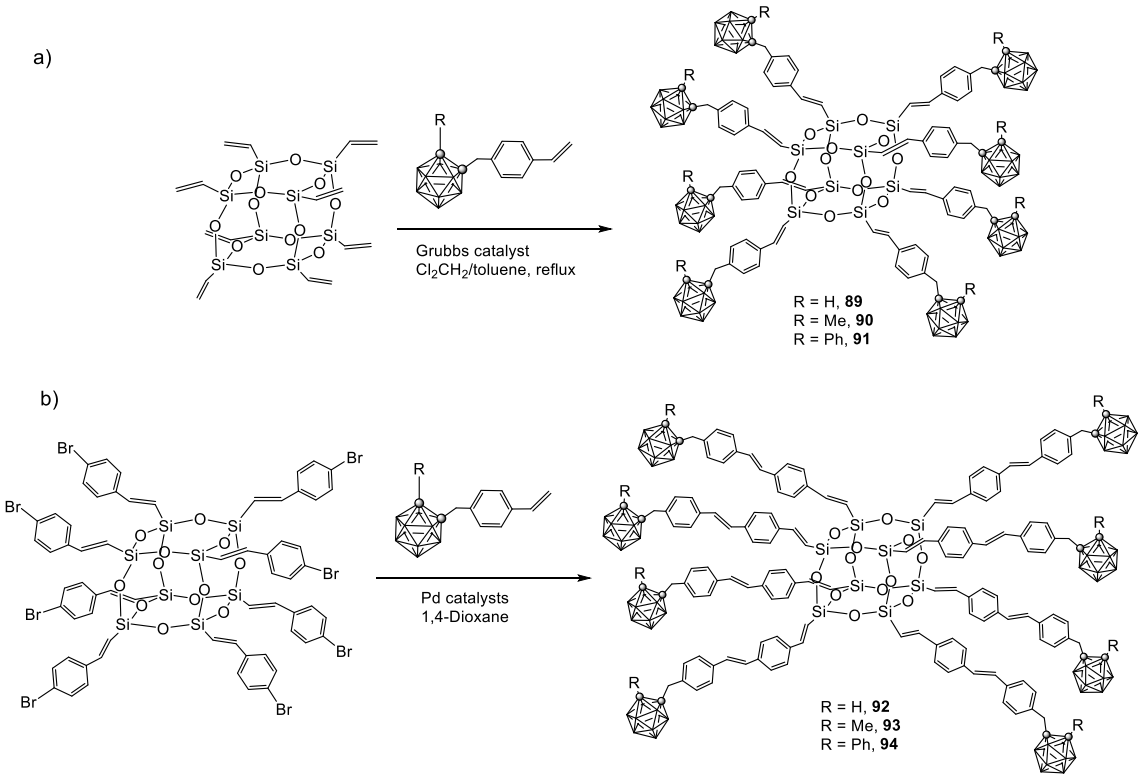

Scheme 21. Synthesis of POSS hybrids decorated with metallacarboranes by cross-methatesis reaction.

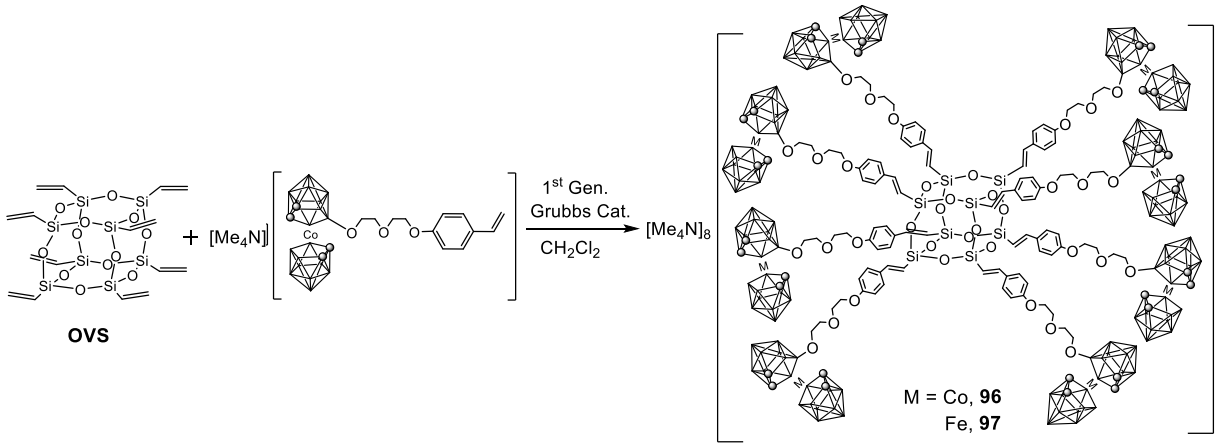

Scheme 22. Synthesis of fluorescent tin complexes bearing boron clusters to be used as cell markers.

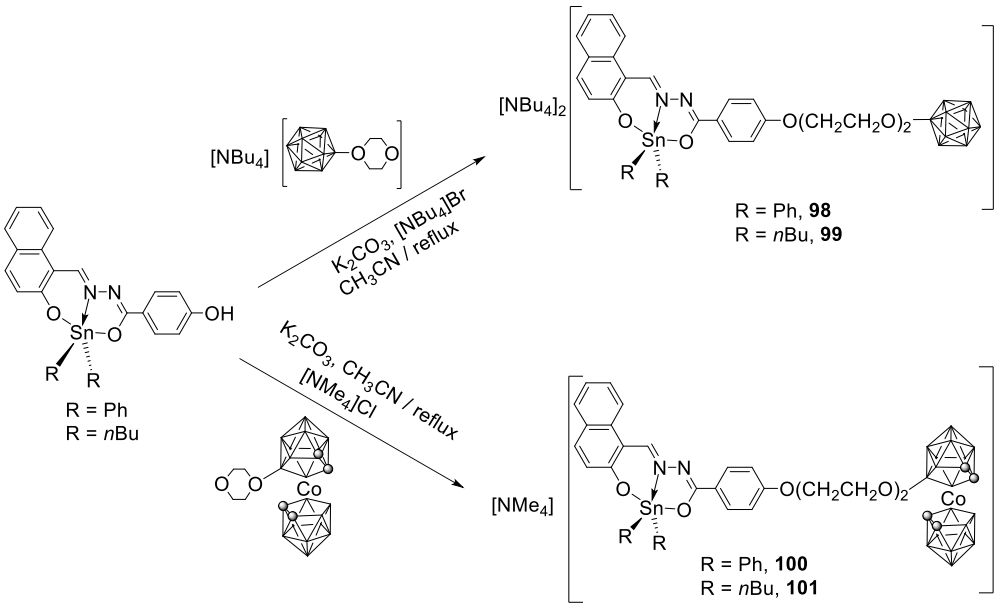

Scheme 23. Procedure to obtain the fluorescent BODIPY-anionic boron cluster conjugates.

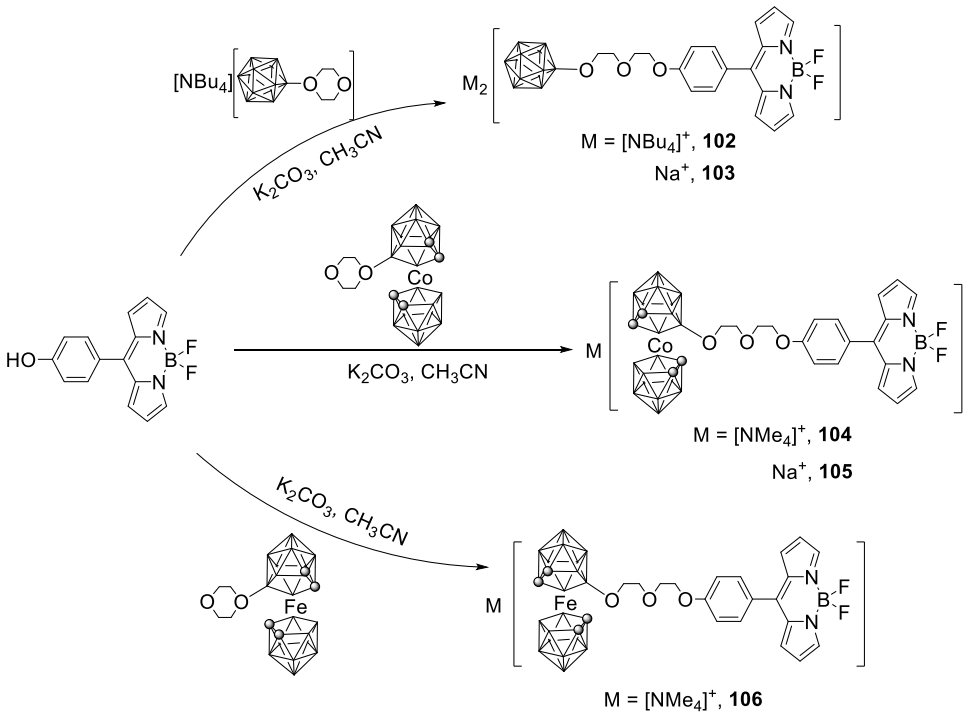

Scheme 24. a) Synthesis of mixed-doubly functionalized [3,3'-Co(1,2-$C_2B_9H_{11}$)$_2$]$^-$ derivative. b) Radiolabelling reactions on [3,3'-Co(8-I-1,2-$C_2B_9H_{10}$)(1',2'-$C_2B_9H_{11}$)]$^-$and [3,3'-Co(8-I-1,2-$C_2B_9H_{10}$)(8'-PEG-1',2'-$C_2B_9H_{10}$)]$^-$ derivatives were performed by palladium catalyzed iodine exchange reaction.

a)

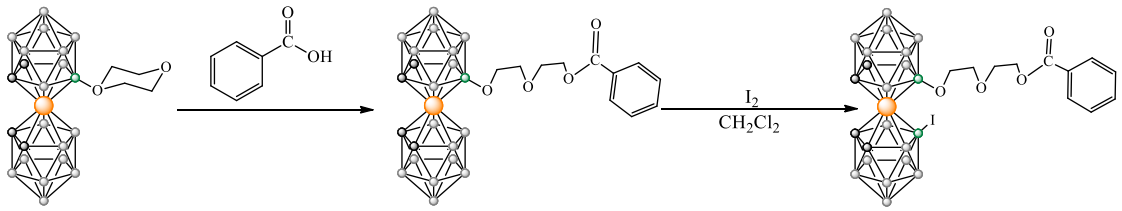

b)

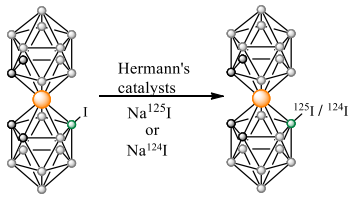

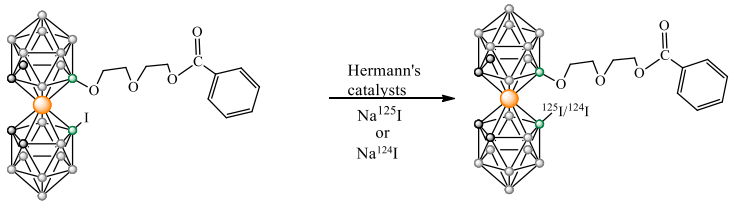

Table 1. Emission properties of Frèchet-type dendrons in different solvents.

		λ_{em} (nm)		
Compound	**Clusters**	**THF**	**Acetone**	**Other solvents**
52	*closo* Ph-*o*	373	374	375 (toluene); 374 ($CHCl_3$)
53	*closo* Me-*o*	366	368	367 (Toluene); 368 ($CHCl_3$)
54	*closo* Ph-*o*	369	-	371 (toluene)
55	*closo* Me-*o*	333	-	363 (toluene)
56	*nido* Ph-*o*	375	375	379 (H_2O)
57	*nido* Ph-*o*	373	375	381 (DMSO)
58	*nido* Me-*o*	363	365	369 (H_2O)
59	*nido* Me-*o*	363	364	370 (DMO)
60	*nido* Ph-*o*	370	-	373 (H_2O)
61	nido Ph-*o*	369	-	371 (DMSO)
62	*nido* Me-*o*	339	-	362 (H_2O)
63	*nido* Me-*o*	338	-	366 (DMSO)

Table 2. Photophysical properties of carboranyl containing dendrimers.

Compound	Nº clusters	λ_{abs} (nm)	λ_{em} (nm)	ϕ_F
69	9	269	366	0.54 [a]
70	9	269	366	0.24[a]
71	9	269	366	0.51[a]
72	9	269	366	0.11[a]
73	9	267	367	0.13[b]
74	9	n.a	n.a	n.a[c]
78	4	423	657	-
79	8	422	656	-
80	8	422	649	-
81	8	423	603, 645	-
82	16	423	596, 643	-
83	16	424	604, 644	-
84	32	424	599, 641	-

[a] Measured in THF; [b] measured in H_2O; [c] unavailable, due to the low solubility of the compound in water

Table 3: Effective dose (ED_{50}) for $[3,3'\text{-}Co(1,2\text{-}C_2B_9H_{11})_2]^-$ and $[8,8'\text{-}I_2\text{-}3,3'\text{-}Co(1,2\text{-}C_2B_9H_{10})_2]^-$ on cell growth

	Compound ED_{50} (mean ±SD, μM)	
Cell type	$Na[3,3'\text{-}Co(1,2\text{-}C_2B_9H_{11})_2]$	$Na[8,8'\text{-}I_2\text{-}3,3'\text{-}Co(1,2\text{-}C_2B_9H_{10})_2]$
HEK293	121 ± 3.8	30 ± 3.8
HeLa	157 ± 8.6	23 ± 2.5
THP-1	154 ± 8.9	44 ± 6.0
3T3	99 ± 5.5	29 ± 0.8
Dictyostelium	2.6 ± 0.3	1.8 ± 0.1
E.coli B/r	nc[1]	53 ± 5.4
Klebsiella pneumonia	nc[1]	65 ± 4.1

[1] not calculated: unable to measure as ED_{50} is greater than 250 μM, above the solubility of $Na[3,3'\text{-}Co(1,2\text{-}C_2B_9H_{11})_2]$ in LB medium.

Table 4: Minimum inhibitory concentration (MIC_{50}) of some cobaltabisdicarbollide complexes on pathogenic microorganisms. Thiamphenicol was used as positive control.

		MIC_{50}				
Microorganism	Number of strains	Na[**111**]	Li[**112**]	Na[**108**]	Na_3[**109**]	Thiam.
S. aureus	4	12.8 ± 7.3	36.0 ± 10.1	10.1 ± 7.3	48.0 ± 9.2	21.3 ± 6.2
S. pyogenes	4	3.1 ± 1.6*	26.0 ± 6.0	2.5 ± 0.6**	48.0 ± 9.2	20.0 ± 9.9
E. coli	4	7.0 ± 1.0*	26.0 ± 6.0	4.0 ± 0.1*	22.0 ± 6.0	12.0 ± 2.3
P. aeruginosa	4	18.0 ± 5.0	22.0 ±6.0	8.0 ± 2.8*	17.0 ± 5.7	20.5 ± 3.8
Candida spp	4	1.4 ± 0.2***	28.0 ± 4.0	2.3 ± 0.4***	32.0 ± 0.1	14.0 ± 2.0

Significantly lower MICs versus wide-spectrum antibiotic thiamphenicol (used as positive control) are presented as follows: *$P < 0.05$, **$P < 0.01$, ***$P < 0.001$ vs. thiamphenicol

Table 5. Minimum inhibitory concentration (MIC_{90}) of some cobaltabisdicarbollide complexes on pathogenic microorganisms. Thiamphenicol was used as positive control.

				MIC_{90}		
Microorganism	Number of strains	Na[**111**]	Li[**112**]	Na[**108**]	Na_3[**109**]	Thiam.
S. aureus	4	25.5 ± 9.2	72.0 ± 20.4	20.3 ± 4.0	88.0 ± 48.0	38.5 ± 10.7
S. pyogenes	4	6.3 ± 5.5*	52.0 ± 24.0	5.0 ± 2.4*	96.0 ± 36.9	34.0 ± 14.4
E. coli	4	14.4 ± 4.0	52.0 ± 24.0	8.0 ± 0.0*	43.5 ± 25.0	25.0 ± 10.4
P. aeruginosa	4	36.0 ± 20.0	43.5 ±25.0	15.0 ± 12.0	34.0 ± 22.0	37.0 ± 10.1
Candida spp	4	2.8 ± 0.8**	56.0 ± 16.0	4.5 ± 1.7**	64.0 ± 0.0***	28.5 ± 7.0

Significantly lower MICs versus wide-spectrum antibiotic thiamphenicol (used as positive control) are presented as follows: *$P < 0.05$, **$P < 0.01$, ***$P < 0.001$ vs. thiamphenicol

Table 6: The effect of the cobaltabisdicarbollide complexes displayed in Figure 8 on the viability and proliferation of cultured Madin-Darby bovine kidney cells (MDBK). Cytotoxicity concentration (CC_{50}, µg/ml) for each compound was determined by thiazolyl blue tetrazolium bromide test (MTT)[113] and neutral red uptake cytotoxicity assay (NR)[114] after 72 h of treatment. All data points represent an average of three independent assays.

Compound	MTT	NR
Na[**111**]	15.3 ± 1.4	12.4 ± 2.1
Na[**107**]	25.7 ± 2.5	29.7 ± 1.9
Na[**108**]	37.4 ± 2.9	40.8 ± 3.1
Li[**112**]	> 100	> 100
Na_3[**109**]	> 100	> 100
Na[**110**]	19.4 ± 1.7	17.2 ± 0.8
H[3,3'-Co(1,2-$C_2B_9H_{11}$)$_2$]	31.2 ± 3.7	26.8 ± 2.2
Thiamphenicol	> 100	> 100

References

(1) Scoire, S. Is boron a prebiotic element? A mini-review of the essentiality of boron for the appearance of life on Earth. *Orig. Life Evol. Biosph*., **2012**, *42* (1), 3-17.

(2) (a) Dembitsky, V. M.; Smoum, R.; Al-Quntar, A. A. A.; Ali, H. A.; Pergament, I.; Srebnik, M. Natural occurrence of boron containing compounds in plants, algae and microorganisms. *Plant Sci*., **2002**, *163*, 931–942. (b) Loomis, W. D.; Durst, R. W. Chemistry and biology of boron. *BioFactors*., **1992**, *3*, 229–239. (c) Dinca, L.; Scorei, R. Boron in human nutrition and its regulations use. *J. Nutr. Ther*., **2013**, *2*, 22–29.

(3) (a) Nielsen, F. H. Is boron nutritionally relevant? *Nutr. Rev*., **2008**, *66* (4), 183-191. (b) Newnham, R. E. Essentiality of boron for healthy bones and joints. *Environ. Health Perspect*., **1994**, *102*, 83–85. (c) Hakki, S. S.; Bozkurt, B. S.; Hakki, E. E. Boron regulates mineralized tissue associated proteins in osteoblasts (MC3T3-E1). *J. Trace. Elem. Med. Biol.*, **2010**, *24* (4), 243-250.

(4) (a) Pizzorno, L. Nothing Boring about Boron. *Eur. J. Integr Med*., **2015**, *14* (4), 35-48. (b) Price, C. T.; Langford, J. R.; Liporace, F. A. Essential nutrients for bone health and a review of their availability in the average North American diet. *Open Orthop. J.*, **2012**, *6*, 143–149. (c) Beattie, J. H.; Peace, H. S. The influence of a low-boron diet and boron supplementation on bone, major mineral and sex steroid metabolism in postmenopausal women. *Br. J. Nutr.,* **1993**, *69* (3), 871-884. (d) Miljkovic, D.; Scorei, R. I.; Cimpoiaşu, V. M.; Scorei, I. D. Calcium fructoborate: plant based dietary boron for human nutrition. *J. Diet. Suppl*., **2009**, *6* (3), 211-226. (e) Stubbs, J. R.; Zhang, S.; Friedman, P. A.; Nolin, T. D. Decreased conversion of 25-hydroxyvitamin D3 to 24,25-dihydroxyvitamin D3 following cholecalciferol therapy in patients with CKD. *Clin. J. Am. Soc. Nephrol.*, **2014**, *9* (11), 1965-1973. (f) Zofková, I.; Nemcikova, P.; Matucha, P. Trace elements and bone health. *Clin. Chem. Lab. Med*., **2013**, *51* (8), 1555-1561.

(5) (a) Viñas, C. The uniqueness of boron as a novel challenging element for drugs in pharmacology, medicine and for smart biomaterials. *Future Med. Chem*., **2013**, *5* (6), 617-619. (b) Chellan, P.; Sadler, P. J. The elements of life and medicines. *Phil. Trans. R. Soc. A.*, **2015**, *373*,

20140182. (c) Pache, W.; Zähner, H. Metabolic products of microorganisms. 77. Studies on the mechanism of action of boromycin. *Arch. Mikrobiol*., **1969**, *67*, 156–165. (d) Soriano-Ursúa, M. A.; Das, B. C.; Trujillo-Ferrara, J. G. Boron-containing compounds: chemico-biological properties and expanding medicinal potential in prevention, diagnosis and therapy. *Expert. Opin. Ther. Pat*., **2014**, *24*, 485–500. (e) Ciaravino, V.; Plattner, J.; Chanda, S. An assessment of the genetic toxicology of novel boron-containing therapeutic agents. *Environ. Mol. Mutagen*., **2013**, *54*, 338–346.

(6) (a) Housecroft, C. E. Boranes and Metalloboranes, Ellis Horwood Limited,: Chichester, UK, **1990**. (b) Housecroft, C. E. Specialist Periodical Reports in Organometallic Chemistry, Abel, E. W.; Stone, F. G. A., Eds.; Royal Society of Chemistry: London, **1991**. (c) Housecroft, C. E., Cluster Molecules of the *p*-Block Elements, Oxford University Press, New York, USA, **1994**.

(7) (a) Wade, K. The Structural Significance of the Number of Skeletal Bonding Electron-pairs in Carboranes, the Higher Boranes and Borane Anions, and Various Transition-metal Carbonyl Cluster Compounds. *J. Chem. Comm. Soc. D.*, **1971**, 792-793. (b) Williams, R. E. Carboranes and Boranes; Polyhedra and Polyhedral Fragments. *Inorg. Chem*., **1971**, *10*, 210-214. (c) Mingos, D. M. P. A General Theory for Cluster and Ring Compounds of the Main Group and Transition Elements. *Nature-Phy. Sci*., **1972**, *236*, 99-102. (d) Rudolph, R. W.; Pretzer, W. R. Hueckel-type rules and the systematization of borane and heteroborane chemistry. *Inorg. Chem*., **1972,** *11*, 1974-1978. (e) Wade, K. Structural and Bonding Patterns in Cluster Chemistry. *Adv. Inorg. Chem. Radiochem*., **1976**, *18*, 1-66. (f) Williams, R. E. Coordination Number Pattern Recognition Theory of Carborane Structures. *Adv. Inorg. Chem. Radiochem*., **1976**, *18*, 67-142. (g) Rudolph, R. W. Boranes and heteroboranes: a paradigm for the electron requirements of clusters? *Acc. Chem. Res*., **1976**, *9*, 446-452.

(8) Grimes, R. N. Carboranes, 3rd Ed.; Elsevier Inc.: New York, **2016**.

(9) (a) Pitochelli, A. R.; Hawthorne, M. F. The isolation of the icosahedral $B_{12}H_{12}^{-2}$ ion. *J. Am. Chem. Soc*., **1960**, *82*, 3228-3229. (b) Miller, H. C.; Miller, N. E.; Muetterties, E. L. Synthesis of Polyhedral Boranes. *J. Am. Chem. Soc.*, **1963**, *85*, 3885-3886.

(10) Poater, J.; Solà, M.; Viñas, C.; Teixidor, F. π Aromaticity and Three-Dimensional Aromaticity: Two sides of the Same Coin? *Angew. Chem. Int. Ed*., **2014**, *53*, 12191–12195.

(11) Peymann, T.; Herzog, A.; Knobler, C. B.; Hawthorne, M. F. Aromatic Polyhedral Hydroxyborates:Bridging Boron Oxides and Boron Hydrides. *Angew. Chem. Int. Ed*., **1999**, *38*, 1061-1064.

(12) Connelly, N. G.; Damhus, T.; Hartshorn, R. M.; Hutton, A. T. *Nomenclature of Inorganic Chemistry, IUPAC Recommendations 2005*, Chapter IR-6, 83-110, RSC publishing, Cambridge, UK, **2005**.

(13) (a) Grimes, R. N. Boron-carbon ring ligands in organometallic synthesis. *Chem. Rev*., **1992**, *92*, 251-268. (b) Saxena, A. K.; Hosmane, N. S. Recent advances in the chemistry of carborane metal complexes incorporating d- and f-block elements. *Chem. Rev*., **1993**, *93*, 1081-1124. (c) Saxena, A. K.; Maguire, J. A.; Hosmane, N. S. Recent Advances in the Chemistry of Heterocarborane Complexes Incorporating s- and p-Block Elements. *Chem. Rev*., **1997**, *97*, 2421-2462.

(14) (a) Fréchet, J. M.; Tomalia, D. A. Eds. Dendrimers and other dendritic polymers, Wiley Series in Polymer Science, Wiley, **2001**. (b) Newkome, G. R.; Moorefield, C. N., Vötgle, F. Dendrimers and Dendrons: Concepts, Synthesis, Applications; Wiley: New York, **2002**. (c) Beletskaya, I. P.; Chuchurjukin, A. V. Synthesis and properties of functionalised dendrimers. *Russ. Chem. Rev.*, **2000**, *69*, 639-660. (d) Astruc, D.; Chardac, F. Dendritic Catalysts and Dendrimers in Catalysis. *Chem. Rev.*, **2001**, *101*, 2991-3024. (e) Newkome, G. R.; Moorefield, C. N.; Vötgle, F. Dendritic Molecules. Concepts, Syntheses, Perspectives; VCH: Weinheim, Germany, **1996**. (f) Vogtle, F.; Richardt, G.; Werner, N. Dendrimer Chemistry: Concepts, Synthesis, Properties, Applications; Wiley: Weinheim, Germany, **2009**. (g) Bosman, A. W.; Janssen, H. M.; Meijer, E. W. About

Dendrimers: Structure, Physical Properties, and Applications. *Chem. Rev.*, **1999**, *99*, 1665-1688. (h) Walter, M. V.; Malkoch, M. Simplifying the synthesis of dendrimers: accelerated approaches. *Chem. Soc. Rev.*, **2012**, *41*, 4593-4609.

(15) (a) Kleij, A. W.; Gossage, R. A.; Gebbink, R. J. M. K.; Brinkmann, N.; Reijerse, E. J.; Kragl, U.; Lutz, M.; Spek, A. L.; van Koten, G. A "Dendritic Effect" in Homogeneous Catalysis with Carbosilane-Supported Arylnickel(II) Catalysts: Observation of Active-Site Proximity Effects in Atom-Transfer Radical Addition. *J. Am. Chem. Soc.*, **2000**, *122*, 12112-12124. (b) Boury, B.; Corriu, J. P. R.; Núñez, R. Hybrid Xerogels from Dendrimers and Arborols. *Chem. Mater.*, **1998**, *10*, 1795-1804.

(16) (a) Yamamoto, K.; Higuchi, M.; Shiki, S.; Tsuruta, M.; Chiba, H. Stepwise radial complexation of imine groups in phenylazomethine dendrimers. *Nature*, **2002**, *415*, 509-511. (b) Frey, H.; Haag, R. Dendritic polyglycerol: a new versatile biocompatible-material. *Rev. Mol. Biotechnol.*, **2002**, *90*, 257-267.

(17) (a) Hecht, S.; Fréchet, J. M. J. Dendritic Encapsulation of Function: Applying Nature's Site Isolation Principle from Biomimetics to Materials Science. *Angew. Chem., Int. Ed.,* **2001**, *40*, 74-91. (b) Stiriba, A.-E.; Frey, H.; Haag, R. Dendritic Polymers in Biomedical Applications: From Potential to Clinical Use in Diagnostics and Therapy. *Angew. Chem., Int. Ed.*, **2002**, *41*, 1329-1334. (c) Oosterom, G. E.; Reek, J. N. ; Kamer, P. C.; van Leeuwen, P.W. Transition Metal Catalysis Using Functionalized Dendrimers. *Angew. Chem. Int. Ed.*, **2001**, *40 (10)*, 1828-1849. (d) Kleij, A. W.; Gossage, R. A.; Jastrezebski, J. T. B. H.; Boersma, J.; van Koten, G. The "Dendritic Effect" in Homogeneous Catalysis with Carbosilane-Supported Arylnickel(ii) Catalysts: Observation of Active-Site Proximity Effects in Atom-Transfer Radical Addition. *Angew. Chem. Int. Ed.*, **2000**, *39*, 176-178.

(18) Reviews of dendrimers: (a) Boas, U.; Heegaard, P. M. H. Dendrimers in drug research. *Chem. Soc. Rev.*, **2004**, *33*, 43-63. (b) Al-Jamal, K. T.; Ramaswamy, C.; Florence, A. T. Supramolecular structures from dendrons and dendrimers. *Adv. Drug. Deliv. Rev.*, **2005**, *57*, 2238-2270. (b) I. J.;

Baker, J. R., Jr. Eds. Dendrimer-Based Nanomedicine; Majoros, Pan Stanford Publishing: Singapore, **2008**. (c) Caminade, A. M.; Majoral, J. -P. Dendrimers and nanotubes: a fruitful association. *Chem. Soc. Rev.*, **2010**, *39*, 2034-2047. (d) Astruc, D.; Boisselier, E.; Ornelas, C. Dendrimers Designed for Functions: From Physical, Photophysical, and Supramolecular Properties to Applications in Sensing, Catalysis, Molecular Electronics, Photonics, and Nanomedicine. *Chem. Rev.*, **2010**, *110*, 1857-1959. (e) Newkome, G. R.; Shreiner C. Dendrimers Derived from 1 → 3 Branching Motifs. *Chem. Rev.*, **2010**, *110*, 6338-6442. (f) Sowinska, M.; Urbanczyk-Lipkowska, Z. Advances in the chemistry of dendrimers. *New J. Chem.*, **2014**, *38*, 2168–2203.

(19) (a) Caminade, A. M. Inorganic dendrimers: recent advances for catalysis, nanomaterials, and nanomedicine. *Chem. Soc. Rev*., **2016**, *45*, 5174-5186. (b) Briz, V.; Serramia, M. J.; Madrid, R.; Hameau, A.; Caminade, A. M.; Majoral, J. P.; Muñoz-Fernández, M. A. Validation of a Generation 4 Phosphorus-Containing Polycationic Dendrimer for Gene Delivery Against HIV-1. *Curr. Med. Chem.*, **2012**, *19*, 5044–5051. (c) Caminade, A. M.; Ouali, A.; Laurent, R.; Turrin, C. O.; Majoral, J. P. Coordination chemistry with phosphorus dendrimers. Applications as catalysts, for materials, and in biology. *Coord. Chem. Rev.*, **2016**, *308*, 478–497. (d) Wang, L., Yang, Y. -X.. Shi, X., Mignani, S., Caminade A. M.; Majoral, J. P. Cyclotriphosphazene core-based dendrimers for biomedical applications: an update on recent advances. *J. Mater. Chem. B.*, **2018**, *6*, 884-895. (e) Serramia, M. J.; Álvarez, S.; Fuentes-Paniagua, E.; Clemente, M. I.; Sánchez-Nieves, J.; Gómez, R.; de la Mata, J.; Muñoz-Fernández, M. A. In vivo delivery of siRNA to the brain by carbosilane dendrimer. *J. Controlled Release.*, **2015**, *200*, 60–70. (f) Sowinska, M.; Urbanczyk-Lipkowska, Z. Advances in the chemistry of dendrimers. *New J. Chem.*, **2014**, *38*, 2168–2203. (g) Caminade, A. M. Phosphorus dendrimers for nanomedicine. *Chem. Commun.*, **2017**, *53*, 9830-9838.

(20) Menjoge, A. R.; Kannan, R. M.; Tomalia, D. A. Dendrimer-based drug and imaging conjugates: design considerations for nanomedical applications. *Drug Discov. Today.*, **2010**, *15*, 171-185.

(21) Cheng, Y. in *Dendrimer-Based Drug Delivery Systems: From Theory to Practice*, Wiley, **2012**, ISBN: 978-1-118-27522-1.

(22) Khandare, J.; Calderón, M.; Diaga, N. M.; Haag, R. Multifunctional dendritic polymers in nanomedicine: opportunities and challenges. *Chem. Soc. Rev*., **2012**, *41,* 2824-2848.

(23) Plesek, J. Potential Applications of the Boron Cluster Compounds. *Chem. Rev*., **1992**, *92*, 269-278.

(24) Sweet, W. N.; Soloway, A. H.; Wright, R. L. Evaluation of boron compounds for use in neutron capture therapy of brain tumors .2. Studies in man. *J. Pharmac. Exp. Ther.*, **1962**, *137*, 263-266.

(25) (a) Newkome, G. R.; Moorefield, C. N.; Keith, J. M.; Baker, G. R.; Escamilla, G. H. Chemistry within a Unimolecular Micelle Precursor: Boron Superclusters by Site- and Depth-Specific Transformations of Dendrimers. *Angew. Chem. Int. Ed. Engl.*, **1994**, *33*, 666-668. (b) Barth, R. F.; Adams, D. M.; Soloway, A. H.; Alam, F.; Darby, M. V. Boronated starburst dendrimer-monoclonal antibody immunoconjugates: Evaluation as a potential delivery system for neutron capture therapy. *Bioconjug. Chem.*, **1994**, *5*, 58-66. (c) Armspach, D.; Cattalini, M.; Constable, E. C.; Housecroft, C. E.; Phillips, D. Boron-rich metallodendrimers—mix-and-match assembly of multifunctional metallosupramolecules. *Chem. Commun*., **1996**, 1823-1824. (d) Qualmann, B.; Kessels, M. M.; Mussiol, H.-J.; Sierralta, W. D.; Jungblut, P.W.; Moroder, L. Synthesis of Boron-Rich Lysine Dendrimers as Protein Labels in Electron Microscopy. *Angew. Chem. Int. Ed. Engl.*, **1996**, *35*, 909-911.

(26) (a) Skukla, M. S.; Gong, W.; Chatterjee, M.; Yang, W.; Sekido, M.; Diop, L. A.; Müller, R.; Sudimack, J. J.; Lee, R. J.; Barth, R. F.; Tjarks, W. Synthesis and Biological Evaluation of Folate Receptor-Targeted Boronated PAMAM Dendrimers as Potential Agents for Neutron Capture Therapy. *Bioconjug. Chem.*, **2003***,* 14, 158-167. (b) Barth, R. F.; Coderre, J. A.; Vicente, M. G. H.; Blue, T. E. Boron neutron capture therapy of cancer: current status and future prospects. *Clin. Cancer Res.*, **2005**, *11*, 3987-4002. (c) Backer, M. V.; Gaynutdinov, T. I.; Patel, V.;

Bandyopadhyaya, A. K.; Thirumamagal, B. T. S.; Tjarks, W.; Barth, R. F.; Claffey, K.; Backer, J. M. Vascular endothelial growth factor selectively targets boronated dendrimers to tumor vasculature. *Mol. Cancer Ther.,* **2005***, 4,* 1423.

(27) (a) Dash, B. P.; Satapathy, R.; Maguire, J. A.; Hosmane, N. S. Boron-enriched star-shaped molecule viacycloaddition reaction. *Chem. Commun*., **2009**, 3267-3269. (b) Dash, B. P.; Satapathy, R.; Gaillsard, E. R.; Maguire, J. A.; Hosmane, N. S. Synthesis and Properties of Carborane-Appended C3-Symmetrical Extended π Systems. *J. Am. Chem. Soc.*, **2010**, *132*, 6578-6587. (c) Dash, B .P.; Satapathy, R.; Maguire, J. A.; Hosmane, N. S. Facile Synthetic Routes to Phenylene and Triazine Core Based Dendritic Cobaltabisdicarbollides. *Organometallics.,* **2010**, *29*, 5230-5235. (d) Dash, B. P.; Satapathy, R.; Gaillsard, E. R.; Norton, K. M.; Maguire, J. A.; Chug, N.; Hosmane, N. S. Enhanced π-Conjugation and Emission via Icosahedral Carboranes: Synthetic and Spectroscopic Investigation. *Inorg. Chem*., **2011**, *50*, 5485-5493.

(28) (a) Parrott, C.; Marchington, E. B.; Valliant, J. F.; Adronov, A. J. Synthesis and Properties of Carborane-Functionalized Aliphatic Polyester Dendrimers. *J. Am. Chem. Soc*., **2005**, *127*, 12081-12089. (b) Parrott, M. C.; Valliant, J. F.; Adronov, A. Thermally Induced Phase Transition of Carborane-Functionalized Aliphatic Polyester Dendrimers in Aqueous Media. *Langmuir*., **2006**, *22*, 5251-5255.

(29) (a) Núñez, R.; González, A.; Viñas, C.; Teixidor, F.; Sillanpää, R.; Kivekäs, R. Approaches to the Preparation of Carborane-Containing Carbosilane Compounds. *Org. Lett*., **2005**, *7*, 231. (b) Núñez, R.; González-Campo, A.; Viñas, C.; Teixidor, F.; Sillanpää, R.; Kivekäs, R. Boron-Functionalized Carbosilanes: Insertion of Carborane Clusters into Peripheral Silicon Atoms of Carbosilane Compounds. *Organometallics.,* **2005**, *24*, 6351-6357.

(30) Juárez-Pérez, E. J.; Viñas, C.; Teixidor, F.; Núñez, R. Polyanionic Carbosilane and Carbosiloxane Metallodendrimers Based on Cobaltabisdicarbollide Derivatives. *Organometallics.*, **2009**, *28*, 5550-5559.

(31) González-Campo, A.; Viñas, C.; Teixidor, F.; Núñez, R.; Sillanpää, R.; Kivekäs, R. Modular Construction of Neutral and Anionic Carboranyl-Containing Carbosilane-Based Dendrimers. *Macromolecules*., **2007**, *40*, 5644-5652.

(32) (a) Ye, Q.; Zhou H.; Xu, J. Cubic Polyhedral Oligomeric Silsesquioxane Based FunctionalMaterials:Synthesis, Assembly, and Applications. *Chem. Asian J.*, **2016**, *11*, 1322-1337. (b) Laine, R. M.; Roll, M. F. Polyhedral Phenylsilsesquioxanes. *Macromolecules.*, **2011**, *44* (55), 1073-1109. (c) Sulaiman, S.; Zhang, J.; Goodson, I. I. I. T.; Laine, R. M. Synthesis, characterization and photophysical properties of polyfunctional phenylsilsesquioxanes: [*o*-$RPhSiO_{1.5}]_8$, [2,5-$R_2PhSiO_{1.5}]_8$, and $[R_3PhSiO_{1.5}]_8$ compounds with the highest number of functional units/unit volume. *J. Mater. Chem.*, **2011**, *21*, 11177-11187. (d) Cordes, D. B.; Lickiss, P. D.; Rataboul, F. Recent developments in the chemistry of cubic polyhedral oligosilsesquioxanes. *Chem. Rev.*, **2010**, *110*, 2081-2173.

(33) Hartmann-Thompson, C. *Applications of Polyhedral Oligomeric Silsesquioxanes*, Springer Netherlands, Midland, **2011**.

(34) (a) Bahrami, M.; Furgal, J. C.; Hashemi, H.; Ehsani, M.; Jahani, Y.; Goodson, T.; Kieffer J.; Laine, R. M. Synthesis and Characterization of Nanobuilding Blocks [o-$RStyrPhSiO_{1.5}]_{10,12}$ (R = Me, MeO, NBoc, and CN). Unexpected Photophysical Properties Arising from Apparent Asymmetric Cage Functionalization as Supported by Modeling Studies. *J. Phys. Chem. C.*, **2015**, *119*, 15846-15858. (b) Zhang, T.; Wang, J.; Zhou, M.; Ma, L.; Yin, G.; Chen G.; Li, Q. Influence of polyhedral oligomeric silsesquioxanes (POSS) on blue light-emitting materials for OLED. *Tetrahedron.*, **2014**, *70* (14), 2478-2486. (c) Furgal, J. C.; Jung, J. H.; Clark, S.; Goodson T.; Laine, R. M. Beads on a Chain (BoC) Phenylsilsesquioxane (SQ) Polymers via F– Catalyzed Rearrangements and ADMET or Reverse Heck Cross-coupling Reactions: Through Chain, Extended Conjugation in 3-D with Potential for Dendronization. *Macromolecules.*, **2013**, *46* (19), 7591-7604. (d) Chan, K. L.; Sonar, P.; Sellinger, A. Cubic silsesquioxanes for use in solution processable organic light emitting diodes (OLED). *J. Mater. Chem.*, **2009**, *19*, 9103-9120. (e) Lo, M. Y.; Ueno, K.; Tanabe, H.;

Sellinger, Silsesquioxane-Based Nanocomposite Dendrimers With Photo-luminescent and Charge Transport Properties. A., *Chem. Rec.*, **2006**, *6*, 157-168.

(35) (a) Maegawa, T.; Miyashita, O.; Irie, Y.; Imoto, H.; Naka, K. Synthesis and properties of polyimides containing hexaisobutyl-substituted T8 cages in their main chains. *RSC. Adv.*, **2016**, *6*, 31751-31757. (b) Huang, S.; Qiu, Z. Enhanced Thermal Stability and Crystallization Rate of Biodegradable Poly(butylene adipate) by a Small Amount of Octavinyl-Polyhedral Oligomeric Silsesquioxanes. *Ind. Eng. Chem. Res.*, **2014**, *53*, 15296-15300. (c) Ro, H. W.; Soles, C. L. Silsesquioxanes in nanoscale patterning applications. *Mater. Today.*, **2011**, *14*, 20-33. (d) Pielichowski, K.; Njuguna, J.; Janowski, B.; Pielichowski, J. in *Supramolecular Polymers Polymeric Betains Oligomers*, Springer Berlin Heidelberg, **2006**, *201*, ch. 77, pp. 225-296.

(36) Ghanbari, H.; Cousins, B. G.; Seifalian, A. M. A Nanocage for Nanomedicine: Polyhedral Oligomeric Silsesquioxane (POSS). *Macromol. Rapid. Commun.*, **2011**, *32*, 1032-1046.

(37) (a) Nemoto, H.; Wilson, J. G.; Nakamura, H.; Yamamoto, Y. Polyols of a cascade type as a water-solubilizing element of carborane derivatives for boron neutron capture therapy. *J. Org. Chem.*, **1992**, *57* (2), 435-435. (b) Nemoto, H.; Cai, J.; Yamamoto, Y. Synthesis of a water-soluble o-carbaborane bearing a uracil moiety via a palladium-catalysed reaction under essentially neutral conditions. *J. Chem. Soc., Chem. Commun.*, **1994**, 577-578.

(38) (a) Knoth, W. H.; Miller, H. C.; England, D. C.; Parshall, G. W.; Muetterties, E. L. Derivative Chemistry of $B_{10}H_{10}^-$ and $B_{12}H_{12}^-$. *J. Am. Chem. Soc.*, **1962**, *84* (6), 1056-1057. (b) Olid, D.; Nuñez, R.; Viñas, C.; Teixidor, F. Methods to produce B–C, B–P, B–N and B–S bonds in boron clusters. *Chem. Soc. Rev.*, **2013**, *42*, 3318-3336.

(39) Hawthorne, M. F.; Carborane Chemistry at Work and at Play, Proceedings of the Ninth International Meeting on Boron Chemistry. In *Advances in Boron Chemistry*, W. Siebert Ed. (Special Publication No. 201, Royal Society of Chemistry, London, **1997**, 261-272.

(40) (a) Maderna, A.; Knobler, C. B.; Hawthorne, M. F. Twelvefold Functionalization of an Icosahedral Surface by Total Esterification of $[B_{12}(OH)_{12}]^{2-}$: 12(12)-Closomers. *Angew. Chem. Int.*

Ed., **2001**, *40* (9), 1661-1664. (b) Peymann, T.; Knobler, C. B.; Khan, S. I.; Hawthorne, M. F. Dodeca(benzyloxy)dodecaborane, B(12)(OCH(2)Ph)(12): A Stable Derivative of hypercloso-B(12)H(12) This work was supported by the U.S. Department of Energy (DE-FG02-95ER61975) and the National Science Foundation (NSF CHE 9730006 and NSF CHE 9871332). *Angew. Chem. Int. Ed*., **2001**, *40*(9), 1664-1667.

(41) Thomas, J.; Hawthorne, M. F. Dodeca(carboranyl)-substituted closomers: toward unimolecular nanoparticles as delivery vehicles for BNCT. *Chem. Commun.*, **2001**, 1884-1885.

(42) (a) Goswami, L. N.; Ma, L. X.; Chakravarty, S.; Cai, Q. Y.; Jalisatgi, S. S.; Hawthorne, M. F. Discrete Nanomolecular Polyhedral Borane Scaffold Supporting Multiple Gadolinium(III) Complexes as a High Performance MRI Contrast Agent. *Inorg. Chem*., **2013**, *52* (4), 1694-1700. (b) Goswami, L. N.; Ma, L. X.; Kueffer, P. J.; Jalisatgi, S. S.; Hawthorne, M. F. Synthesis and Relaxivity Studies of a DOTA-Based Nanomolecular Chelator Assembly Supported by an Icosahedral Closo-B-12(2-)-Core for MRI: A Click Chemistry Approach. *Molecules.*, **2013**, *18* (8), 9034-9048.

(43) Goswami, L. N.; Khan, A. A.; Jalisatgi, S. S.; Hawthorne, M. F. Synthesis and in vitro assessment of a bifunctional closomer probe for fluorine (^{19}F) magnetic resonance and optical bimodal cellular imaging. *Chem. Commun*., **2014**, *50*, 5793-5795.

(44) (a) Sibrian-Vazquez, M.; Vicente, M. G. H. *Boron Tumor-Delivery for BNCT: Recent Developments and Perspectives in Boron Science: New Technologies and Applications* (ed. Hosmane, N.S.) 209 (Taylor & Francis, Bosa Roca), **2012**. (b) Scholz, M.; Hey-Hawkins, E. Carbaboranes as Pharmacophores: Properties, Synthesis, and Application Strategies. *Chem. Rev.*, **2011**, *111*, 7035-7062. (c) Sivaev, I.B.; Bregadze, V.V. Polyhedral Boranes for Medical Applications: Current Status and Perspectives. *Eur. J. Inorg. Chem*., **2009**, 1433-1450. (d) Bregadze, V. I.; Sivaev, I. B.; Glazun, S. A. Polyhedral boron compounds as potential diagnostic and therapeutic antitumor agents. *Anticancer Agents Med. Chem*., **2006**, *6*, 75-109. (e) Lesnikowski, Z. J. Challenges and Opportunities for the Application of Boron Clusters in Drug

Design. *J. Med. Chem*., **2016**, *59(17)*, 7738-7758. (f) Valliant, J. F.; Guenther, K. J.; King, A. S.; Morel, P.; Schaffer, P.; Sogbein, O. O.; Stephenson, K. A. The medicinal chemistry of carboranes. *Coord. Chem. Rev*., **2002**, *232*, 173-230. (g) Armstrong, A. F.; Valliant, J. F. The bioinorganic and medicinal chemistry of carboranes: from new drug discovery to molecular imaging and therapy. *Dalton Trans*., **2007**, 4240-4251. (h) Hawthorne, M. F.; Maderna, A. Applications of Radiolabeled Boron Clusters to the Diagnosis and Treatment of Cancer. *Chem. Rev*., **1999**, *99*, 3421-3434. (i) Issa, F.; Kassiou, M.; Rendina, L.M. Boron in Drug Discovery: Carboranes as Unique Pharmacophores in Biologically Active Compounds. *Chem. Rev*., **2011**, *111(9)*, 5701-5722.

(45) Takagaki, M.; Tomaru, T.; Maguire, J.A. & Hosmane, N.S. *Future Applications of Boron and Gadolinium Neutron Capture Therapy in Boron Science: New Technologies and Applications* 243 (Taylor & Francis, Bosa Roca), **2012**.

(46) (a) Luderer, M.J.; de la Puente, P.; Azab, A.K. Advancements in Tumor Targeting Strategies for Boron Neutron Capture Therapy. *Pharm. Res.*, **2015**, *32*, 2824-2836. (b) Matuszewski, M.; Kiliszek, A.; Rypniewski, W.; Lesnikowski, Z.J.; Olejniczak, A. B. Nucleoside bearing boron clusters and their phosphoramidites-building blocks for modified oligonucleotide synthesis. *New J. Chem.*, **2015**, *39*, 1202-1221.

(47) Hiroyuki, N. Boron lipid-based liposomal boron delivery system for neutron capture therapy: recent development and future perspective. *Future Med. Chem.*, **2013**, *5*, 715-730.

(48) (a) Leśnikowski, Z. J. Challenges and Opportunities for the Application of Boron Clusters in Drug Design. *J. Med. Chem.*, **2016**, *59*, 7738-7758. (b) Ban, H.S.; Nakamura, H. Boron-Based Drug Design. *Chem. Rec.*, **2015**, *15*, 616-635.

(49) Barth, R.F.; *Vicente, M. G.; Harling O. K.; Kiger, W.S.; Riley, K. J.; Binns, P. J.; Wagner, F. M.; Suzuki, M.; Aihara, T.; Kato, I.; Kawabata, S.* Current status of boron neutron capture therapy of high grade gliomas and recurrent head and neck cancer. *Radiat. Oncol.*, **2012**, *7*, 146-146.

(50) Hawthorne, M. F.; Young, D. C.; Wegner, P. A. Carbametallic Boron Hydride Derivatives. I. Apparent Analogs of Ferrocene and Ferricinium Ion. *J. Am. Chem. Soc.*, **1965**, *87*, 1818-1819.

(51) Masalles, C.; Llop, J.; Viñas, C.; Teixidor, F. Extraordinary Overoxidation Resistance Increase in Self-Doped Polypyrroles by Using Non-conventional Low Charge-Density Anions. *Adv. Mater*., **2002**, *14*, 826-829.

(52) (a) Sivaev, I. B.; Bregadze, V. I. Chemistry of Cobalt Bis(dicarbollides). A Review. *Collect. Czech. Chem. Commun.* **1999**, *64*, 783-805. (b) Juárez-Pérez, E. J.; Núñez, R.; Viñas, C.; Sillanpää, R.; Teixidor, F. The Role of C–H···H–B Interactions in Establishing Rotamer Configurations in Metallabis(dicarbollide) Systems. *Eur. J. Inorg. Chem.*, **2010**, 2385-2392. (C) Dash, B. P.; Satapathy, R.; Swain, B. R.; Mahanta, C. S.; Jena, B.; Hosmane, N. S. Cobalt bis(dicarbollide) anion and its derivatives. *J. Organomet. Chem.,* **2017**, *849-850*, 170-194.

(53) (a) Chamberlin, R. M.; Scott, B. L.; Melo, M. M.; Abney, K. D. Butyllithium Deprotonation vs Alkali Metal Reduction of Cobalt Dicarbollide: A New Synthetic Route to C-Substituted Derivatives. *Inorg. Chem.*, **1997**, *36* (5), 809-817. (b) Rojo, I.; Teixidor, F.; Viñas, C.; Kivekäs, R.; Sillanpää, R. Synthesis and Coordinating Ability of an Anionic CobaltabisdicarbollideLigand Geometrically Analogous to BINAP. *Chem. Eur. J.*, **2004**, *10* (21)*,* 5376-5385. (c) Juárez-Pérez, E. J.; Viñas, C.; González-Campo, A.; Teixidor, F.; Kivekäs, R.; Sillanpää R.; Núñez, R. Controlled Direct Synthesis of C-Mono- and C-Disubstituted Derivatives of $[3,3'\text{-}Co(1,2\text{-}C_2B_9H_{11})_2]^-$ with Organosilane Groups: Theoretical Calculations Compared with Experimental Results. *Chem. Eur. J.*, **2008**, *14* (16), 4924. (d) Juárez-Pérez, E. J.; Viñas, C.; Teixidor, F.; Núñez, R. First example of the formation of a Si–C bond from an intramolecular Si–H···H–C diyhydrogen interaction in a metallacarborane: A theoretical study. *J. Organomet. Chem.*, **2009**, *694* (11), 1764-1770.

(54) (a) Viñas, C.; Pedrajas, J.; Bertrán, J.; Teixidor, F.; Kivekäs, R.; Sillanpää, R. Synthesis of Cobaltabis(dicarbollyl) Complexes Incorporating Exocluster SR Substituents and the Improved Synthesis of $[3,3'\text{-}Co(1\text{-}R\text{-}2\text{-}R'\text{-}1,2\text{-}C_2B_9H_9)_2]^-$ Derivatives. *Inorg. Chem.*, **1997**, *36* (11), 2482-2486. (b) Viñas, C.; Gómez, S.; Bertrán, J.; Teixidor, F.; Dozol, J. F.; Rouquette, H. Cobaltabis(dicarbollide) derivatives as extractants for europium from nuclear wastes. *Chem. Commun.*, **1998**, 191-192. (c) Viñas, C.; Gómez, S.; Bertrán, J.; Teixidor, F.; Dozol, J. F.; Rouquette,

H. New Polyether-Substituted Metallacarboranes as Extractants for ^{137}Cs and ^{90}Sr from Nuclear Wastes. *Inorg. Chem.*, **1998**, *37*(14), 3640-3643. (d) Viñas, C.; Bertrán, J.; Gómez, S; Teixidor, F.; Dozol, J. F.; Rouquette, H.; Kivekäs, R.; Sillanpää, R. Aromatic substituted metallacarboranes as extractants of ^{137}Cs and ^{90}Sr from nuclear wastes. *J. Chem. Soc. Dalton. Trans.,* **1998**, 2849-2854. (e) Viñas, C.; Pedrajas, J.; Teixidor, F.; Kivekäs R.; Sillanpää, R.; Welch, A. First Example of a Bis(dicarbollide) Metallacarborane Containing a B,C′-Heteronuclear Bridge. *J. Inorg. Chem*., **1997,** *36* (14), 2988-2991.

(55) (a) Teixidor, F.; Viñas, C.; Demonceau, A.; Nuñez, R. Boron clusters: Do they receive the deserved interest? *Pure. Appl. Chem*., **2003**, *75* (9), 1305-1313. (b) Grimes, R. N. *Carboranes*, 2nd Edn, Academic Press: Burlington, MA, **2011**.

(56) Teixidor, F.; Barberà, G.; Vaca, A.; Kivekäs, R.; Sillanpää, R.; Oliva, J.; Viñas, C. Are Methyl Groups Electron-Donating or Electron-Withdrawing in Boron Clusters? Permethylation of o-Carborane. *J. Am. Chem. Soc.*, **2005**, *127* (29), 10158-10159.

(57) Puga, A. V.; Teixidor, F.; Sillanpää, R.; Kivekäs, R.; Arca, M.; Barberà, G.; Viñas, C. From Mono- to Poly-Substituted Frameworks: A Way of Tuning the Acidic Character of C_c-H in o-Carborane Derivatives. *Chem. Eur. J.,* **2009**, *15*, 9755–9763.

(58) Núñez, R.; González-Campo, A.; Laromaine, A.; Teixidor, F.; Sillanpää, R.; Kivekäs, R.; Viñas, C. Synthesis of Small Carboranylsilane Dendrons as Scaffolds for Multiple Functionalizations. *Org. Lett.*, **2006**, *8* (20), 4549-4552.

(59) (a) Gómez, F. A.; Hawthorne, M. F. A simple route to C-monosubstituted carborane derivatives. *J. Org. Chem.*, **1992**, *57* (5), 1384-1390. (b) Wang, S.; Yang, Q.; Mak, T. C. W.; Xie, Z. Carbon versus Silicon Bridges. Synthesis of a New Versatile Ligand and Its Applications in Organolanthanide Chemistry. *Organometallics.,* **2000**, *19* (3), 334-343. (c) Xie, Z. Cyclopentadienyl−Carboranyl Hybrid Compounds: A New Class of Versatile Ligands for Organometallic Chemistry. *Acc. Chem. Res*, **2003**, *36* (1), 1-9. (d) González-Campo, A.; Boury, B.;

Teixidor, F.; Núñez, R. Carboranyl Units Bringing Unusual Thermal and Structural Properties to Hybrid Materials Prepared by Sol−Gel Process. *Chem. Mater.* **2006**, *18* (18), 4344-4353.

(60) Farràs, P.; Teixidor, F.; Kivekäs, R.; Sillanpää, R.; Viñas, C; Grüner, B.; Cisarova, I. Metallacarboranes as Building Blocks for Polyanionic Polyarmed Aryl-Ether Materials. *Inorg. Chem.*, **2008**, *47* (20), 9497-9508.

(61) Viñas, C.; Núñez, R.; Teixidor, F. Large Molecules Containing Icosahedral Boron Clusters Designed for Potential Applications in Boron Science, Hosmane, N. S. Ed.; CRC Press Taylor & Francis Group: Boca Raton, **2012**.

(62) Šícha, V.; Farràs, P.; Štíbr, B.; Teixidor, F.; Grüner, B.; Viñas, C. Syntheses of C-substituted icosahedral dicarbaboranes bearing the 8-dioxane-cobalt bisdicarbollide moiety. *J. Organomet. Chem.*, **2009**, *694* (11), 1599-1601.

(63) Llop, J.; Masalles C.; Viñas C.; Teixidor F.; Sillanpää R.; Kivekäs, R. The $[3,3'\text{-}Co(1,2\text{-}C_2B_9H_{11})_2]^-$ anion as a platform for new materials: synthesis of its functionalized monosubstituted derivatives incorporating synthons for conducting organic polymers. *Dalton Trans.*, **2003**, *4*, 556-561.

(64) (a) Sivaev, I. B.; Starikova, Z. A.; Sjöberg S.; Bregadze, V. I. Synthesis of functional derivatives of the $[3,3'\text{-}Co(1,2\text{-}C_2B_9H_{11})_2]^-$ anion. *J. Organomet. Chem.*, **2002**, *649*, 1-8. (b) Sivaev, I. B.; Sjöberg S.; Bregadze, V. I., Materials of the Next Century, Nizhny Novgorod, Russia, May 29-June **2000**.

(65) Plešek, J.; Grüner, B.; Heřmánek, S.; Báča, J.; Mareček, V.; Jänchenová, J.; Lhotský, A.; Holub, K.; Selucký, P.; Rais, J.; Císařová, I.; Čáslavský, J. Synthesis of functionalized cobaltacarboranes based on the *closo*-$[(1,2\text{-}C_2B_9H_{11})_2\text{-}3,3'\text{-}Co]$ ion bearing polydentate ligands for separation of M^{3+} cations from nuclear waste solutions. Electrochemical and liquid-liquid extraction study of selective transfer of M^{3+} metal cations to an organic phase. Molecular structure of the *closo*-$[(8\text{-}(2\text{-}CH_3O\text{-}C_6H_4\text{-}O)\text{-}(CH_2CH_2O)2\text{-}1,2\text{-}C_2B_9H_{10})\text{-}(1',2'\text{-}C_2B_9H_{11})\text{-}3,3'\text{-}Co]Na$ determined by X-ray diffraction analysis. *Polyhedron.*, **2002**, *21*, 975-986.

(66) Grüner, B.; Plešek, J.; Báča, J.; Císařová, I.; Dozol, J.-F.; Rouquette, H.; Viňas, C.; Selucký, P.; Rais, J. Cobalt bis(dicarbollide) ions with covalently bonded CMPO groups as selective extraction agents for lanthanide and actinide cations from highly acidic nuclear waste solutions. *New J. Chem.*, **2002**, *26*, 1519-1527.

(67) Teixidor, F.; Pedrajas, J.; Rojo, I.; Viñas, C.; Kivekäs, R.; Sillanpää, R.; Sivaev, I.; Bregadze, V.; Sjöberg, S. Chameleonic Capacity of $[3,3'\text{-}Co(1,2\text{-}C_2B_9H_{11})_2]^-$ in Coordination. Generation of the Highly Uncommon S(thioether)−Na Bond. *Organometallics.*, **2003**, *22* (17), 3414-3423.

(68) (a) Grüner, B.; Mikulasek, L.; Baca, J.; Cisarova, I.; Böhmer, V.; Danila, C.; Reinoso-Garcia, M. M.; Verboom, W.; Reinhoudt, D. N.; Casnati, A.; Ungaro, R. Cobalt Bis(dicarbollides)(1–) Covalently Attached to the Calix[4]arene Platform: The First Combination of Organic Bowl-Shaped Matrices and Inorganic Metallaborane Cluster Anions. *Eur. J. Org. Chem.*, **2005**, *10*, 2022-2039. (b) Mikulasek, L.; Grüner, B.; Danila, C.; Bohmer, V.; Caslavsky, J.; Selucky, P. Synergistic effect of ligating and ionic functions, prearranged on a calix[4]arene. *Chem. Commun.* **2006**, *38*, 4001-4003.

(69) (a) Olejniczak, A. B.; Plesek, J.; Kriz, O.; Lesnikowski, Z. J. A Nucleoside Conjugate Containing a Metallacarborane Group and Its Incorporation into a DNA Oligonucleotide. *Angew. Chem. Int. Ed.* **2003**, *42*, 5740-5743. (b) Leśnikowski, Z. J.; Paradowska, E.; Olejniczaka, A. B.; Studzińska, M.; Seekamp, P.; Schüßler, U.; Gabel, D.; Schinazi, R. F.; Plešek, J. Towards new boron carriers for boron neutron capture therapy: metallacarboranes and their nucleoside conjugates. *Bioorg. Med. Chem.*, **2005**, *13*, 4168-4175. (c) Olejniczak, A. B.; Plesek, J.; Lesnikowski, Z. J. Nucleoside–Metallacarborane Conjugates for Base-Specific Metal Labelingof DNA. *Chem. Eur. J.*, **2007**, *13*, 311-318.

(70) Farràs, P.; Cioran, A. M.; Šícha, V.; Teixidor, F.; Štíbr, B.; Grüner, B.; Viñas, C. Toward the Synthesis of High Boron Content Polyanionic Multicluster Macromolecules. *Inorg. Chem*., **2009**, *48*, 8210–8219.

(71) (a) Wiesboeck, R. A.; Hawthorne, M. F. Dicarbaundecaborane(13) and Derivatives. *J. Am. Chem. Soc.*, **1964**, *86*, 1642-1643. (b) Garret, P. M.; Tebbe, F. N.; Hawthorne, M. F. The Thermal Isomerization of C-Phenyldicarbaundecaborate(12). *J. Am. Chem. Soc*., **1964***, 86* (22), 5016-5017. (c) Hawthorne, M. F.; Young, D. C.; Garret, P. M.; Owen, D. A.; Schwerin, S. G.; Tebbe, F. N.; Wegner, P. M. Preparation and characterization of the (3)-1,2- and (3)-1,7-dicarbadodecahydroundecaborate(-1) ions. *J. Am. Chem. Soc.*, **1968***, 90* (4)*,* 862-868.

(72) (a) Zakharkin, L. I.; Kalinin, V. N. On the reaction of amines with barenes. *Tetrahedron Lett.,* **1965**, *6* (7), 407-409. (b) Zakharkin, L. I.; Kirillova, V. S. Cleavage of o-carboranes to (3)-l,2-dicarbaundecarborates by amines. *Izv. Akad. Nauk SSSR, Ser. Khim*., **1975**, 24, 2596-2598. (c) Taoda, Y.; Sawabe, T.; Endo, Y.; Yamaguchi, K.; Fujii, S.; Kagechika, H. Identification of an intermediate in the deboronation of ortho-carborane: an adduct of ortho-carborane with two nucleophiles on one boron atom. *Chem. Commun.*, **2008**, 2049-2051.

(73) (a) Fox, M. A.; Gill, W. R.; Herbertson, P. L.; MacBride, J. A. H.; Wade, K. Deboronation of c-substituted ortho- and meta-closo-carboranes using "wet" fluoride ion solutions. *Polyhedron.,* **1996**, *16*, 565-571. (b) Fox, M. A.; MacBride, J. A. H.; Wade, K. Fluoride-ion deboronation of p-fluorophenyl-ortho- and -meta-carboranes. NMR evidence for the new fluoroborate, $HOBHF_2^-$. *Polyhedron.*, **1997**, *16*, 2499-2507. (c) Fox, M.A.; Wade, K. Cage-fluorination during deboronation of meta-carboranes. *Polyhedron.*, **1997**, *16*, 2517-2525. (d) Yoo, J.; Hwang, J. W.; Do, Y. Facile and Mild Deboronation of o-Carboranes Using Cesium Fluoride. *Inorg. Chem.*, **2001**, *40* (3), 568-570.

(74) Davidson, M. G.; Fox, M. A.; Hibbert, T. G.; Howard, J. A. K.; Mackinnon, A.; Neretin, I. S.; Wade, K. Deboronation of ortho-carborane by an iminophosphorane: crystal structures of the novel carborane adduct *nido*-$C_2B_{10}H_{12}{\cdot}HNP(NMe_2)_3$ and the borenium salt $[(Me_2N)_3PNHBNP(NMe_2)_3]_2O^{2+}(C_2B_9H_{12}^-)_2$. *Chem. Commun.*, **1999**, 1649-1650.

(75) Teixidor, F.; Sillanpää, R.; Pepiol, A.; Lupu, M.; Viñas. C. Synthesis of Globular Precursors. *Chem. Eur. J.,* **2015**, *21*, 12778 – 12786

(76) Cigler, P.; Kožišek, M.; Řezačova, P.; Brynda, J.; Otwinowski, Z.; Pokorna, J.; Plešek, J.; Grüner, B.; Doleckova-Marešova, L.; Maša, M.; Sedlaček, J.; Bodem, J.; Krausslich, H. G.; Kral, V.; Konvalinka, J. From nonpeptide toward noncarbon protease inhibitors: Metallacarboranes as specific and potent inhibitors of HIV protease. *Proc. Natl. Acad. Sci. U. S. A.,* **2005**, *102* (43), 15394-15399.

(77) (a) Cioran, A. M.; Musteti, A. D.; Teixidor, F.; Krpetić, Ž.; Prior, I. A.; He, Q.; Kiely, C. J.; Brust, M.; Viñas, C. Mercaptocarborane-Capped Gold Nanoparticles: Electron Pools and Ion Traps with Switchable Hydrophilicity. *J. Am. Chem. Soc.*, **2012**, *134* (1), 212-221. (b) Grzelczak, M. P.; Danks, S. P.; Klipp, R. C.; Belic, D.; Zaulet, A.; Kunstmann-Olsen, C.; Bradley, D. F.; Tsukuda, T.; Viñas, C.; Teixidor, F.; Abramson, J. J.; Brust, M. Ion Transport across Biological Membranes by Carborane-Capped Gold Nanoparticles. *ACS Nano*., **2017**, *11* (12), 12492−12499. (c) Oleshkevich, E.; Teixidor, F.; Rosell, A.; Viñas, C. Merging Icosahedral Boron Clusters and Magnetic Nanoparticles: Aiming toward Multifunctional Nanohybrid Materials. *Inorg. Chem*., **2018**, *57* (1), 462−470. (d) Saha, A.; Oleshkevich, E.; Viñas, C.; Teixidor, F. Biomimetic Inspired Core–Canopy Quantum Dots: Ions Trapped in Voids Induce Kinetic Fluorescence Switching. *Adv. Mater*., **2017**, *29*, 1704238-1704245.

(78) Janczak, S.; Olejniczak, A.; Balabańska, S.; Chmielewski, M. K.; Lupu, M.; Viñas, C.; Lesnikowski, Z. J. Boron clusters as a platform for new materials: synthesis of functionalized *o*-carborane ($C_2B_{10}H_{12}$) derivatives incorporating DNA fragments. *Chem. Eur. J.*, **2015**, *21*, 15118-15122.

(79) Cheung, M.-S.; Chan, H.-S.; Xie, Z. Synthesis and structural characterization of hydroxyethyl- and alkoxyethyl-*o*-carboranes and their alkali and rare earth metal complexes. *Organometallics.*, **2004**, *23*, 517-526.

(80) Brown, T.; Brown, D. J. S. Oligonucleotides and analogues. A Practical Approach, Ed.: F. Eckstein, IRL Press, Oxford, **1991**, p1-24.

(81) Teixidor, F.; Pepiol, A.; Viñas, C. Synthesis of Periphery-Decorated and Core-Initiated Borane Polyanionic Macromolecules. *Chem. Eur. J*., **2015**, *21*, 10650–10653.

(82) Lerouge, F.; Viñas, C.; Teixidor, F.; Núñez, R.; Abreu, A.; Xochitiotzi, E.; Santillán, R.;Farfán, N. High boron content carboranyl-functionalized aryl ether derivatives displaying photoluminescent properties. *Dalton Trans*., **2007**, 1898-1903.

(83) Lerouge, F.; Ferrer-Ugalde, A.; Viñas, C.; Teixidor, F.; Núñez, R.; Abreu, A.; Xochitiotzi, E.; Santillán, R.; Farfán, N. Synthesis and fluorescence emission of neutral and anionic di and tetra carboranyl compounds. *Dalton Trans*., **2011**, 40, 7541-7550.

(84) Núñez, R.; Juárez-Pérez, E. J.; Teixidor, F.; Santillan, R.; Farfán, N.; Abreu, A.; Yépez, R.; Viñas, C. Decorating Poly(alkyl aryl-ether) Dendrimers with Metallacarboranes. *Inorg. Chem*., **2010**, *49*, 9993-10000.

(85) González-Campo, A.; Ferrer-Ugalde, A.; Viñas, C.; Teixidor, F.; Sillanpää, R.; Rodríguez-Romero, J.; Santillan, R.; Farfán, N.; Núñez, R. A Versatile Methodology for the Controlled Synthesis of Photoluminescent High-Boron-Content dendrimers. *Chem. Eur. J.* **2013**, *19*, 6299-6312.

(86) Wu, W.; Zhang, X. Y.; Kang, S. X.; Gao, Y. M. *Chin. Chem. Lett.* **2010**, 21, 312-316.

(87) Juárez-Pérez, E. J.; Viñas, C.; Teixidor, F.; Santillan, R.; Farfán, N.; Abreu, A.; Yépez, R. Núñez, R. Polyanionic Aryl Ether Metallodendrimers Based on Cobaltabisdicarbollide Derivatives. Photoluminescent Properties. *Macromolecules*, **2010**, *43*, 150-159.

(88) Cabrera-González, J.; Xochitiotzi-Flores, E.; Viñas, C.; Teixidor,F.; García-Ortega, H.; Farfán, N.; Santillan, R.; Parella, T.; Núñez, R. High-Boron-Content Porphyrin-Cored Aryl Ether Dendrimers: Controlled Synthesis, Characterization, and Photophysical Properties. *Inorg. Chem.* **2015**, *54*, 5021−5031.

(89) Ferrer-Ugalde, A.; Juárez-Pérez, E. J.; Teixidor, F.; Viñas, C.; Pérez-Inestrosa, E.; Sillanpää, R.; Núñez, R. Synthesis and Characterization of New Fluorescent Styrene-Containing Carborane

Derivatives: The Singular Quenching Role of a Phenyl Substituent. *Chem. Eur. J.* **2012**, *18*, 544-553

(90) González-Campo, A.; Juárez-Pérez, E. J.; Viñas, C.; Boury, B.; Kivekäs, R.; Sillanpää, R.; Núñez, R. Carboranyl Substituted Siloxanes and Octasilsesquioxanes: Synthesis, Characterization, and Reactivity. *Macromolecules* **2008**, *41*, 8458-8466.

(91) (a) Bassindale, A. R.; Mackinnon, I. A.; Maesano, M. G.; Taylor. P. G. The preparation of hexasilsesquioxane (T6) cages by "non aqueous" hydrolysis of trichlorosilanes.*Chem. Commun*. **2003**, 1382. (b) Brook M. A. In *Silicon in Organic, Organometallic, and Polymer Chemistry*, John Wiley & Sons, Inc.: New York, 2000; p.256. (c) Le Roux, C.; Yang, H.; Wenzel, S.; Brook, M. A. Using "Anhydrous" Hydrolysis To Favor Formation of Hexamethylcyclotrisiloxane from Dimethyldichlorosilane. *Organometallics* **1998**, *17*, 556-564. (d) Lu, P.; Paulasaari, J. K.; Weber, W. P. *Organometallics* **1996**, *15*, 4649. (e) Arkhireeva, A.; Hay, J. N.; Manzano, M. Preparation of Silsesquioxane Particles via a Nonhydrolytic Sol−Gel Route. *Chem. Mater.* **2005**, *17*, 875-880.

(92) (a) Itami, Y.; Marciniec, B.; Kubicki, M. Functionalization of Octavinylsilsesquioxane by Ruthenium-Catalyzed Silylative Coupling versus Cross-Metathesis. *Chem. Eur. J.* **2004**, *10*, 1239-1248. (b) Sulaiman, S.; Bhaskar, A.; Zhang, J.; Guda, R.; Goodson III T.; Laine, R. M. Molecules with Perfect Cubic Symmetry as Nanobuilding Blocks for 3-D Assemblies. Elaboration of Octavinylsilsesquioxane. Unusual Luminescence Shifts May Indicate Extended Conjugation Involving the Silsesquioxane Core. *Chem. Mater.*, **2008**, *20*, 5563-5573. (c) Cheng, G.; Vautravers, N. R.; Morris, R. E.; Cole-Hamilton, D. Synthesis of Functional Cubes from Octavinylsilsesquioxane (OVS). *J. Org. Biomol. Chem.* **2008**, *6*, 4662-4667.

(93) Ferrer-Ugalde, A.; Juárez-Pérez, E. J.; Viñas, C.; Teixidor, F.; Núñez, R. Synthesis, Characterization, and Thermal Behavior of Carboranyl–Styrene Decorated Octasilsesquioxanes: Influence of the carborane clusters on photoluminescence. *Chem. Eur. J.* **2013**, 19, 17021–17030.

(94) Cabrera-González, J.; Ferrer-Ugalde, A.; Bhattacharyya, S.; Chaari, M.; Teixidor, F.; Gierschner, J.; Núñez, R. Fluorescent carborane–vinylstilbene functionalised octasilsesquioxanes: synthesis, structural, thermal and photophysical properties. *J. Mater. Chem. C*, **2017**, *5*, 10211-10219.

(95) Cabrera-González, J., Sánchez-Arderiu, V.; Viñas, C.; Parella, T.; Teixidor, F.; Núñez R. Redox-Active Metallacarborane-Decorated Octasilsesquioxanes. Electrochemical and Thermal Properties. *Inorg. Chem.* **2016**, *55 (22)*, 11630–11634

(96) Hosmane, N. S. Boron Science: New Technologies and Applications. CRC Press, Boca Raton. **2012**.

(97) Cigler, P.; Kozisek, M.; Rezacova, P.; Brynda, J.; Otwinowski, Z.; Pokorna, J.; Plesek, J.; Grüner, B.; Doleckova-Maresova, L.; Masa, M.; Sedlacek, J.; Bodem, J.; Krausslich, H. G.; Kral, V.; Konvalinka, J. From nonpeptide toward noncarbon protease inhibitors: Metallacarboranes as specific and potent inhibitors of HIV protease. *Proc. Natl. Acad. Sci. U. S. A*., **2005**, *102* (43), 15394-15399.

(98) (a) Rezacova, P.; Pokorna, J.; Brynda, J.; Kozisek, M.; Cigler, P.; Lepsik, M.; Fanfrlik, J.; Rezac, J.; Saskova, K. G.; Sieglova, I.; Plesek, J.; Sicha, V.; Grüner, B.; Oberwinkler, H.; Sedlacek, J.; Krausslich, H. G.; Hobza, P.; Kral, V.; Konvalinka, J., Design of HIV Protease Inhibitors Based on Inorganic Polyhedral Metallacarboranes. *J. Med. Chem*. **2009**, *52* (22), 7132-7141. (b) Kozisek, M.; Cigler, P.; Lepsik, M.; Fanfrlik, J.; Rezacova, P.; Brynda, J.; Pokorna, J.; Plesek, J.; Grüner, B.; Saskova, K. G.; Vaclavikova, J.; Kral, V.; Konvalinka, J. Inorganic Polyhedral Metallacarborane Inhibitors of HIV Protease: A New Approach to Overcoming Antiviral Resistance. *J. Med. Chem*., **2008**, *51* (15), 4839-4843.

(99) Bauduin, P.; Prevost, S.; Farràs, P.; Teixidor, F.; Diat, O.; Zemb, T. A Theta-Shaped Amphiphilic Cobaltabisdicarbollide Anion: TransitionFrom Monolayer Vesicles to Micelles. *Angew. Chem. Int. Ed*., **2011**, *50*, 5298-5300.

(100) Brusselle, D.; Bauduin, P.; Girard, L.; Zaulet, A.; Viñas, C.; Teixidor, F.; Ly, I.; Diat, O. Yotropic Lamellar Phase Formed from Monolayered q-ShapedCarborane-Cage Amphiphiles. *Angew. Chem. Int. Ed.*, **2013**, *52*, 12114-12118.

(101) Zaulet, A.; Teixidor, F.; Bauduin, P.; Diat, O.; Hirva, P.; Ofori, A.; Viñas, C. Deciphering the role of the cation in anionic cobaltabisdicarbollide clusters. *J. Organomet. Chem*., **2018**, *865*, 214-225.

(102) Verdia-Baguena, C.; Alcaraz, A.; Aguilella, V. M.; Cioran, A.M.; Tachikawa, S.; Nakamura, H.; Teixidor, F.; Viñas, C. Amphiphilic COSAN and I_2-COSAN crossing synthetic lipid membranes: planar bilayers and liposomes. *Chem. Commun.*, ***2014**, 50*, 6700-6703.

(103) (a) Montal, M.; Mueller, P. Formation of Bimolecular Membranes from Lipid Monolayers and a Study of Their Electrical Properties. *Proc. Natl. Acad. Sci. U. S. A.*, **1972**, *69* (12), 3561-3566. (b) Bezrukov, S. M.; Vodyanoy, I. Probing alamethicin channels with water-soluble polymers. Effect on conductance of channel states. *Biophys. J*., **1993**, *64* (1), 16-25.

(104) Tarrés, M.; Canetta, E.; Paul, E.; Forbes, J.; Azzouni, K.; Viñas, C.; Teixidor, F.; Harwood, J. A. Biological interaction of living cells with COSAN-based synthetic vesicles. *Sci. Rep*., **2015**, *5*, 7804.

(105) (a) Kessin, R. H. The evolution of the cellular slime molds: Dictyostelium - A model system for cell and developmental biology. Universal Academy Press, Columbia, **1997**. (b) Olie, R. A.; Durrieu, F.; Cornillon, S.; Loughran, G.; Gross, J.; Earnshaw, W. C.; Golstein, P. Apparent caspase independence of programmed cell death in *Dictyostelium*. *Curr. Biol.*, **1998**, *8*, 955-958.

(106) Tarrés, M.; Canetta, E.; Viñas, C.; Teixidor, F.; Harwood, A. J. Imaging in living cells using *v*B–H Raman spectroscopy: monitoring COSAN uptake. *Chem. Commun*., **2014**, *50*, 3370-3372.

(107) Muñoz-Flores, B. M.; Cabrera-González. J.; Viñas, C.; Chávez-Reyes, A.; Dias, H. V. R., Jiménez-Pérez, V. M.; Núñez, R. Organotin Dyes Bearing Anionic Boron Clusters as Cell-Staining Fluorescent Probes. *Chem. Eur. J.* **2018**, *4*, 5601-5612.

(108) Chaari, M.; Gaztelumendi, N.; Cabrera-González, J.; Peixoto-Moledo, P., Viñas, C.; Xochitiotzi-Flores, E., Farfan, N.; Ben Salah, A.; Nogues, C.; Nuñez R. Fluorescent BODIPY-anionic boron cluster conjugates as potential agents for cell tracking. *Bioconjugate Chem.* 2018 DOI: 10.1021/acs.bioconjchem.8b00204.

(109) Gona, K. B.; Zaulet, A.; Gómez-Vallejo, V.; Teixidor, F.; Llop J.; Viñas, C. COSAN as a molecular imaging platform: synthesis and "in vivo" imaging. *Chem. Commun.*, **2014**, *50*, 11415-11417.

(110) (a) Baker, S. J.; Akama, T.; Zhang, Y. K.; Sauro, V.; Pandit, C.; Singh, R.; Kully, M.; Khan, J.; Plattner, J.; Benkovic, S. J.; Lee, V.; Maples, K. R. Identification of a novel boron-containing antibacterial agent (AN0128) with anti-inflammatory activity, for the potential treatment of cutaneous diseases. *Bioorg. Med. Chem. Lett.*, **2006**, *16*, 5963-5967. (b) Mendes, R. E.; Alley, M. R. K.; Sader, H. S.; Biedenbach, D. J.; Jones, R. N. Potency and Spectrum of Activity of AN3365, a Novel Boron-Containing Protein Synthesis Inhibitor, Tested against Clinical Isolates of Enterobacteriaceae and Nonfermentative Gram-Negative Bacilli. Antimicrob. *Agents Chemother*. **2013**, *57* (6), 2849-2857. (c) Gorovoy, A. S.; Gozhina, O. V.; Svendsen, J. S.; Domorad, A. A.; Tetz, G. V.; Tetz, V. V.; Lejon, T. Boron-Containing Peptidomimetics – A Novel Class of Selective Anti-tubercular Drugs. *Chem. Biol. Drug. Des*., **2013**, *81*, 408-413.

(111) Popova, T.; Zaulet, A.; Teixidor, F.; Alexandrova, R.; Viñas, C. Investigations on antimicrobial activity of cobaltabisdicarbollides. *J. Organomet. Chem*., **2013**, *747*, 229-234.

(112) Zheng, Y.; Liu, W. W.; Chen, Y.; Jiang, H.; Yan, H.; Kosenko, I.; Chekulaeva, L.; Sivaev, I.; Bregadze, V.; Wang, X. M. A Highly Potent Antibacterial Agent Targeting Methicillin-Resistant Staphylococcus aureus Based on Cobalt Bis(1,2-Dicarbollide) Alkoxy Derivative. *Organometallics*., **2017**, *36* (18), 3484-3490.

(113) Mosmann, T. Rapid Colorimetric Assay for Cellular Growth and Survival: Application to Proliferation and Cytotoxicity Assays. *J. Immunol. Methods.,* **1983**, *65*, 55-63.

(114) Borenfreund, E.; Puerner, J. Toxicity determined in vitro by morphological alterations and neutral red absorption. *Toxicol. Lett*., **1985**, *24*, 119-250.